ENERGY DISSIPATION IN CULVERTS BY FORCING A HYDRAULIC JUMP AT THE OUTLET

By

EMILY ANNE LARSON

A thesis submitted in partial fulfillment of
the requirements for the degree of

MASTER OF SCIENCE IN CIVIL ENGINEERING

WASHINGTON STATE UNIVERSITY
Department of Civil and Environmental Engineering

December 2004

To the faculty of Washington State University:

The members of the Committee appointed to examine the thesis of EMILY ANNE LARSON find it satisfactory and recommend that it be accepted.

Chair

ACKNOWLEDGMENT

I would like to thank Dr. Rollin Hotchkiss for advice, guidance, and coaching throughout the development of this thesis. I would also like to thank my committee members Dr. Michael Barber and Dr. Joan Wu for their valuable comments and review. Without Dr. Wu's tireless encouragement for me to continue my education, I would not have attempted this thesis. I would like to thank Dr. David Admiraal at the University of Nebraska for his close involvement with the model design and providing valuable advice throughout the experimental process and data analysis. The assistance of undergraduate researchers Brandon Billings, Brian Drake, and Chris Frei have allowed me to expand the scope of research and still graduate in a timely manner. The model would never have been constructed or operational without the skills and knowledge of Pat Simms, Norm Martel, and Stan. The support of my fellow graduate students at Albrook Hydrailics Laboratory has been invaluable in keeping me sane and on track during my research. My family, as always, has been the foundation of all of my achievements.

The ideas of Kevin Donahoo, Hydraulic Engineer, Roadway Design Division, Nebraska Department of Roads, were the basis the designs researched. The project was fully funded by the Nebraska Department of Roads.

REDUCING ENERGY AT CULVERT OUTLETS BY FORCING A HYDRAULIC JUMP INSIDE THE CULVERT BARREL

Abstract

By Emily Anne Larson
Washington State University
December 2004

Chair: Rollin H. Hotchkiss

Riprap and concrete stilling basins are often built at culvert outlets to keep high-energy flows from scouring the streambed. The effectiveness of two simple alternatives to building large and complex basins is examined: an end weir on a horizontal apron and a drop structure with an end weir. The two designs are intended to create a hydraulic jump within the culvert barrel, without the aid of tailwater, to reduce the energy of the flow at the outlet. This research examines the jump geometry, the effectiveness of each jump type, and proposes a design procedure for practicing engineers. The B-jump, with its toe located at drop, was found to be most effective in dissipating energy, momentum, and velocity. The outlet momentum was reduced 10-48% from the approach momentum, while relative dimensionless energy loss was reduced 6-71%. The reduction in velocity was dependent on approach velocity and varied from 0.7 to 8.5 ft/s (0.21–2.59 m/s). The design procedure is applicable to culverts with approach Froude numbers from 2.6-6.0. Both designs are effective in reducing outlet velocity, momentum, and energy, all of which will decrease the need for downstream scour mitigation. The layout of the designs will also allow easy access for maintenance activities.

TABLE OF CONTENTS

Page

LIST OF TABLES

LIST OF FIGURES

NOTATION

B = Culvert width [L]

C_d = Drag coefficient [1]

E' = Dimensionless energy [1]

Fr_1 = Approach Froude number [1]

g = gravity [LT^{-2}]

H_1 = Depth of upstream water surface above weir crest [L]

h_d = Drop height [L]

h_w = Weir height [L]

L_d = Distance between the drop and the weir [L]

L_j = Length from jump toe to stagnation point [L]

L_w = Distance between the jump toe and the weir [L]

M = Momentum per unit width [L^2]

Q = Discharge [L^3T^{-1}]

q = Unit discharge [L^2T^{-1}]

y = Flow depth [L]

y' = Dimensionless depth, y/y_c [1]

y_1 = Approach flow depth [L]

y_2 = Flow depth just upstream from the weir [L]

y^*_2 = Depth of classic hydraulic jump [L]

y_3 = Downstream or outlet flow depth [L]

y_3' = Outlet depth found assuming no energy loss [L]

$y'_{3adjusted}$ = Outlet depth adjusted to account for energy loss [L]

y_c = Critical depth [L]

V_1 = Approach velocity [LT^{-1}]

V_2 = Velocity between drop and weir [LT^{-1}]

V_3 = Downstream or outlet velocity [LT^{-1}]

γ = Specific weight [$ML^{-2}T^{-2}$]

ρ = Density [ML^{-3}]

CHAPTER ONE

INTRODUCTION AND OBJECTIVES

Introduction

Culverts are used to pass water under roadways and other structures. Some topographic situations require a steeply sloped culvert, which increases the water velocity and produces high-energy flow at the culvert outlet. This high-energy water can scour and erode the natural channel bed and cause undercutting of the culvert outlet.

One of the most efficient means of energy dissipation for culvert outflows is to induce a hydraulic jump. A hydraulic jump occurs at the transition from supercritical flow to subcritical flow. It is characterized by a sudden increase in water depth and loss in energy. Current mitigations for scour include building large riprap basins or rigid concrete structures downstream from the culvert outlet (*1*). These solutions require significant additional cost for material and right-of-way. The effectiveness of two simple energy dissipators, located at the culvert outlet, were modeled. Both are intended to force a hydraulic jump and stabilize its location without the assistance of tailwater, or subcritical flow depth downstream. The two designs tested were [1] a rectangular weir placed on a horizontal apron (Design I) and [2] a vertical drop structure followed downstream by a rectangular weir (Design II). A schematic of each design is provided in Figure 1.

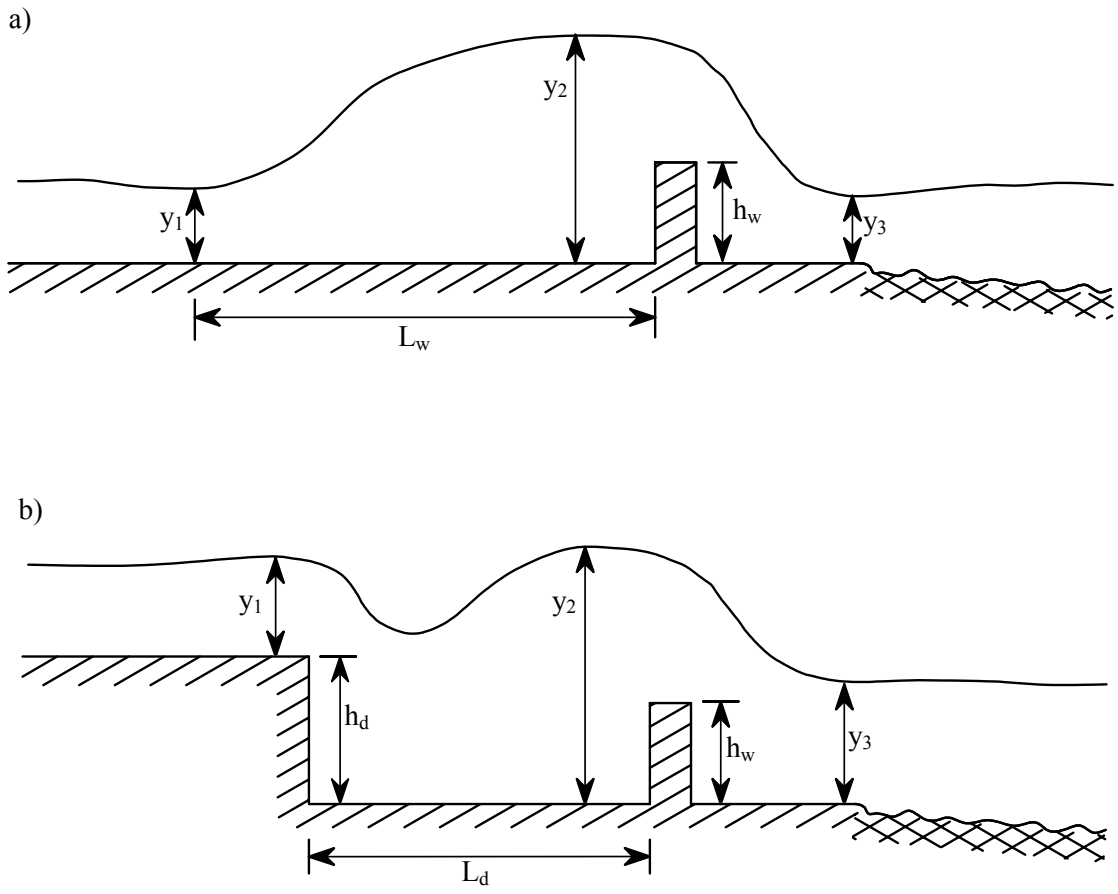

Figure 1. Elevation views (not to scale) of experimental setup, a) Design I: horizontal apron with a rectangular weir; b) Design II: vertical drop structure with a rectangular weir, where y_1 = Approach flow depth, y_2 = Flow depth just upstream from weir, y_3 = downstream flow depth, L_w = Distance from jump toe to weir, h_w = weir height, L_d = distance from drop to weir, h_d = drop height.

Insuring that a jump occurs does not guarantee a protected streambed downstream from the weir. Tailwater acts as a cushion against downstream channel erosion (*2*), and without it, protection is required. Scour holes downstream from weirs have been observed in the literature (*3,4*), and their depth and length are dependent on weir height, tailwater depth, and bed material in the downstream channel. This thesis will not address this issue.

Research Objectives

1. Experimentally evaluate two simple alternatives for energy dissipation of high velocity flow exiting from culverts.
2. Use successful test results to create a design procedure for practicing engineers.

CHAPTER TWO

LITERATURE REVIEW

Hydraulic Jumps Forced by Weirs

Extensive research has been completed on the use of rectangular weirs and sills to force hydraulic jumps in horizontal rectangular channels (*2-11*). Sills and weirs are used to force a hydraulic jump and to stabilize the jump location on the apron. Hydraulic jumps forced by sills and weirs dissipate more energy than classic hydraulic jumps (*3*). A classic hydraulic jump is a jump caused by subcritical downstream flow depth in a constant width horizontal rectangular channel, with no appurtenances.

Difference Between Weirs and Sills

A weir has a head over crest to weir height ratio (H_1/h_w) less than ten, and a sill has an H_1/h_w greater than ten (*5*). The current research was performed using weirs.

Hydraulic Jump Geometry

Hydraulic jump geometry describes the jump length, depth, and shape. Tests reveal that a hydraulic jump can be forced with a weir, independent of downstream flow depth (*2,5,6*). Hydraulic jump geometry is similar for jumps induced by sharp-crested nonaerated weirs (*6*), broad-crested nonaerated weirs (*5*), and sharp-crested aerated weirs (*2*).

Determining Weir Height and Location

Assuming a uniform velocity distribution upstream from the weir, weir height, jump length, and jump depth can be predicted using the weir equation and the momentum equation (*6*), this is the line labeled "Theoretical" in Figure 2. Experimental data curves approached predicted results when the jump ended at the weir. The distance to the end of the jump is approximated by five times the jump depth (*6*):

$$L_w = 5y_2 \tag{1}$$

where L_w is the distance from the jump toe to the weir and y_2 is the depth of the jump just before the weir. The minimum weir height that creates a jump terminating at the weir was found by Forester and Skrinde:

$$h_w = y_1\left(0.0331 \cdot Fr_1^2 + 0.4385 \cdot Fr_1 - 0.6534\right) \tag{2}$$

where h_w is the weir height, y_1 is the approach flow depth, and Fr_1 is the approach Froude number. This is the equation for line "$L_w/y_2 = 5$" from Figure 2.

Flow Characteristics Downstream from Weir

The early tests focused on how tailwater influenced the jump. Flow depth downstream from the weir was controlled to study its affect on jump behavior.

When the tailwater depth is not known, the momentum equation can be used to predict downstream flow characteristics if the drag coefficient (C_d) is known. The drag coefficient on a weir has been found empirically (*7-11*).

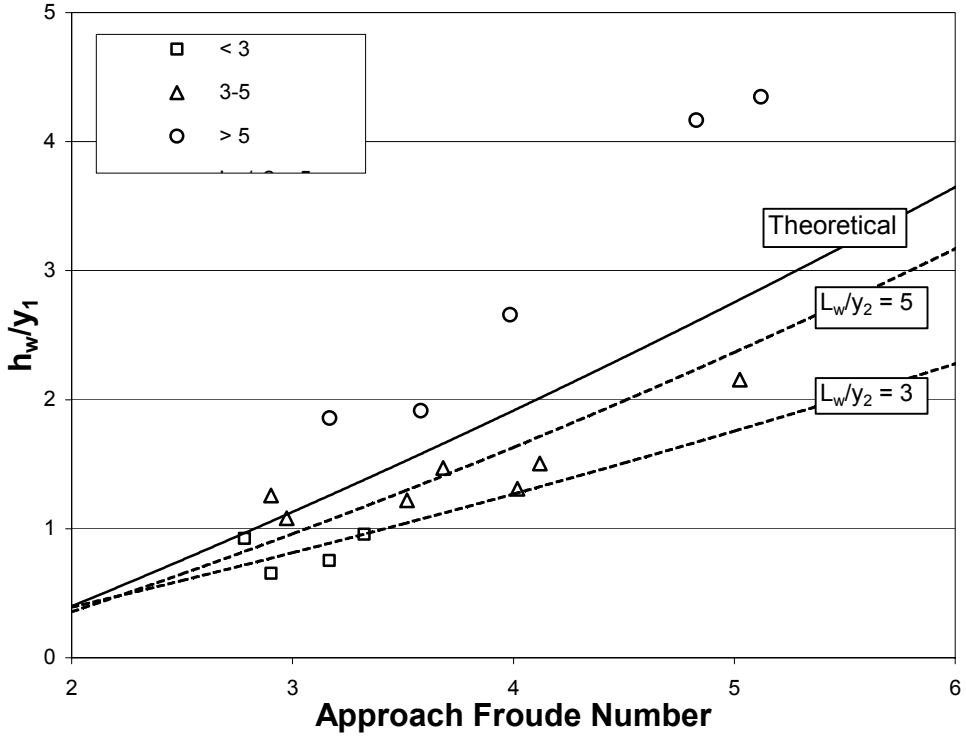

Figure 2. The data from this study compared to research by Forester and Skrinde (*6*).

Energy Dissipation Loss Over Weirs

When the discharge, approach depth, and tailwater depth are known the relative energy loss over a weir can be calculated using the energy equation. When the tailwater depth is not known there are too many unknowns, and so the energy equation must be solved empirically. The relative energy loss over the weir is a function of the approach Froude number, drag coefficient, and the weir height (*7*). The literature only provides solutions for submerged weirs.

Drop Influence on Hydraulic Jumps

Design engineers have used drops in channels the reduce to channel slope (*12*), dissipate energy (*13*), and stabilize the jump location (*14*). There are two main categories of flow over a drop: free and submerged. A free overfall occurs when the flow over the drop is not impeded by tailwater (*13*). A submerged drop occurs when the downstream depth is deep enough to influence nappe behavior. In the current research a submerged flow occurs at the drop and a free flow drop occurs downstream from the weir.

Energy Loss at a Free Flow Drop

Energy loss in free falls over drops has been extensively studied (*12-13,15-19*). When the approach flow is subcritical, the flow energy over the drop can be computed using critical depth and drop height. Assuming no energy loss, the energy at the base of the drop is equal to the energy at the top of the drop:

$$h_w + y_c + \frac{\left(\frac{Q}{By_c}\right)^2}{2g} = y_3 + \frac{\left(\frac{Q}{2y_3}\right)^2}{2g} \tag{3}$$

Where y_c is the critical depth, B is the channel width, g is gravity, y_3 is the flow depth downstream from the drop, and Q is the flow rate. The energy at the base of the drop can also be found experimentally. The difference between the experimental and theoretical energies is the energy loss over the drop (Figure 3). The energy loss over a free overfall is not negligible and varies with relative drop height (*13*).

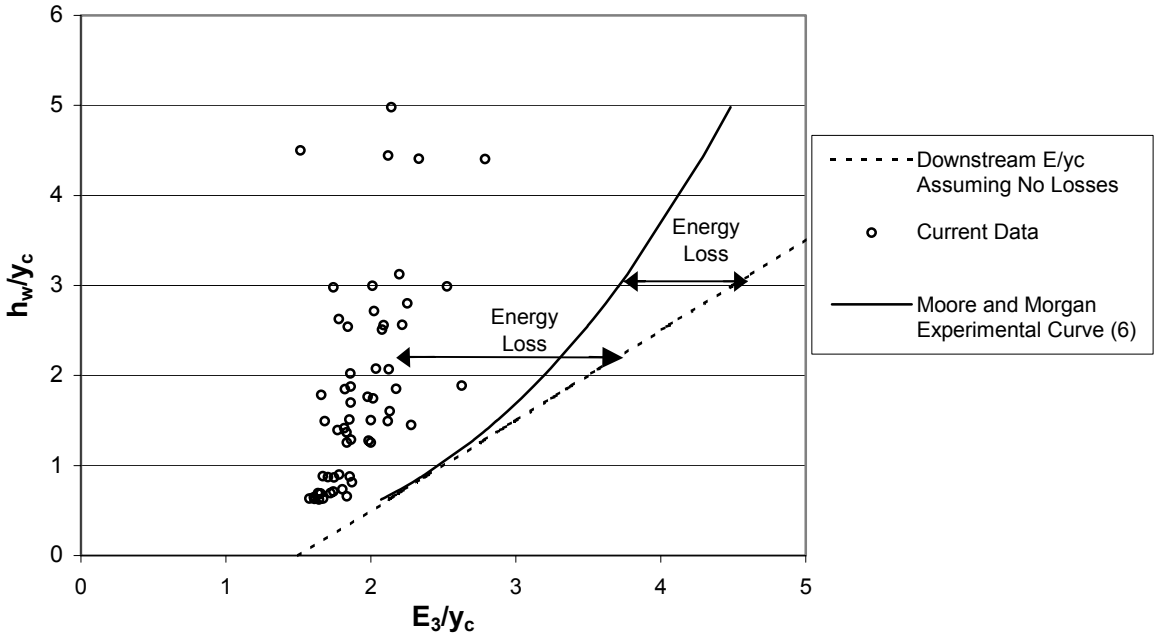

Figure 3: Energy loss over a drop.

Submerged Drop Jump Type

Subcritical tailwater depth is required to force a hydraulic jump at a drop. Depending on the tailwater depth, different jump types have been observed (*14,20-21*). The jump type names and descriptions are listed in Table 1 and shown in Figure 4.

Table 1. Submerged Drop Hydraulic Jump Types

Type of Jump	**Description**	**Reference**
Sloped A-Jump	Requires the highest downstream depth to force the jump toe upstream into the sloped culvert section.	Observed in current research, considered a submerged jump in the literature.
A-Jump	The jump toe is located upstream from the drop.	(14,20-21)
Wave Jump	Occurs when the downstream depth is between that required for an A-Jump and a B-Jump. It is characterized by a standing wave, which can be 1.5 times the height of the tailwater depth.	(14,20-21)
Wave Train	A highly oscillatory wave jump. This category also includes what the current research terms undular jumps. At very low flows smooth surfaced waves start at the toe and propagate far downstream.	21
B-Jump	The jump toe located at the drop.	(14,20-21)
Minimum-B-Jump	The tailwater is lower than that of a B-jump. The flow plunges at the drop and the toe begins downstream from the drop.	(20,21)
Plunging Jet	The tailwater is lowered so that the nappe at the drop is aerated. The flow plunges into the pool between the drop and the weir.	Also called a limited jump (21)

Submerged Drop Sequent Depth

The downstream depth required to force a hydraulic jump at a drop can be predicted using the momentum equation. The force on the drop face has been measured with manometer taps and found to approximate a hydrostatic pressure distribution.

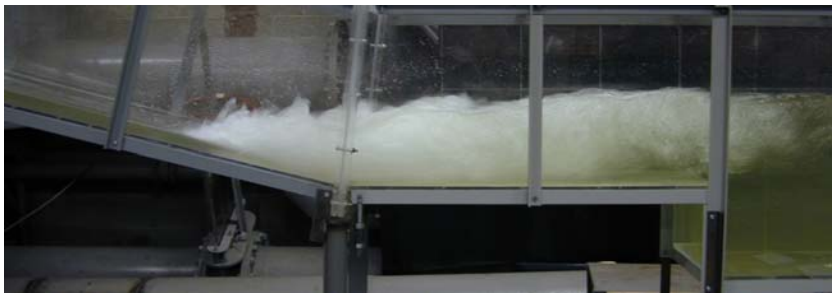

a)

b)

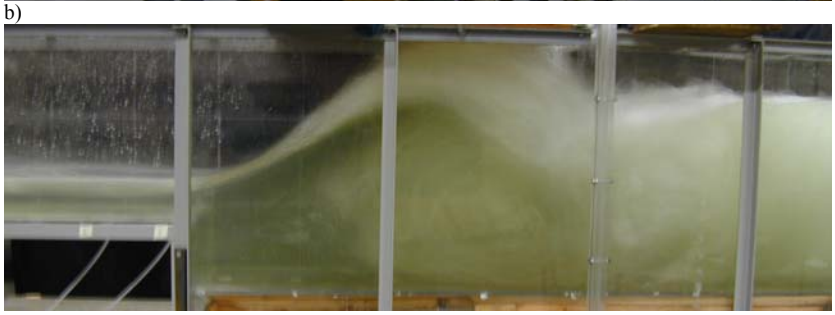

c)

d)

e)

Figure 4. Hydraulic Jump Types. a) Sloped-A-Jump b) A-Jump c) Wave Jump d) B-Jump e) Minimum-B-Jump.

CHAPTER THREE

EXPERIMENTAL SETUP

All tests were conducted in Albrook Hydraulics Laboratory at Washington State University.

The 2 ft (0.61 m) wide box culvert was constructed with acrylic and supported by a steel frame. The model consisted of two sections: a 7.54 ft (2.3 m) long sloped section with a 0.248 slope, and a 14 ft (4.3 m) long horizontal runout section. The total horizontal length of the model from inlet to outlet was 21.35 ft (6.51 m). The horizontal apron section had a vertical drop located 4 ft (1.2 m) downstream from the break in slope, so the last 10 ft (3.1 m) of the apron were lower than the break. The drop height was adjustable with a false floor downstream from the drop. Experiments were run with 0.0, 0.32, 0.71, and 1.0 ft (0.10, 0.22, 0.31 m) drops.

A removable rectangular acrylic weir was 0.75 in (0.02 m) thick, spanned the entire culvert width, and was secured in place with screws. Design I experiments were performed with 0.25, 0.375, 0.5, and 1.0 ft (0.076, 0.114, 0.15, 0.31 m) high weirs. Design II experiments were performed with the weir located 3, 5, and 7 ft (0.91, 1.52, 2.13 m) downstream from the drop, and weir heights of 0.5, 1.0 and 1.5 ft (0.15, 0.31, and 0.46 m).

A point gage mounted over the sloped section was used to measure depth at the toe of Sloped A-Jumps. Another point gage on a rail over the horizontal section enabled depth to be easily measured at any location.

Flow into the model was controlled with a gate valve on the inflow pipe and a butterfly bypass valve near the pump. Flow was measured with a sharp-crested, 90^o V-notch weir located in the flume head tank. Model discharge capacity ranged from 0.25 cfs to 8.35 cfs (7.08-236.5 liters/s). The approach Froude number, measured at the jump toe, ranged from 2.6-6.0. The culvert outlet was uncontrolled; the water fell freely into the tailwater tank where it returned to the sump.

Gravitational forces dominate the flow in the model, so results can be scaled using Froude similarity. All experiments conformed to the Froude law constraints listed in Table 2.

Table 2. Modeling Limitations using Froude Law

Modeling Limitation	Reason	Source
Model/Prototype<1/60	Minimize scale effects	22
y > 15 mm	Eliminate surface tension	25
V > 230 mm/s	For gravitational waves to occur	25
h_w > 3 mm	Reduce effect of viscous forces	26

The turbulence through the jump and over the weir insufflates air bubbles into the water. The modeling process is complicated by the fact that surface tension forces, not gravitational forces, dominate bubbles in two-phase flow. So the bubbles in the model will be the same size as the bubbles in the prototype, resulting in faster rising velocities of bubbles in the model (*22*). Air entrainment also causes the flow velocity to increase (*23*). There is conflicting research results on the effect of air entrainment on the performance of stilling basins, but research has shown that reasonable conjugate depth predictions can be made assuming no air entrainment (*24*). According to Sharp (*22*) "Nevertheless the problems are more apparent than real because there is a general

consensus that Froudian models, provided they are sufficiently large, will provide a reasonable approximation to the performance throughout the two-phase flow stage."

CHAPTER FOUR

EXPERIMENTAL PROCEDURE

Ninety test runs were completed on Design II. Most combinations of three step heights, three weir locations, three weir heights, and four flow rates were tested. Some combinations were not tested due to repetitiveness (Table 3).

Twenty tests were run for Design I. Four flow rates were tested with four different weir heights at one or two locations.

Villemonte's (*27*) equations for a submerged V-notch weir were used to find discharge. Depth measurements were taken, in the headtank upstream and downstream from the weir.

Point gage water depth measurements were taken at the jump toe, the weir, and at the culvert outlet. The jump toe location, the length from the toe to the stagnation point, and the length from the toe to the weir were recorded. For each run digital photographs were taken and visual observations were recorded.

Since Design I experimentation has been described by earlier research, Design I data were compared to theoretical and experimental data of Forester and Skrinde (*6*). To verify the data repeatability gathered from Design II, twenty runs were repeated.

Table 3. Design II Configurations and Jump Types.

h_w	h_d	~Q	Run #	$L_w = 3$	Run #	$L_w = 5$	Run #	$L_w = 7$
1	1	.32	5	Wave Train			20	Wave Train
1	1	2	7	Skimming	31	Skimming	18	Wave/Skimming
1	1	5	6	Skimming	29-30	Undeveloped	17	Wave Train
1	1	8	8	Skimming	32	Undeveloped	19	Wave Train
1	.71	2	65	Undeveloped	55	A-Jump	41	A-Jump
1	.71	5	64	Undeveloped	54	Wave	42	Wave
1	.71	7	63	Undeveloped	53	Wave	43	Wave
1	.71	8	66	Undeveloped	52	Wave	40	Wave
1	.32	2	78	Sloped A-Jump	85	Sloped A-Jump		
1	.32	5	77	Sloped A-Jump	84	Sloped A-Jump		
1	.32	7	76	Sloped A-Jump	86	Sloped A-Jump		
1	.32	8	75	Sloped A-Jump	83	Sloped A-Jump		
.5	1	.32	1	Plunging Jet			21	Plunging Jet
.5	1	2	2	Plunging Jet	35	Plunging Jet	22	Plunging Jet
.5	1	5	3	Skimming Flow	34	Min-B-Jump	23	Min-B-Jump
.5	1	8	4	Skimming Flow	33	Min-B-Jump	24	Min-B-Jump
.5	.71	2	60	Min-B-Jump	48	Min-B-Jump	36	Min-B-Jump
.5	.71	5	61	Skimming Flow	49	Min-B-Jump	37	Min-B-Jump
.5	.71	7	62	Skimming Flow	50	Min-B-Jump	38	Min-B-Jump
.5	.71	8	59	Skimming Flow	51	Min-B-Jump	39	Min-B-Jump
.5	.32	2	71	Undeveloped	79	A-Jump	89	B-Jump
.5	.32	5	72	A-Jump	80	B-Jump	88	B-Jump
.5	.32	7	73	A-Jump	81	B-Jump	87	B-Jump
.5	.32	8	74	A-Jump	82	B-Jump	90	B-Jump
1.5	1	.32	12	Sloped-A-Jump			13	Sloped-A-Jump
1.5	1	2	11	Sloped-A-Jump	26	Sloped-A-Jump	14	Sloped -A-Jump
1.5	1	4			28	Sloped-A-Jump		
1.5	1	5	10	A-Jump	27	A-Jump	15	A-Jump
1.5	1	8	9	Undeveloped	25	A-Jump	16	Wave
1.5	.71	2	70	Sloped-A-Jump			47	Sloped-A-Jump
1.5	.71	5	69	Sloped-A-Jump	57	Sloped-A-Jump	46	Sloped-A-Jump
1.5	.71	7	68	Sloped-A-Jump	56	Sloped-A-Jump	45	Sloped-A-Jump
1.5	.71	8	67	Sloped-A-Jump	58	Sloped-A-Jump	44	Sloped-A-Jump

CHAPTER FIVE

RESULTS AND DISCUSSION

Design I

As stated in the literature review, extensive research has been completed on Design I. A limited number of tests were completed to compare results with previous studies. There are some differences between the current research and the literature data. First, the approach supercritical flow is developed with a steeply sloped channel, not a sluice gate. Also, the depth of flow downstream from the weir was uncontrolled and analyzed to find the change in energy, outlet momentum, and outlet velocity.

Hydraulic Jump Types

Weir heights were selected to test a full range of jumps. Submerged jumps, complete jumps, and standing waves were all observed during Design I testing (Figure 5).

Jump Effectiveness

Momentum at the outlet, energy loss, and reduction in velocity were used to determine jump effectiveness. The specific momentum function was used to find the approach and outlet momenta:

$$M = \frac{q^2}{g \cdot y} + \frac{y^2}{2} \tag{4}$$

Where M is the specific momentum and y is the flow depth. For equal approach momenta jumps forced by a weir had a lower outlet momenta than an apron with no

a)

b)

c)

Figure 5. Design I Observed Jumps: a) Standing Wave $L_w/y_{2,}$ =0.9 b) Complete Jump L_w/y_2 = 5, and c) Submerged Jump L_w/y_2 = 9.

appurtenances (Figure 6). For equal approach momenta Design I jumps had greater momenta at the outlet than A-jumps, B-jumps, and Minimum B-Jumps observed in Design II testing.

Dimensionless energy was used to determine the energy loss between the approach and the outlet:

$$y' = \frac{y}{y_c} \tag{5}$$

$$E' = y' + \frac{1}{2 \cdot (y')^2} \tag{6}$$

Where y′ is the dimensionless depth and E′ is dimensionless energy. For equal dimensionless approach energies, Design I dissipated more energy than an apron with no appurtenances (Figure 7). Design I dissipates more energy than Sloped A-jumps and A-jumps, and less energy than B-jumps and Minimum B-Jumps observed in Design II tests.

The velocity change is compared to the approach velocity in Figure 8. Design I has a greater reduction in velocity than an apron with no appurtenances.

Comparison to Literature

The current weir data were compared with the trend lines from Forester and Skrinde (Figure 2). For a given approach Froude number and h_w/y_1 value, the Forester and Skrinde data for L_w/y_2 are higher than measured. The high discrepancy seen in the L_w/y_2 values greater than 5 is likely due to the jump toe occurring in the culvert sloped section of this study.

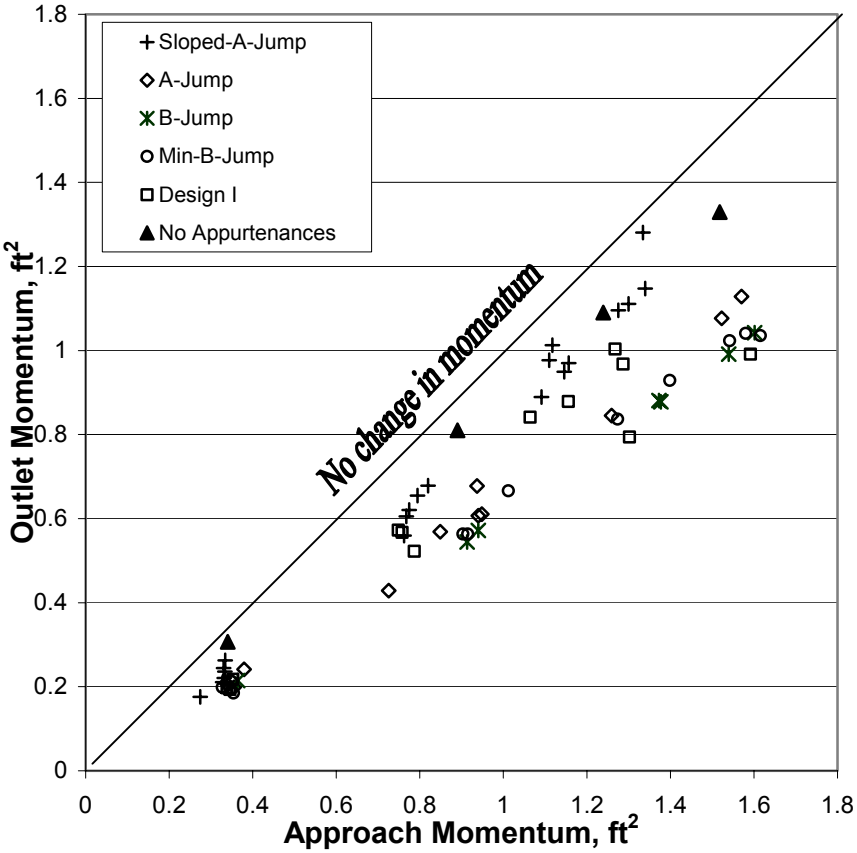

Figure 6. Outlet Momentum vs. Approach Momentum.

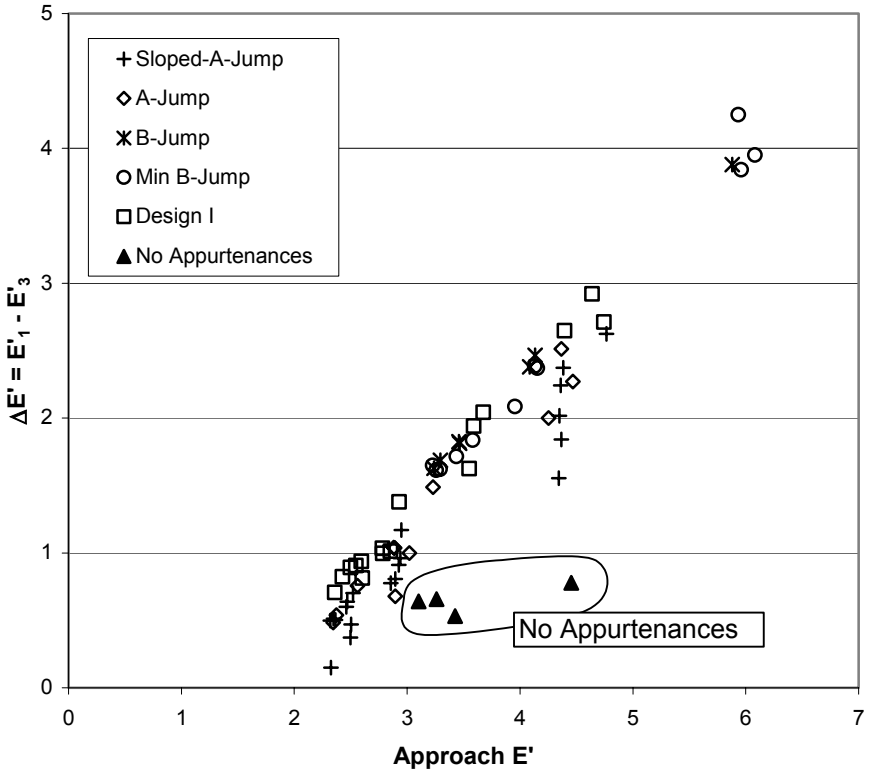

Figure 7. Change in Dimensionless Energy, E′.

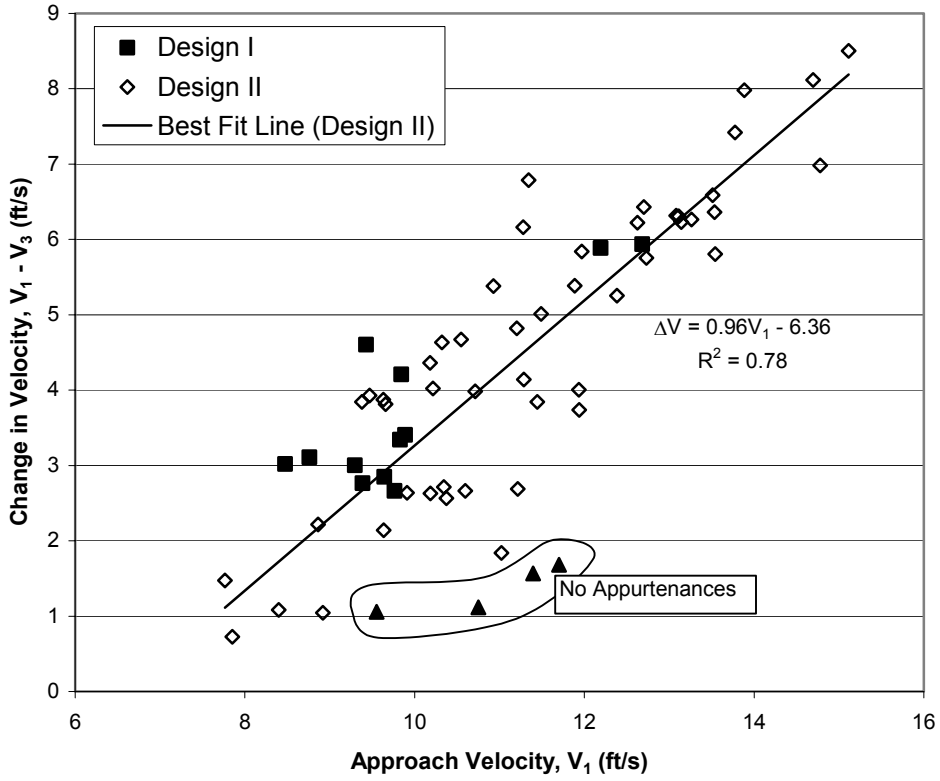

Figure 8. Change in velocity vs. approach velocity.

Determining Weir Location

Forester and Skrinde (*6*) recommend that jump length (L_w) be five times the jump depth. Figure 5a and 5c verify that when L_w/y_2 is less than five the jump is not complete, and when this value is greater than five the increased energy dissipation is minimal. The weir should be placed so that the hydraulic jump begins at the slope break. The jump depth (y_2) can be estimated using the sequent depth for a classic hydraulic jump (y^*_2) or $h_w + y_c$. Determining jump length with y^*_2 over-predicts the length by about 13%, while determining the jump length with $h_w + y_c$ underpredicts the distance by about 10%. For a slightly conservative design, it is recommended that the distance between the slope break and the weir equal the jump length:

$$L_w = 5 \cdot y_2^* \tag{7}$$

Where L_w is the distance from the jump toe to the weir and y^*_2 is the sequent depth for a classic hydraulic jump.

Determining Weir Height

The weir height can be designed using an empirical equation fitted to data from jumps with a length five times the jump depth (Equation 2).

Predicting Outlet Conditions

An alternate means of predicting flow conditions downstream from the weir is by treating the weir as a free overfall. This requires two assumptions: that the flow over the weir is critical and that there is no energy loss between the weir and outlet.

The measured depth just upstream from the weir minus the weir height, was generally greater than critical depth (Figure 9). To see the sensitivity the depth over the weir has on the outlet depth prediction, y_3 was predicted using both the measured depth just upstream from the weir minus the weir height and critical depth over the weir. It was found that the y_3 predictions from each method were very similar (Figure 10). Therefore, the first assumption has little effect on the predicted outlet depth.

The second assumption, that there is no energy loss between the flow over the weir and the outlet, was not witnessed during testing (Figure 3). The outlet depth, y_3' found assuming no energy loss, under predicts the flow depth at the culvert outlet (Figure 11). The difference between the predicted and measured outlet depths is the energy loss downstream from the weir. An empirical equation was used to fit the y_3' assuming no energy loss to the measured depth:

$$y_3 = 1.23y_3' + 0.05 \quad (8)$$

Where y_3' is the outlet depth assuming no energy loss and y_3 is the outlet depth adjusted to account for energy loss. With the y_3, known channel width and design discharge, all hydraulic values at the outlet may be calculated.

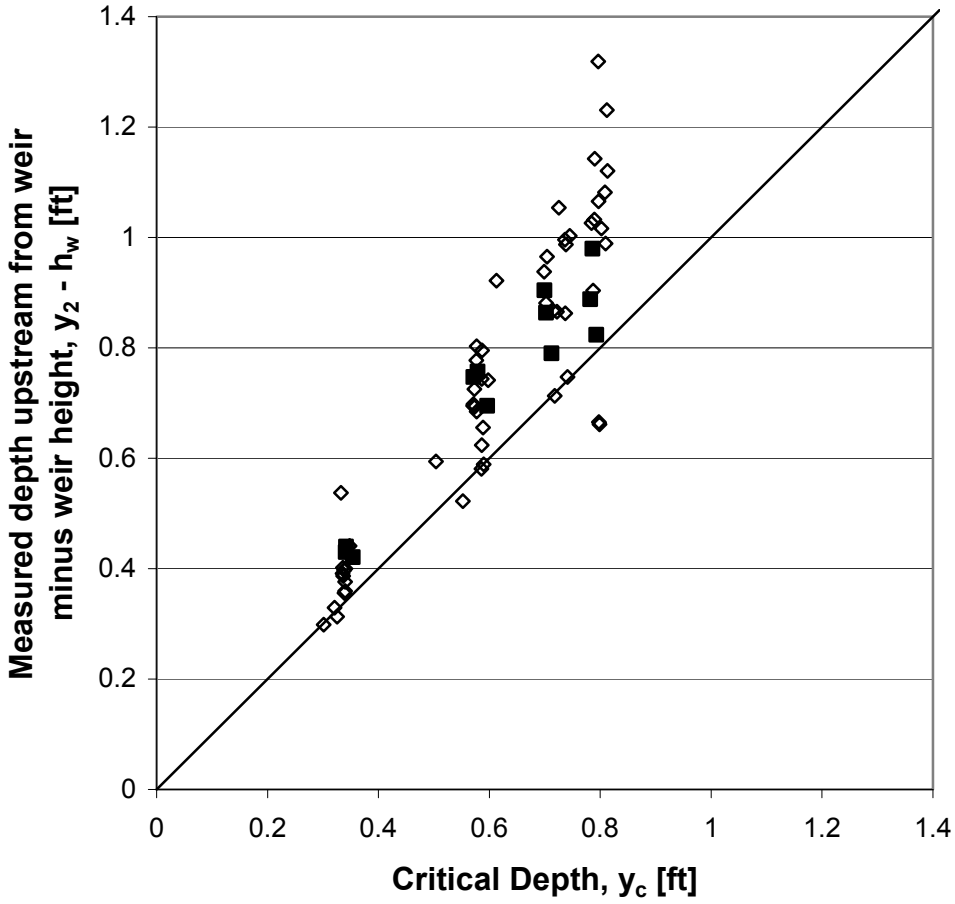

Figure 9. Measured depth just upstream from the weir minus the weir height compared with critical depth.

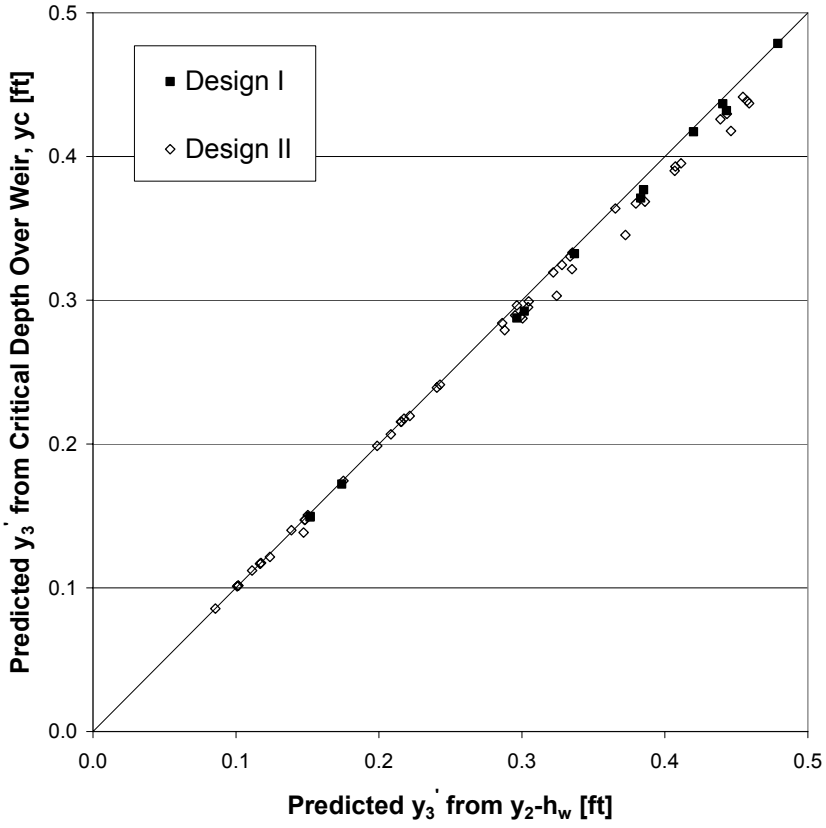

Figure 10. y_3' from measured depth just upstream from the weir minus the weir height, $y_2 - h_w$, compared with y_3' from assuming critical depth over the weir.

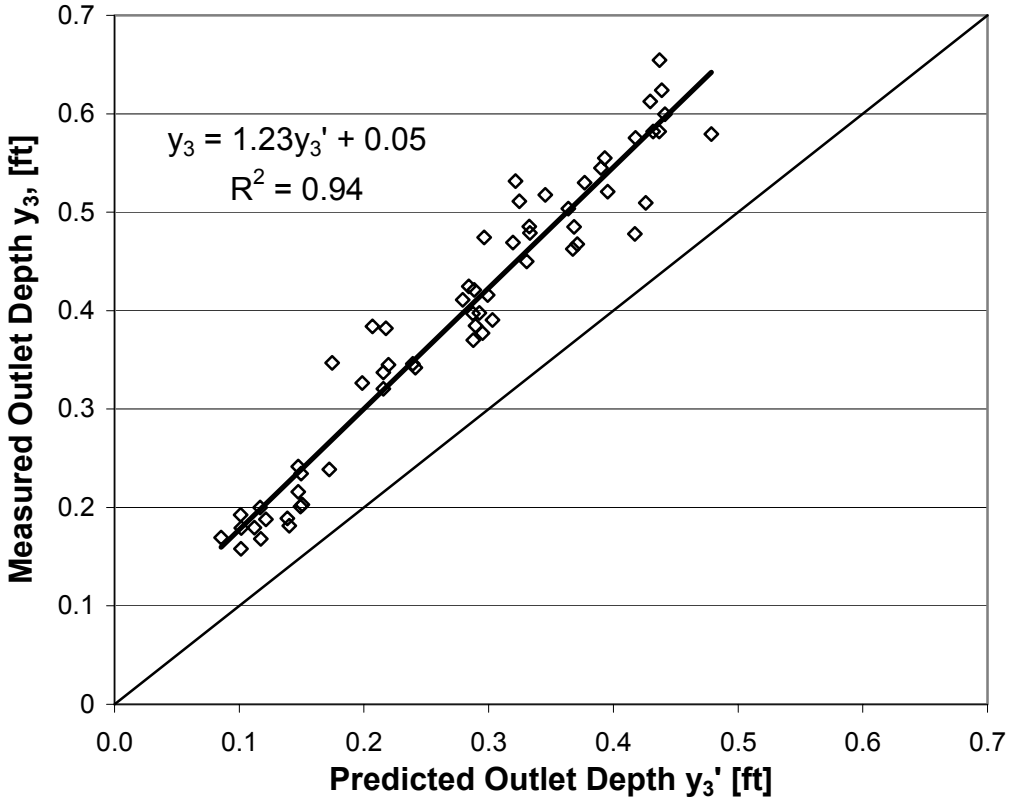

Figure 11. Predicted outlet depth assuming no energy loss, y_3' compared to measured outlet depth, y_3.

Design II

Hydraulic Jump Types

Each jump type reviewed (Table 1) was observed during testing. Some runs did not produce a jump; the flow either skimmed over the weir or the weir was too close to the drop to allow the jump to fully develop. Analysis was performed on Sloped A-Jumps, A-Jumps, B-Jumps, and Minimum-B-Jumps. Wave Jumps were not analyzed due to unstable, unpredictable, and undesirable behavior for design. The Wave Train and Plunging Jet jumps occurred too rarely to collect sufficient data for analysis.

The jump type is a function of approach Froude number and depth, drop height, weir height, and weir location (Figure 12).

Effectiveness of Jump Types

Momentum at the outlet, energy loss, and reduction in velocity were used to determine which type of jump was the most effective for reducing downstream erosion potential. For equal approach characteristics a B-Jump results in the lowest momentum at the outlet (Figure 6) and the greatest decrease in energy (Figure 7). Design II has a lower outlet velocity than an apron with no appurtenances (Figure 8). The B-Jump produced the most complete and stable jump using the shortest weir height.

Comparison to Literature

The jump types created with a drop and weir match those created with tailwater described in the literature (*19-21*). The geometric characteristics of these jumps match the theoretical data derived by Rouse (*19*) and the experimental data presented by Moore and Morgan (*20*) (See Appendix D).

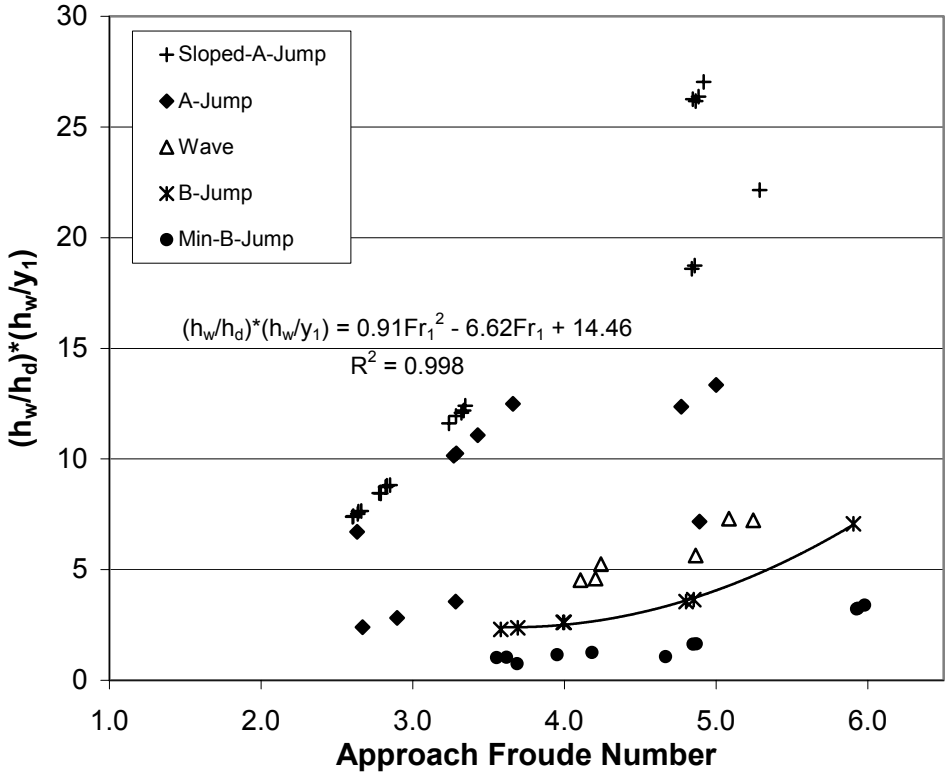

Figure 12. Hydraulic jump geometry. The fitted polynomial is for design.

Experimental free overfall data (*13*) and the current data are compared in Figure 3. The two data sets show similar trends, though Moore measured significantly less energy loss. This can be attributed to the fact that Moore's data was collected at the toe immediately downstream from the nappe, and the current data were collected at the outlet of the model. Also, Moore's data had a smooth approach and an aerated nappe, while many of the current experiments had a turbulent nonaerated nappe.

Verification

Results from the twenty repeated runs were within 10% in most cases (Table 4).

Table 4. Repeatability of Runs

	Percent of Repeated Runs Within:			
Depths	**5%**	**10%**	**15%**	**20%**
$\mathbf{y_1}$	63	94	94	100
$\mathbf{y_2}$	75	100	100	100
$\mathbf{y_3}$	50	63	69	94

Testing proved that over ninety-percent of the time y_1 and y_2 could be replicated within 10%, and that y_3 could be replicated to with 20%. The increased difficulty in repeating y_3 measurements was caused by the highly turbulent and aerated nature of the flow downstream from the weir. The difficulties in measuring turbulent two-phase flow are discussed throughout the literature and there is no standard for how to mitigate the problem. Studies comparing the performance of different measuring instruments and techniques commonly show relative errors of $\pm$20%, and several instances with relative error values of $\pm$50% (*28,29*).

Determining Weir Location

Figure 12 does not include the weir location, because location determines only if a jump occurs. For instance, if the weir were located too close to the drop, the jump would not have space to fully develop (Appendix D). The length of a classic hydraulic jump, L_j, is approximated as six times the sequent depth, y_2, for $4<Fr_1<12$ (30,31). This approximation is a good estimate for jump length, L_w in the current study. The distance between the drop and the weir can be found using the equation for a classic hydraulic jump by substituting L_d for L_j and approximating y_2 with $y_c + h_w$:

$$L_d = 6\left(y_c + h_w\right) \tag{9}$$

Where L_d is the distance between the drop and the weir.

Determining Weir Height

Weir height is found using Figure 13 and a desired outlet Froude number, to find a corresponding y_3/h_w value. The outlet depth, y_3, can be calculated from the selected outlet Froude number, Fr_3, and the design discharge.

Determining Drop Height

The drop height (h_d) is found using B-jump geometry data, the most effective jump type. The known values of y_1 and Fr_1 are used with the equation fitted to the B-jump data in Figure 12.

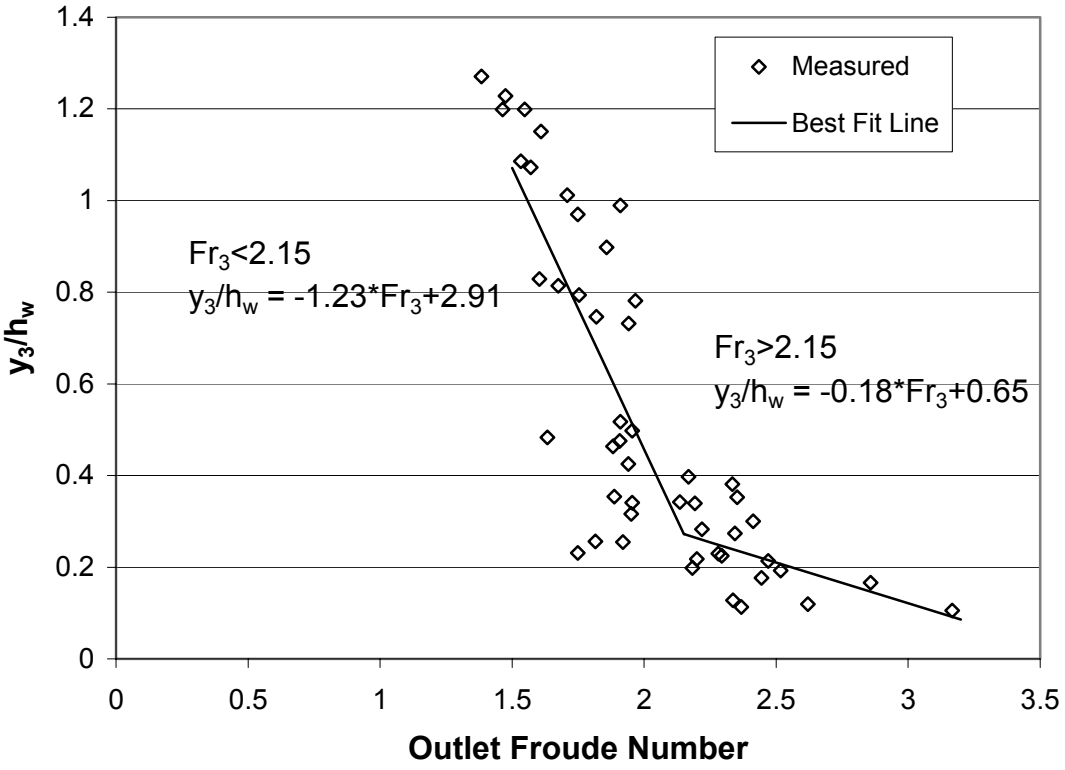

Figure 13. Weir height relationship to outlet conditions.

Predicting Outlet Conditions

The outlet conditions can be found using free overfall theory, as is outlined in the Design I discussion. Equation 8 is used to fit the predicted outlet depth to the measured outlet depth for Design II:

Weir With Drain Holes

All experimental runs for Design I and II were performed with a solid rectangular weir. If this weir were used on the prototype the area upstream of the weir would fill with sediment and reduce the design effectiveness. Eight runs were performed with a weir with drain holes to determine its effect on outlet conditions and jump type. The effectiveness of the jump was found to be comparable to a weir without drain holes (Appendix E). The jets coming through the slots were observed to break up at the nappe base. Jump type did not change.

CHAPTER SEVEN

DESIGN PROCEDURE

Design I

For a horizontal runout section with an end weir the following design procedure was developed using empirical data found this study, combined with data from past research.

Given: The design discharge (Q), approach Froude number (Fr_1), and culvert width (B).

1. Use known design parameters to calculate approach depth and critical depth:

$$y_1 = \sqrt[3]{\frac{\left(\frac{Q}{B}\right)^2}{Fr_1^2 g}} \tag{10}$$

$$y_c = \sqrt[3]{\frac{\left(\frac{Q}{B}\right)^2}{g}} \tag{11}$$

2. Use approach Froude number (Fr_1) and approach depth (y_1) to find sequent depth (y^*_2):

$$y_2^* = \frac{y_1}{2}\left(-1 + \sqrt{1 + 8Fr_1^2}\right) \tag{12}$$

3. Use Equation 2 to determine weir height:

$$h_w = y_1\left(0.0331 \cdot Fr_1^2 + 0.4385 \cdot Fr_1 - 0.6534\right) \tag{2}$$

4. Use Equation 7 to determine distance between change in slope and weir:

$$L_w = 5 \cdot y_2^* \tag{7}$$

5. Solve energy equation (Equation 3) for outlet depth (y_3). There are three solutions to Equation 3; the correct solution is $0 < y_3 < y_c$:

$$h_w + y_c + \frac{V_c^2}{2g} = y_3 + \frac{\left(\frac{Q}{2y_3}\right)^2}{2g} \quad (3)$$

6. Adjust predicted y_3 found above for energy loss with Equation 8:

$$y_3 = 1.23y_3' + 0.05 \quad (8)$$

7. Use outlet depth (y_3), culvert width (B), and design discharge (Q) to determine outlet Froude number (Fr_3), velocity (V_3), and energy (E_3):

$$V_3 = \frac{Q}{By_3} \quad (13)$$

$$Fr_1 = \frac{V_3}{\sqrt{gy_3}} \quad (14)$$

$$E_3 = y_3 + \frac{V_3^2}{2g} \quad (15)$$

Design II

For a horizontal runout section with a negative step and end weir the following design procedure was developed using empirical data found in this study, combined with data from past research.

Given: The design discharge (Q), approach Froude number (Fr_1), and culvert width (B).

1. Use known design parameters to calculate approach depth and critical depth:

$$y_1 = \sqrt[3]{\frac{\left(\frac{Q}{B}\right)^2}{Fr_1^2 g}} \tag{10}$$

$$y_c = \sqrt[3]{\frac{\left(\frac{Q}{B}\right)^2}{g}} \tag{11}$$

2. Use approach Froude number (Fr_1) and approach depth (y_1) to find sequent depth (y^*_2):

$$y_2^* = \frac{y_1}{2}\left(-1 + \sqrt{1 + 8Fr_1^2}\right) \tag{12}$$

3. Select a desired outlet Froude number (Fr_3), and use this with design discharge (Q) and culvert width (B) to find an outlet flow depth (y_3):

$$y_3 = \sqrt[3]{\frac{\left(\frac{Q}{B}\right)^2}{Fr_3^2 g}} \tag{16}$$

4. Use Fr_3 and y_3 from step 3 in Figure 13 to obtain first estimate of weir height (Fr_3<2.15):

$$h_w = \frac{y_3}{\left(-1.23Fr_3 + 2.91\right)} \tag{17}$$

5. Use Equation 9 to determine distance between the drop and the weir:

$$L_d = 6\left(y_c + h_w\right) \tag{9}$$

6. Use Figure 12 to determine drop height:

$$h_d = \frac{h_w^2}{\left(0.9326 \cdot Fr_1^2 - 6.8218 \cdot Fr_1 + 14.859\right) \cdot y_1} \tag{18}$$

7. Solve energy equation (Equation 3) for outlet depth (y_3). There are three solutions to Equation 3, the correct solution is $0 < y_3 < y_c$:

$$h_w + y_c + \frac{V_c^2}{2g} = y_3 + \frac{\left(\frac{Q}{2y_3}\right)^2}{2g} \tag{3}$$

8. Adjust predicted y_3 found above for energy loss with Equation 8:

$$y_3 = 1.23 y_3' + 0.05 \tag{8}$$

9. Use outlet depth (y_3), culvert width (B), and design discharge (Q) to find determine outlet Froude number (Fr_3), velocity (V_3), and energy (E_3):

$$V_3 = \frac{Q}{B y_3} \tag{13}$$

$$Fr_3 = \frac{V_3}{\sqrt{g y_3}} \tag{14}$$

$$E_3 = y_3 + \frac{V_3^2}{2g} \tag{15}$$

10. Use Fr_3 from Equation 15 and y_3 from Equation 10 in Equation 18. Repeat steps 4-9 until outlet conditions match.

CHAPTER EIGHT

SUMMARY AND CONCLUSIONS

The first objective of this project was to experimentally evaluate two simple alternatives for energy dissipation of rapidly-moving water exiting from culverts.

1. All of the hydraulic jumps were classified into types based on their water surface profile. These profiles matched those observed in previous research.
2. Analysis of the outlet momentum, change in dimensionless energy, and change in velocity showed that Design I and Design II were more effective at reducing momentum and dissipating energy than no appurtenances.
3. For Design II the most effective jump type was a B-jump, followed in order by a Min-B-Jump, A-Jump, and Sloped-A-Jump.

The second objective was to use test results to create a set of design procedures for practicing engineers. A design procedure for practicing engineers was developed based on the energy equation and measured data.

This study provides simply constructed alternatives for dissipating energy at culvert outlets. Both designs are effective in reducing outlet velocity, momentum, and energy, all of which will decrease the need for downstream scour mitigation. The layout of the designs will also allow easy access for maintenance activities.

REFERENCES

1. Corry, M., P. Thompson, F. Watts, J. Jones, and D. Richards. *Hydraulic design of energy dissipators for culverts and channels (HEC-14).* Publication FHWA-EPD-86-110. FHWA, U.S. Department of Transportation, 1983.

2. Rand, W. An Approach to Generalized Design of Stilling Basins. *The New York Academy of Sciences*, 1957, p. 173-191.

3. Hager, W.H. and D. Li. Sill-controlled Energy Dissipator. *Journal of Hydraulic Research*, Vol. 30, No. 2, 1992, p.165-181.

4. Rand, W. Sill-controlled Flow Transitions and Extent of Erosion. *Proc. ASCE J. Hydr. Div*., Vol. 96, No. HY4, 1970, p. 7212.

5. Kandaswamy, P.K. and H. Rouse. Characteristics of Flow Over Terminal Weirs and Sills. *Proc. ASCE J. Hydr. Div.,* Vol. 83, No. HY4, 1957, p.1345.

6. Forster, J.W. and R.A. Skrinde. Control of Hydraulic Jump by Sills. *Tran. ASCE,* Vol.115, 1950, p. 973-987.

7. Rajaratnam, N. The Forced Hydraulic Jump *Water Power,* 1964, p. 14-19 and 61-65.

8. Rajaratnam, N. and M.R. Chamani. Energy Loss at Drops. *Journal of Hydraulic Research*, Vol. 33, No. 3, 1995.Rand, Walter. An approach to generalized design of stilling basins. *The New York Academy of Sciences*. 1957,p. 173-191.

9. Ohtsu, I., Yasuda, Y., Yamanaka, Y. Drag on vertical sill of forced jump. *Journal of Hydraulic Research*, Vol. 29, No. 1, 1991, p. 29-47.

10. Narayanan, R. and L.S. Schizas. Force on sill of forced jump. *Proc. ASCE J. Hydr. Div*., Vol. 106, No. HW4, 1980, p. 15368.

11. Narayanan, R. and L.S. Schizas. Force on sill of forced jump. *Proc. ASCE J. Hydr. Div*., Vol. 106, No. HW7, 1980, p. 15552.

12. Rajaratnam, N. and M.R. Chamani. Energy loss at drops. *Journal of Hydraulic Research,* Vol. 33, No. 3, 1995.

13. Moore, W.L. Energy loss at the base of free overfall. *Tran. ASCE,* Vol. 108, 1943, p. 1343-1360.

14. White, M.P. Discussion of Moore. *Tran. ASCE,* Vol. 108, 1943, p. 1361-1364.

15. Gill, M.A. Hydraulics of Rectangular Vertical Drop Structures. *Journal of Hydraulic Research*, Vol. 17, No. 4, 1979.

16. Moore, W.L. Discussion of Moore. *Tran. ASCE,* Vol. 108, 1943.

17. Chamani, M.R. and M.K. Beirami. Flow Characteristics at Drops. *Journal of Hydraulic Research*, Vol. 128, No. 8, 2002.

18. Rouse, H. Discussion of Moore. *Trans. ASCE*, Vol. 108, 1943.

19. Rouse, H., Bhoota, B., Hsu, En-Yun. Design of Channel Transition. *Proc. ASCE,* Nov. 1949, p. 1369-1385.

20. Moore, W.L. and C.W. Morgan. The Hydraulic Jump at an Abrupt Drop. *Proc. ASCE J. Hydr. Div.,* Vol. 83, No. HY6, 1957, pp. 1449.

21. Ohtsu, I, Yasuda, Y. Transition From Supercritical to Subcritical Flow at an Abrupt Drop. *Journal of Hydaulic Research,* Vol. 29, No. 3, 1991, p. 309-238.

22. Sharp, J.J. *Hydraulic Modelling*. Butterworth, London, 1981.

23. Straub, L.G., and A.G. Anderson. Self Aerated Flow in Open Channels. *Trans. ASCE.,* Vol. 125, 1960, p. 456-486.

24. Falvey, H.T. *Air-Water Flow in Hydraulic Structures*. Publication Engineering Monograph No. 41. United States Department of the Interior. 1980.

25. Novak, P. and J. Čăbelka. *Models in Hydraulic Engineering Physical Principles and Design Applications*. Pitman Advanced Publishing Program, Boston, 1981.

26. Ohtsu, I., Yasuda, Y., Yamanaka, Y. Drag on vertical sill of forced jump. *Journal of Hydraulic Research,* Vol. 29, No. 1, 1991, p. 29-47.

27. Villimonte, J.R. Submerged-Weir Discharge Studies. *Eng. News-Record*, Dec. 25, 1947.

28. Cartellier, A., Achard, J.L. Local phase detection probes in fluid/fluid two-phase flows. *Rev. Sci. Instrum.,* Vol. 62, No. 2, 1990, p. 874-886.

29. Liu, M., Zhu, D., and N. Rajaratnam. Evaluation of ADV Measurements in Bubbly Two-Phase Flows. *ASCE Conference: Hydraulic Measurements and Experimental Methods,* Estes Park, CO., Jul 28-Aug1 2002.

30. Bradley, J.N., Peterka, A.J. The Hydraulic Design of Stilling Basins. *Proc. ASCE Hyd. Div.,* Vol. 83, No. HY5, 1957.

31. S.C. *Open-Channel Flow*. John Wiley & Sons, Inc., New York, 2001.

APPENDIX

APPENDIX A

EXAMPLE DESIGN PROBLEMS

Example Problem
Design I

Given:

$Q := 500\frac{ft^3}{s}$ Design Discharge

$Fr_1 := 4.5$ Froude Number at the break, found using BCAP

$B := 14 \cdot ft$ Culvert Width

$g = 32.174\frac{ft}{s^2}$ Gravity

1. Use known design parameters to calculate approach and critical depth:

$$y_1 := \sqrt[3]{\frac{\left(\frac{Q}{B}\right)^2}{Fr_1^{\,2} \cdot g}} \qquad y_1 = 1.251ft$$ Depth of flow at the break.

$$y_c := \sqrt[3]{\frac{\left(\frac{Q}{B}\right)^2}{g}} \qquad y_c = 3.41ft$$ Critical depth.

2. Use approach Froude number and approach depth to find sequent depth:

$$y_2 := \frac{y_1}{2} \cdot \left(-1 + \sqrt{1 + 8 \cdot Fr_1^{\,2}}\right) \qquad y_2 = 7.36ft$$ Sequent depth.

3. Use Equation 2 to determin weir height:

$$h_w := y_1 \cdot \left(0.0331 \cdot Fr_1^{\,2} + 0.4385 Fr_1 - 0.6534\right)$$

$h_w = 2.49ft$ Weir height.

4. Use Equation 7 to determine distance between change in slope and weir:

$L_w := 5 \cdot y_2$ $L_w = 36.801ft$ Distance between break in slope and weir.

5. Solve Equation 3 for outlet depth.

$y_3 := 1.856\text{ft}$

The predicted outlet depth needs to be between 0 and critical depth.

6. Adjust predicted outlet depth from Equation 8:

$y_{3adjusted} := 1.23 \cdot y_3 + 0.05 \cdot \text{ft}$

$y_{3adjusted} = 2.333\text{ft}$

Adjusted outlet depth.

7. Use adjusted outlet depth, culvert width, and design discharge to determine outlet conditions.

$V_3 := \frac{Q}{B \cdot y_{3adjusted}}$ $\quad V_3 = 15.309\frac{\text{ft}}{\text{s}}$ Outlet Velocity

$Fr_3 := \frac{V_3}{\sqrt{g \cdot y_{3adjusted}}}$ $\quad Fr_3 = 1.767$ Outlet Froude Number

$E_3 := y_{3adjusted} + \frac{V_3^2}{2g}$ $\quad E_3 = 5.975\text{ft}$ Outlet Energy

Example Problem
Design II

Given:

$Q := 500\frac{ft^3}{s}$ Design Discharge

$Fr_1 := 4.5$ Froude Number at the break, found using BCAP

$B := 14 \cdot ft$ Culvert Width

$g = 32.174\frac{ft}{s^2}$ Gravity

1. Use known design parameters to calculate approach and critical depth:

$$y_1 := \sqrt[3]{\frac{\left(\frac{Q}{B}\right)^2}{Fr_1^{\,2} \cdot g}} \qquad y_1 = 1.251ft$$ Depth of flow at the break.

$$y_c := \sqrt[3]{\frac{\left(\frac{Q}{B}\right)^2}{g}} \qquad y_c = 3.41ft$$ Critical depth.

2. Use approach Froude number and approach depth to find sequent depth:

$$y_2 := \frac{y_1}{2} \cdot \left(-1 + \sqrt{1 + 8 \cdot Fr_1^{\,2}}\right) \qquad y_2 = 7.36ft$$ Sequent depth.

3. Select a desired outlet Froude number (Figure 13), and use this with design discharge and culvert width to find outlet flow depth.

$Fr_3 := 1.677$ Selected outlet Froude number from Figure 13.

$$y_3 := \sqrt[3]{\frac{\left(\frac{Q}{B}\right)^2}{Fr_3^{\,2} \cdot g}} \qquad y_3 = 2.416ft$$ Selected outlet depth.

4. Use selected outlet Froude number and depth to estimated weir height.

$$h_w := \frac{y_3}{-1.23 \cdot Fr_3 + 2.91} \qquad h_w = 2.851\,ft$$ Weir height.

5. Use Equation 9 to determin distance between the drop and the weir:

$$L_d := 6 \cdot (y_c + h_w) \qquad L_d = 37.565\,ft$$ Distance between drop and weir.

6. Use Figure 12 to determine drop height:

$$h_d := \frac{h_w^{\,2}}{y_1 \cdot \left(0.9326 \cdot Fr_1^{\,2} - 6.8218 \cdot Fr_1 + 14.859\right)}$$

$$h_d = 2.133\,ft$$ Predicted Drop Height

7. Solve energy equation (Equation 3) for outlet depth.

$$y_3 := 1.923 \cdot ft$$ Predicted outlet depth, no energy loss.

8. Adjust predicted outlet depth for energy loss using Equation 8:

$$y_{3adjusted} := 1.23 \cdot y_3 + 0.05 \cdot ft$$

$$y_{3adjusted} = 2.415\,ft$$ Adjusted outlet depth.

9. Use adjusted outlet depth, culvert width, and design discharge to determine outlet conditions.

$$V_3 := \frac{Q}{B \cdot y_{3adjusted}} \qquad V_3 = 14.787 \frac{ft}{s}$$ Outlet Velocity

$$Fr_{3a} := \frac{V_3}{\sqrt{g \cdot y_{3adjusted}}} \qquad Fr_{3a} = 1.677$$ Outlet Froude Number

$$E_3 := y_{3adjusted} + \frac{V_3^{\,2}}{2g} \qquad E_3 = 5.813\,ft$$ Outlet Energy

10. Iterate until outlet Froude number in step 9 matches outlet Froude number in step 3.

APPENDIX B

LITERATURE REVIEW

Introduction

A hydraulic jump occurs at the transition from supercritical flow to subcritical flow and is characterized by a steep change in water surface profile. Hydraulic jumps are extremely turbulent which is the cause of most of the energy loss (*1*). A classical hydraulic jump (CHJ) occurs in a horizontal rectangular channel with a constant width and no appurtenances. For a CHJ, the energy loss increases with the Froude number. For example, a jump with a Froude number of 2 dissipates about 7% of the flows energy, but a jump with a Froude number of 9 dissipates 70% of the flows energy (*2*).

For energy dissipation structures, the length of the structure should equal the length of the jump. For a CHJ the length of the jump is a function of the upstream Froude number and the depth of the tailwater. A design requirement for this project is that it dissipates energy without any tailwater. By adding appurtenances, such as sills, drops, and chutes, a hydraulic jump can be forced. A forced jump's location can be controlled and, in general, the length of the jump can be shortened significantly. This saves construction cost by shortening the length of the runout section. Appurtenances can also reduce the amount of tailwater required for a jump to occur.

Jumps over a Weir

Hydraulic Jump Geometry

Forster and Skinde (*3*) researched hydraulic jumps over sharp-crested, non-aerated sills when the downstream flow is supercritical. The results showed that the flow upstream of the sill is independent of tailwater, if the tailwater depth is less than that needed to submerge the sill crest. Mathematically, the flow is independent of tailwater depth if:

$$y_3 < (y_2 - 3/4 * h_w) \quad (1)$$

An equation is derived with L_w/y_2 as a function of Froude number and h_w/y_1. This relationship is plotted as the line labeled "Theoretical" in Figure 6. The experimental data, with the sill located in different locations in relation to the toe of the jump, are lower then the theoretical due to the assumption of uniform flow that was not always the case during the experiments. The authors recommend that the design be based on the curve $L_w/y_2 = 5$ for maximum discharge. If the conditions are above and to the left of the curve, the sill is too high, which pushes the jump upstream and may drown the source. If the flow is below and to the right of the curve, the sill is too low and the jump will not occur. Kandaswamy and Rouse (*4*) found similar results with an aerated weir.

Rand (*5*) established relationships between flow characteristics and basin geometry for a concrete basin with a drop at the beginning to create supercritical approach flow and a broad-crested steel end sill to force the jump. He varied the sill position (L_w), the weir height (h_w), the tailwater depth (y_3), and the Froude number (from 3 to 7). The paper results in a series of tables and graphs relating dimensionless combinations of the above variables. Besides showing that hydraulic jumps will occur

for a wide range of related L_w and h_w values, he also shows that the jump can be triggered and its position controlled independent of tailwater depth. Rand concluded that jumps can occur independent of tailwater depth, but warns that tailwater can act as a cushion against downstream erosion.

Rand (*6*) identified five dimensionless variables. One of these, K, is used to define a forced jump.

$$K = \frac{\left(\frac{L_w}{y_1} - \frac{L_{\min}}{y_1}\right)}{\left(\frac{L_{\max}}{y_1} - \frac{L_{\min}}{y_1}\right)} \qquad (2)$$

Where L_{max} = distance from the toe to the weir when K = 1, L_{min} = shortest possible L_w without submerging the jump. Rand created several plots of the various dimensionless variables in relation to each other.

Hager and Li (7) described the flow pattern over and around a sill. They only examined submerged jumps, because non-submerged jumps have supercritical flow downstream from the weir and therefore they are incomplete energy dissipators. Jumps are classified into different types. Results show velocity vectors for flow at various transverse, vertical, and streamwise cross-sections. Erosion downstream of the sill is also examined for protected and unprotected beds. The effect of the sill is found to increase along with the efficiency as the height of the sill increases and the distance between the toe of the jump and the sill decreases. However, if the sill is too high, or too close to the toe the jump looses quality and energy dissipation is reduced, so a balance must be made.

Erosion Downstream of Weirs

Rand (*8*) expands his work on sills to include the scour downstream from dentated and broad-crested sills. Predicting scour hole length enables us to design the a protective apron that is the correct length.. Rand found the length of the scour hole, not the depth. He used sediment size that was "larger or equal to what is needed in the case of impending motion." Rand found that streamwise length is independent of sill type and equal to:

$$\frac{L_e}{L_t} = 1.15 \tag{3}$$

Where L_t = the length from the toe of the jump to the end of transitional flow and L_e = the distance from the toe to the end of scour hole.

Drag Forces on Weir

The momentum equation can be used to predict the depth of flow downstream of the weir if the drag coefficient on the weir is known.

$$\frac{\gamma \cdot y_1^2}{2} - C_d \frac{\rho \cdot V_1^2 \cdot h_w}{2} - \frac{\gamma \cdot y_3^2}{2} = \frac{\gamma \cdot q}{g}\left[V_3 - V_1\right] \tag{4}$$

There are three different methods outlined in the literature of how to find the drag coefficient. The drag on the sill can be measured indirectly by measuring the depth of flow upstream and downstream of the sill and solving the momentum equation for drag (*9*). The value of the drag coefficient is dependent on the distance of the toe of the jump from the weir. For a weir with no tailwater, the drag coefficient found using the indirect method ranged from 0.46 to 0.62. The drag on the weir can also be calculated by

installing manometer taps along both sides of the weir. These point measurements can then be integrated to find the drag over the entire weir (*10,11*). The drag force over the entire weir can be found using a transducer (*12,13*). The maximum drag coefficient values found using a transducer were 0.3-0.45.

Jumps over Vertical Drops

Vertical drops have been used, in place of a sluice gate, to increase Froude number and create supercritical flow (*14,15*). Due to the energy loss in the impact of the fall, negative drops have also been studied as energy dissipators themselves (*15*). Drops have also been studied as triggers of hydraulic jumps (*16*).

Moore (*15*) examined energy loss over vertical drops in the channel. The paper also evaluates hydraulic jumps that form downstream from a drop when the tailwater depth is properly adjusted. The experimental data were found to closely match the momentum equation given by Bakhmeteff (*17*):

$$\frac{d_3}{d_1} = \frac{1}{2}\left[-1+\sqrt{1+8\left(\frac{d_c}{d_1}\right)^3}\right] \tag{5}$$

The experimental data showed that the length of a jump below a negative drop is 20% longer then the length of a jump below a sluice gate. For unsubmerged jumps, the high velocity jet dissipated by the time the surface profile indicated the end of the jump. For submerged jumps the jet travels farther downstream.

Rand (*14*) found geometric relationships for flow over a vertical drop with subcritical flow upstream and downstream and an aerated nappe over the drop. In this

study, the drop was used to create supercritical flow and subcritical tailwater was used to control jump location.

Moore and Morgan (*16*) examined vertical drops as a trigger for a hydraulic jump. The authors conclude that an abrupt drop stabilized the hydraulic jump for a large range of tailwater depths. This is discussed in the main body of the thesis.

Jumps on Rough Beds

Nebraska Department of Roads has actually proposed three designs. Design III looks at the effect of roughness of the channel bed and walls on inducing a jump. This research is being conducted by the Federal Highway Administration in Washington D.C.

Rajaratnam (*18*) examined the effect channel bed roughness had on hydraulic jump characteristics. Five types of roughness were studied: four beds had various types of wire screens and one bed was lined with gravel. It was found that for relative roughness values greater then 0.05, the length of the roller and the length of the jump were approximately one half that of an equivalent jump on a smooth bed. The tailwater depth required for the jump to occur was a function of Froude number and relative roughness, and was significantly reduced with rougher beds. The loss of energy occurring with a rough bed jump was up to 1.5 times the loss of energy occurring in a smooth bed jump.

Hughes and Flack (*19*) tested the effect of bed roughness on hydraulic jump characteristics. Five beds were tested: three beds with varying sizes of gravel as the roughness element and two beds with square bars in the bed running transverse to the flow. They varied the relative roughness from 0.0-0.9 and the Froude number from 3-10.

It was found that bed roughness reduces the sequent depth and the length of the jump, and that these reductions were a function of Froude number and bed roughness.

Ead et.al. (*20*) assessed velocity fields in circular corrugated pipes with varying flow (30-200 L/s) and slope (0.55, 1.14, and 2.55%). The main concern in this paper was with velocity profiles and fish passage. The velocity near the boundaries of the pipe was relatively slow, so fish passage there may be possible. Flow in the center of the pipe was rough and turbulent.

Ead and Rajaratnam (*21*) ran a series of experiments in a rectangular flume with a corrugated aluminum bed laid so that the crest is the same height as upstream bed. It was found that tailwater depth required to form a jump is smaller if the bed is rough:

$$\frac{d_2}{d_1} = F_1 \text{ and } \frac{d_{2^*}}{d_1} = \sqrt{2}F_1 \tag{6}$$

The above relationships are true for crests heights equal to upstream bed, not for crest heights protruding into flow. It was also found that the length of jumps are shorter on rough beds.

$$L_R = \frac{2}{3}L_j \tag{7}$$

Where L_R is the length scale for rough beds and L_j is the length scale for smooth beds.

Jumps at Expansions

Rajaratnam and Subramany (22) examined hydraulic jumps that occur at abrupt channel expansions. The jumps were classified into two categories, R- and S-jumps. With low tailwater depths, water flows into an expansion and expands freely until it

meets the new width. As the tailwater depth increases, a jump forms with a face not perpindicular to the flow, and with a further increase in tailwater depth, a jump forms normal to the flow. This is an R-jump; any further increase in tailwater depth causes the jump to collapse and the tailwater spills on to the upstream supercritical flow. If the tailwater depth is further increased the jump will eventually move to the outlet and resemble a stable submerged jump. The S-jump is the minimum tailwater depth at which this stable flow occurs. The flow between the S- and R-jumps is highly oscillatory and unstable.

Jumps in Sloping Channels

Smith and Chen (*23*) examined jumps in steeply sloping (up to 30 degrees) square conduits. The authors attempted to derive an equation for the dimensionless jump height, but it cannot be solved because there are too many variables. The equation:

$\frac{H_j}{D} = f\left(Fr_1, \frac{y_1}{D}, \theta\right)$, where H_j is vertical jump height, can only be found experimentally.

Tests were run for various combinations of y_1/D and slope, H_j/D and Fr were then measured for each run. D is the depth of the conduit. The paper also discussed the "blowback" phenomenon. This occurs when air bubbles are entrained in the flow and buoyancy causes them to rise to the top of the pipe where they form long flat air pockets. In sloped pipes, buoyancy acts to push the pocket upstream and drag forces act to move the pocket downstream. When the air pocket becomes large enough, the buoyancy forces are dominant and the air pocket moves rapidly upstream. This is blowback, and it is accompanied by surges in the jump position and downstream pressure. The authors also

discussed the violent horizontal surging and pressure fluctuations that occur when an incomplete jump takes place. The frequency and magnitude of horizontal surging is increased because the roof suppresses vertical surging. The walls of the culvert experience significant loads and vibrations due to these surges.

Ohtsu and Yasuda (*24*) examined the length of and velocity change in B- and D-jumps, with slopes varying from 0 to 60 degrees and Froude numbers ranging from 4 to 14. In D-jumps with slopes from 23-60 degrees, the high velocity is maintained and the flow simulates a wall jet. This also occurs in steep B-jumps, except the jet accelerates at the junction. For B- and D-jumps with slopes less then 19 degrees a surface roller may form and the velocity decay is greater.

Husain et. al. (*25*) discuss the difficulty in measuring K and L consistently (also found by Gunal (*26*)). There are several different methods of measurement; they use USBR. 440 different runs were completed on sloped channels with positive and negative slopes. Linear regression was than completed to find coefficients for the following five equations: $K = f(\theta, F_1, S)$, $d_2/d1 = f_2(K, \theta, F_1, S)$, $L/d1 = f_3(K, \theta, F_1, S)$, $L/d_2 = f_4(K, \theta, F_1, S)$, $L/(d_2-d_1) = f_5(K, \theta, F_1, S)$, where θ = slope, and S is the ratio of step to depth. They concluded that negative step is regarded as a better energy dissipater over the positive step in designing the stilling basins on sloping floor for both stability and compaction of hydraulic jump.

Gunal and Narayanan (*26*) discussed the theory that hydraulic jump predictors assume hydrostatic pressure in the jump, like a wall jet. The authors contend that this is not a good assumption in jumps because of the vertical velocity in the jumps cannot be

neglected. By assuming hydrostatic pressure one can overestimate the water surface profile. This paper discussed incorporating an empirical pressure correction to account for this. The authors also concluded that visual estimates of roller length can be 1.6 times the length obtained from mean velocity profiles.

Stilling Basins

The United States Bureau of Reclamation has designed several stilling basins for use at the base of dam spill basin (*2*). HEC-14 (*27*), entitled Hydraulic Design of Energy Dissipators for Culverts and Channels, is published by the Federal Highway Administration. This document includes design criteria for many of the USBR Basins as well as some other commonly used energy dissipators like the Contra Costa basin and the St. Anthony Falls basin.

Name of Stilling Basin	Description	Applicability
USBR I	Horizontal Apron	Follows rules of CHJ
USBR II	Chute blocks at the base of slope and dentated end sill.	o 4<Fr<14 o Q<500 cfs/unit width o Requires tailwater equal to sequent depth o Jump length shorter than USBR I
USBR III	Chut blocks at the base of slope, one row of baffle blocks along apron, end sill.	o 4<Fr<17 o Q<200 cfs/unit width o V<50 ft/s o Requires tailwater equal to sequent depth o Jump length shorter than USBR I and USBR II
USBR IV	A drop stucture with a horizontal slotted grate.	o 2.5<Fr<4.5 o Several alternate design all intended to increase Fr so a jump is more stable.
USBR V	Sloping Apron	o Discussed in previously in literature review.
USBR VII	Culvert opens into rectangular spilling basin with a wall across one end that flow must go over or under.	o Does not trigger a hydraulic jump, but for a given Fr dissipates more energy then a jump. o Q<339 cfs o V<30 ft/s o Requires no tailwater.
USBR VII-X	Include flip buckets and baffles on sloped aprons.	o Not applicable to this design project.
St. Anthony Falls (SAF)	Chute blocks, baffles, and end sill	o 1.7<Fr<17
Contra Costa	Culvert opens into trapezoidal stilling basin with two rows of baffles and an end sill.	o 1<Fr<10 o No Tailwater Required.
Hook Type or Aero-type	Expanding trapezoidal basin with three hooks staggered across and an end sill	o 1.8<Fr<3.0 o Developed for low tailwater situations

Methods of Measuring Aerated Flow

The literature was consulted for a standard on how to measure the turbulent two-phase flow downstream of the weir. Below is a list compiled from the literature of methods that have been used.

1. Use an electric probe to measure mean air concentration. (*28*) Lamb and Killen 1950)
2. Use a point gage to measure depth. Various statistical methods used to find actual depth. (*29*) US Bureau of Rec.)
3. Prandtl tube w/ flushing manometer. (Rajaratnam)
4. High speed cameras or video. (Rajaratnam, and others)
5. Use empirical equations to find mean air concentration.
6. Salt velocity method. (Thomas, C.W.)
7. Stagnation tube. (Sorensen)
8. Scales. (Sorensen)
9. Platinum Probe.
10. Fiber optics. (Hager, Rajaratnam)
11. ADV. (Liu,Zhu, Rajartnam; and Matos et. al.)
12. Current Meter. (Crowe, Marshal)

LITERATURE REVIEW REFERENCES

1. Chaudhry, M. H. *Open-Channel Flow*. Prentice-Hall, Englewood Cliffs, NJ, 1993.
2. Peterka, A. J. *Hydraulic Design of Stilling Basins and Energy Dissipators* A Water Resources Technical Publication, Engineering Monograph No. 25. U.S. Department of the Interior and U.S. Bureau of Reclamation, 1964.
3. Forster, J.W. and R.A. Skrinde. Control of Hydraulic Jump by sills. *Tran. Am. Soc. Civil. Eng.,* Vol.115, 1950, pp. 973-987.
4. Kandaswamy, P.K. and H. Rouse. Characteristics of flow over terminal weirs and sills. *Proc. ASCE J. Hydr. Div.* Vol. 83, No. HY4, 1957, pp.1345.
5. Rand, Walter. An approach to generalized design of stilling basins. *The New York Academy of Sciences*. 1957, pp. 173-191.
6. Rand, Walter. Flow over a vertical sill in an open channel. *Proc. ASCE J. Hydr. Div.* Vol. 91, No. HY4, 1965, pp. 4408.
7. Hager, W.H. and D. Li. Sill-controlled energy dissipator. *Journal of Hydraulic Research*. Vol. 30, No. 2, 1992, pp.165-181.
8. Rand, Walter. Sill-controlled flow transitions and extent of erosion. *Proc. ASCE J. Hydr. Div*. Vol. 96, No. HY4, 1970, pp. 7212.
9. Rajaratnam, N. The Forced Hydraulic Jump *Water Power* 1964 pp. 14-19 and 61-65.
10. Rajaratnam, N. and V. Murahari. A contribution to forced hydraulic jumps. *Journal of Hydraulic Research*. Vol. 9, No. 2, 1971, pp. 217-240.

11. Ohtsu, I., Yasuda, Y., Yamanaka, Y. Drag on vertical sill of forced jump. *J. of Hyd. Res.* Vol. 29, No. 1, 1991, pp. 29-47.

12. Narayanan, R. and L.S. Schizas. Force on sill of forced jump. *Proc. ASCE J. Hydr. Div*. Vol. 106, No. HW4, 1980, pp. 15368.

13. Narayanan, R. and L.S. Schizas. Force on sill of forced jump. *Proc. ASCE J. Hydr. Div*. Vol. 106, No. HW7, 1980, pp. 15552.

14. Rand, Walter. Flow Geometry at Straight Drop Spillways. *Proc. Am. Soc. Civil Eng*. Vol. 81, 1955, pp. 791.

15. Moore, W.L. Energy loss at the base of free overfall. *Tran. Am. Soc. Civil. Eng.* Vol. 108, 1943, pp. 1343-1360.

16. Moore, W.L. and C.W. Morgan. The hydraulic jump at an abrupt drop. *Proc. ASCE J. Hydr. Div.* Vol. 83, No. HY6, 1957, pp. 1449.

17. Bakhmeteff, B.A. *Hydraulics of Open Channels*. McGraw-Hill Book Company, Inc., New York and London, 1932.

18. Rajaratnam, N. Hydraulic Jumps in Rough Beds. *Transactions of the Engineering Institute of Canada.* Vol.11, No. A-2, 1968, pp. I-VIII.

19. Hughes, W.C. and J.E. Flack. Hydraulic Jump Properties Over a Rough Bed *Journal of Hydraulic Engineering*. Vol.110, No. 12, 1984, pp. 1755-1771.

20. Ead, S.A., N. Rajaratnam, and C. Katopodis. Turbulent Open-Channel Flow in Circular Corrugated Culverts. *Journal of Hydraulic Engineering*. Vol. 126, No. 10, 2000, pp. 750-757.

21. Ead, S.A., and N. Rajaratnam. Hydraulic Jumps on Corrugated Beds. *Journal of Hydraulic Engineering*. Vol.128, No. 7, 2002, pp. 656-663.

22. Rajaratnam, N. and Subramany, K. (1968) "Hydraulic jumps below abrupt symmetrical expansions" Proc. ASCE J. Hydr. Div. 94(HY2) paper 5860.

23. Smith, C.D. and Wentao Chen. (1989) *The Hydraulic jump in a steeply sloping square conduit.* Ournal of Hydraulic Research, 27(3): 385-399.

24. Ohtsu, Iwao and Youichi Yasuda. (1991) *Hydraulic Jump in Sloping Channels.* Journal of Hydraulic Engineering. 117(7): 905-921.

25. Husain, D., Negm, Abdel-Azim M., and A.A. Alhamid. (1994) *Length and depth of hydraulic jump in sloping channels.* Journal of Hydraulic Research. 32(6): 899-910.

26. Gunal, Mustafa and Rangaswami Narayanan. (1996) *Hydraulic Jump in Sloping Channels.* Journal of Hydraulic Engineering. 122(8): 436-442.

27. HEC-14 (1983) "Hydraulic Design of energy dissipators for culverts and channels" Federal Highway Administraion, Washington, D.C. Hydraulics Branch.

APPENDIX C

DATA AND DATA COLLECTION

Order of Operations

1. Close all of the drains, there are two on the head tank.

2. Inspect the head tank, channel, and tailwater tank for foreign object and remove them if found.

3. Adjust valves to the desired settings.

4. Check the level of water in the sump, it should be around the first rung of the ladder. Fill or drain water as needed to adjust water level.

5. Make sure the red valve that controls the lubrication of the pumps is open (horizontal).

6. Turn on the pump.

7. Allow the flow to equilibrate. To check this measure the water level above and below the weir, then check again in 5 minutes. If nothing has changed then you are equilibrated, if different repeat.

8. Take pictures with the camera of the culvert entrance, Reach 1, Drop and weir, reach 3, and anything else that is of interest.

9. Use point gages to measure depths in the channel.

10. Note if a stagnation point exists, if so measure the distance from the toe to the stagnation point. Also measure from the toe to the sill.

11. Observe the flow and make qualitative observations.

12. Measure the water level above and below the weir in the headtank.

13. Turn off pumps.

14. If you are doing more runs, start over at step one.

15. If you are done:
    a. Turn the pump lubrication valve to closed (vertical).
    b. Open the drains on the head tank.
    c. Empty the drip collecting buckets.
    d. Sweep up any major puddles on the floor.
    e. Turn off the lights.

NOTATION

Run = The run number.

L_d = The distance between the drop and the weir.

h_d = The drop height.

h_w = The weir height

y_1 high = The point gage reading for the highest water surface in ununiform flow.

y_1 low = The point gage reading for the loweste water surface in ununiform flow.

y_1 ref = The point gage reading for the channel bed

y_2 high = The point gage reading for the highest water surface in ununiform flow.

y_2 low = The point gage reading for the loweste water surface in ununiform flow.

y_2 ref = The point gage reading for the channel bed

y_3 high = The point gage reading for the highest water surface in ununiform flow.

y_3 low = The point gage reading for the loweste water surface in ununiform flow.

y_3 ref = The point gage reading for the channel bed

H1 = The water surface reading upstream from the weir.

H1 ref = The crest of the V-notch weir.

H2 = The water surface reading downstream from the weir

H2 ref = The crest of the V-notch weir.

Run	Lw	hd	hw	y1 high	y1 low	y1 ref	y2 high	y2 low	y2 ref	y3 high	y3 low	y3 ref	H1	H1 ref	H2	H2 ref
1	3	1	0.5	1.053	1.053	1.017	0.629	0.629	0.018	0.623	0.623	0.566	1.013	0.578	0	0.693
2	3	1	0.5	1.125	1.125	1.016	1.181	1.021	0.019	0.822	0.721	0.566	1.515	0.578	0.76	0.693
3	3	1	0.5	1.206	1.206	1.017	0.838	0.838	0.016	1.049	0.773	0.567	1.927	0.578	1.18	0.693
4	3	1	0.5	1.305	1.305	0.997	0.914	0.914	0.018	0.994	0.994	0.567	2.235	0.578	1.53	0.693
5	3	1	1	1.043	1.043	1.01	1.124	1.061	0.007	0.623	0.623	0.566	1.017	0.578	0	0.693
6	3	1	1	1.198	1.198	1.009	1.415	1.323	0.008	0.939	0.939	0.566	1.91	0.578	1.16	0.693
7	3	1	1	1.123	1.123	1.01	1.303	1.177	0.007	0.849	0.673	0.566	1.501	0.578	0.76	0.693
8	3	1	1	1.29	1.29	1.01	1.588	1.588	0.007	1.079	1.079	0.566	2.242	0.578	1.54	0.693
9	3	1	1.5	1.313	1.313	1.01	2.197	2.197	0.007	1.063	1.063	0.566	2.242	0.578	1.54	0.693
10	3	1	1.5	2.268	2.077	1.008	2.023	2.151	0.006	0.794	0.977	0.565	1.927	0.578	1.18	0.693
11	3	1	1.5	1.991	1.892	1.013	1.872	1.872	0.01	0.812	0.711	0.569	1.538	0.578	0.77	0.693
12	3	1	1.5	1.619	1.619	1.009	1.619	1.619	0.01	0.603	0.603	0.569	1.022	0.578	0	0.693
13	7	1	1.5	1.599	1.599	1.008	2.159	2.159	0.566	0.664	0.664	0.569	1.024	0.578	0	0.693
14	7	1	1.5	1.173	1.096	0.193	1.925	1.879	0.002	0.163	0.163	0.005	1.541	0.578	0.78	0.693
15	7	1	1.5	1.329	0.998	0.193	2.015	2.167	0.002	0.569	0.205	0.005	1.934	0.578	1.19	0.693
16	7	1	1.5	Manometer Data									2.249	0.578	1.54	0.693
17	7	1	1	Manometer Data									1.893	0.578	1.14	0.693
18	7	1	1	Manometer Data									1.473	0.578	0.71	0.693
19	7	1	1	Manometer Data									2.256	0.578	1.55	0.693
20	7	1	1	Manometer Data									1.019	0.578	0	0.693
21	7	1	0.5	Manometer Data									1.014	0.578	0	0.693
22	7	1	0.5	Manometer Data									1.488	0.578	0.71	0.693
23	7	1	0.5	Manometer Data									1.896	0.578	1.14	0.693
24	7	1	0.5	Manometer Data									2.235	0.578	1.55	0.693
25	5	1	1.5	0.518	0.501	0.17	2.131	1.82	-0.19	0.746	0.292	0.008	2.235	0.578	1.54	0.693
26	5	1	1.5	1.027	1.1	0.191	1.812	1.877	1.546	0.142	0.273	0.038	1.472	0.578	0	0.693
27	5	1	1.5	0.381	0.381	0.193	2.158	1.979	1.546	0.198	0.537	0.041	1.877	0.578	1.12	0.693
28	5	1	1.5	0.401	0.401	0.191	1.997	2.285	1.547	0.203	0.573	0.041	1.817	0.578	1.21	0.693
29	5	1	1	0.391	0.391	0.191	1.444	1.583	1.051	0.205	0.541	0.04	1.932	0.578	1.21	0.693
30	5	1	1	0.394	0.394	0.193	1.282	1.474	1.05	0.211	0.481	0.042	1.889	0.578	1.15	0.693
31	5	1	1	0.291	0.291	0.193	1.304	1.423	1.05	0.211	0.342	0.044	1.477	0.578	0.72	0.693
32	5	1	1	0.487	0.487	0.191	1.423	1.665	1.05	0.33	0.585	0.042	2.221	0.578	1.55	0.693
33	5	1	0.5	0.486	0.486	0.191	1.53	1.839	0.042	0.462	0.773	0.042	2.226	0.578	1.55	0.693
34	5	1	0.5	0.404	0.404	0.19	1.338	1.579	0.037	0.334	0.529	0.041	1.97	0.578	1.25	0.693
35	5	1	0.5	0.289	0.289	0.191	0.926	1.008	0.041	0.3	0.217	0.041	1.511	0.578	0	0.693
36	7	0.7	0.5	0.291	0.291	0.191	1.179	1.179	0.335	0.485	0.578	0.35	1.507	0.578	0.75	0.693
37	7	0.7	0.5	0.385	0.385	0.19	1.485	1.665	0.335	0.599	0.872	0.351	1.91	0.578	1.18	0.693
38	7	0.7	0.5	0.465	0.465	0.19	1.742	1.964	0.335	0.872	0.872	0.351	2.163	0.578	1.48	0.693
39	7	0.7	0.5	0.492	0.492	0.19	1.794	2.147	0.335	1.146	0.863	0.35	2.252	0.578	1.55	0.693
40	7	0.7	1	0.487	0.487	0.181	2.121	2.71	0.332	0.832	0.832	0.353	2.23	0.578	1.52	0.693

Run	Lw	hd	hw	y1 high	y1 low	y1 ref	y2 high	y2 low		y3 high	y3 low	y3 ref	H1	H1 ref	H2	H2 ref
41	7	0.7	1	0.287	0.287	0.187	1.607	1.719	0.332	0.451	0.614	0.353	1.515	0.578	0.73	0.693
42	7	0.7	1	0.374	0.374	0.181	1.947	2.143	0.332	0.596	0.949	0.352	1.907	0.578	1.18	0.693
43	7	0.7	1	0.449	0.449	0.181	2.132	2.33	0.332	0.728	0.728	0.352	2.104	0.578	1.43	0.693
44	7	0.7	1.5	0.354	0.354	0	2.71	2.71	0	0.732	0.732	0.348	2.228	0.578	1.52	0.693
45	7	0.7	1.5	0.313	0.313	0	2.398	2.71	0	0.653	0.873	0.352	2.132	0.578	1.43	0.693
46	7	0.7	1.5	0.219	0.219	0	1.686	2.71	1.042	0.531	0.939	0.351	1.906	0.578	1.157	0.693
47	7	0.7	1.5	0.083	0.125	0	1.455	2.71	1.042	0.158	0.423	-0.01	1.528	0.578	0.74	0.693
48	5	0.7	0.5	0.273	0.273	0.176	0.837	0.916	-0.02	0.171	0.282	-0.02	1.531	0.578	0.74	0.693
49	5	0.7	0.5	0.37	0.37	0.174	1.407	1.159	-0.02	0.298	0.498	0.001	1.915	0.578	1.17	0.693
50	5	0.7	0.5	0.426	0.426	0.171	1.322	1.568	-0.02	0.414	0.56	0.002	2.104	0.578	1.41	0.693
51	5	0.7	0.5	0.482	0.482	0.171	1.422	1.57	-0.02	0.442	0.759	0.001	2.243	0.578	1.57	0.693
52	5	0.7	1	0.482	0.482	0.171	1.528	1.769	-0.02	0.035	0.927	0.005	2.233	0.578	1.54	0.693
53	5	0.7	1	0.424	0.424	0.174	1.263	1.763	-0.2	0.293	0.687	0.005	2.124	0.578	1.43	0.693
54	5	0.7	1	0.369	0.369	0.174	1.426	1.849	-0.02	0.191	0.576	0.007	1.931	0.578	1.18	0.693
55	5	0.7	1	0.292	0.292	0.178	1.359	1.445	-0.01	0.164	0.226	0.007	1.553	0.578	0.76	0.693
56	5	0.7	1.5	0.292	0.292	0	1.914	1.753	-0.53	0.284	0.571	0.003	2.128	0.578	1.425	0.693
57	5	0.7	1.5	0.229	0.229	0	1.642	1.777	-0.532	0.264	0.430	0.002	1.946	0.578	1.209	0.693
58	5	0.7	1.5	0.375	0.375	0	2.044	1.87	-0.53	0.333	0.573	0.003	2.247	0.578	1.54	0.693
59	3	0.7	0.5	0.471	0.471	0.171	0.913	1.022	-0.01	0.437	0.679	0.006	2.237	0.578	1.5	0.693
60	3	0.7	0.5	0.292	0.292	0.179	0.951	1.104	-0.01	0.166	0.23	0.009	1.527	0.578	0.76	0.693
61	3	0.7	0.5	0.37	0.37	0.177	0.810	0.81	-0.01	0.566	0.303	0.009	1.919	0.578	1.17	0.693
62	3	0.7	0.5	0.426	0.426	0.173	0.839	0.94	-0.01	0.387	0.646	0.006	2.103	0.578	1.38	0.693
63	3	0.7	1	0.423	0.423	0.173	1.750	1.488	-0.01	0.322	0.766	0.006	2.103	0.578	1.41	0.693
64	3	0.7	1	0.396	0.396	0.177	1.838	1.327	-0.01	0.29	0.571	0.007	1.935	0.578	1.2	0.693
65	3	0.7	1	0.306	0.306	0.175	1.114	1.335	-0.01	0.283	0.155	0.007	1.544	0.578	0.73	0.693
66	3	0.7	1	0.478	0.478	0.175	1.500	1.745	-0	0.368	0.733	0.006	2.252	0.578	1.55	0.693
67	3	0.7	1.5	0.4	0.4	0	1.717	2.71	-0.52	0.388	0.689	0.007	2.251	0.578	1.55	0.693
68	3	0.7	1.5	0.35	0.35	0	1.647	1.814	-0.52	0.366	0.597	0.007	2.153	0.578	1.44	0.693
69	3	0.7	1.5	0.25	0.25	0	1.555	1.658	-0.52	0.251	0.439	0.008	1.928	0.578	1.18	0.693
70	3	0.7	1.5	0.145	0.145	0	1.322	1.363	-0.52	0.15	0.224	0.008	1.54	0.578	0.77	0.693
71	3	0.3	0.5	0.288	0.288	0.171	1.335	1.815	0.375	0.517	0.604	0.366	1.545	0.578	0.77	0.693
72	3	0.3	0.5	0.366	0.366	0.171	1.589	1.778	0.373	0.679	0.811	0.368	1.942	0.588	1.24	0.72
73	3	0.3	0.5	0.416	0.416	0.171	1.704	1.948	0.373	0.746	0.911	0.366	2.11	0.588	1.45	0.72
74	3	0.3	0.5	0.462	0.462	0.171	1.783	2.057	0.379	0.773	0.978	0.366	2.228	0.588	1.57	0.72
75	3	0.3	1	1.311	1.454	0.938	2.263	2.319	0.375	1.011	0.744	0.374	2.229	0.588	1.55	0.72
76	3	0.3	1	1.286	1.407	0.938	2.189	2.319	0.375	0.73	0.956	0.374	2.129	0.588	1.45	0.72
77	3	0.3	1	1.196	1.308	0.938	2.007	2.154	0.375	0.634	0.804	0.373	1.923	0.588	1.23	0.72
78	3	0.3	1	1.064	1.064	0.938	1.782	1.782	0.373	0.51	0.572	0.373	1.547	0.588	0.81	0.72
79	5	0.3	0.5	0.274	0.274	0.176	1.245	0.13	0.36	0.547	0.615	0.365	1.543	0.588	0.81	0.72
80	5	0.3	0.5	0.35	0.35	0.171	1.577	1.72	0.363	0.678	0.9	0.368	1.927	0.588	1.23	0.72
81	5	0.3	0.5	0.415	0.415	0.171	1.729	2.005	0.363	0.738	1.086	0.367	2.17	0.588	1.55	0.72

Run	Lw	hd	hw	y1 high	y1 low	y1 ref	y2 high	y2 low	y2 ref	y3 high	y3 low	y3 ref	H1	H1 ref	H2	H2 ref
82	5	0.3	0.5	0.444	0.444	0.171	1.795	2.111	0.363	0.883	1.101	0.368	2.259	0.588	1.58	0.72
83	5	0.3	1	0.444	0.444	0.171				1.027	0.748	0.37	2.248	0.588	1.6	0.72
84	5	0.3	1	1.187	1.187	0.936	2.013	2.098	0.363	0.634	0.788	0.369	1.927	0.588	1.22	0.72
85	5	0.3	1	1.061	1.049	0.938	1.724	1.793	0.364	0.525	0.611	0.368	1.544	0.588	0.81	0.72
86	5	0.3	1	1.357	1.264	0.938	2.150	2.319	0.364	0.71	0.986	0.369	2.165	0.588	1.52	0.72
87	7	0.3	0.5				1.660	2.064	0.364	0.785	1.063	0.369	2.165	0.588	1.51	0.72
88	7	0.3	0.5				1.521	1.714	0.363	0.625	0.939	0.366	1.941	0.588	1.24	0.72
89	7	0.3	0.5				1.229	1.271	0.363	0.517	0.627	0.369	1.55	0.588	0.81	0.72
90	7	0.3	0.5				1.740	2.075	0.364	0.813	1.15	0.369	2.235	0.588	1.57	0.72
91	3	0	0.5				2.209	2.126	0.688	1.364	1.162	0.681	2.235	0.588	1.6	0.72
93	3	0	0.5				2.003	1.867	0.688	1.079	1.029	0.684	1.918	0.588	1.21	0.72
94	3	0	0.5				2.196	1.989	0.688	1.22	1.087	0.686	2.11	0.588	1.45	0.72
95	3	0	0.5				1.596	1.658	0.687	0.867	0.907	0.686	1.552	0.588	0.8	0.72
96	5	0	0.5				1.598	1.632	0.685	0.962	0.885	0.689	1.552	0.588	0.81	0.72
97	5	0	0.5				1.886	1.992	0.682	1.04	1.133	0.689	1.931	0.588	1.24	0.72
98	5	0	0.5				1.856	2.235	0.682	1.132	1.306	0.689	1.468	0.588	2.12	0.72
99	5	0	0.5				2.250	1.89	0.682	1.095	1.447	0.689	2.232	0.588	1.6	0.72
100	3	0	0.3				1.342	1.39	0.694	1.149	1.392	0.691	2.217	0.588	1.57	0.72
101	3	0	0.3				1.368	1.458	0.696	1.043	1.295	0.691	2.133	0.588	1.48	0.72
102	3	0	0.3				1.402	1.467	0.694	1.283	1.074	0.693	1.932	0.588	1.21	0.72
103	3	0	0.3				1.399	1.292	0.687	0.875	0.968	0.683	1.55	0.588	0.81	0.72
104		0	0										1.551	0.588	0.81	0.72
105		0	0										1.947	0.588	1.23	0.72
106		0	0										2.121	0.588	1.46	0.72
107		0	0										2.245	0.588	1.6	0.72
108	5	0	1										1.556	0.588	0.82	0.72
109	5	0	1										1.943	0.588	1.25	0.72
110	5	0	1										2.145	0.588	1.49	0.72
111	5	0	1										2.245	0.588	1.58	0.72
112	5	0	0.4										2.243	0.588	1.6	0.72
113	5	0	0.4										2.128	0.588	1.46	0.72
114	5	0	0.4										1.954	0.588	1.25	0.72
115	5	0	0.4										1.574	0.588	0.84	0.72
116	5	0.3	0.5										1.542	0.588	0.84	0.72
117	5	0.3	0.5										1.943	0.588	1.24	0.72
118	5	0.3	0.5										2.114	0.588	1.45	0.72
119	5	0.3	0.5										2.233	0.588	1.6	0.72
120	3	0.3	1										2.232	0.588	1.56	0.72
121	3	0.3	1										2.182	0.588	1.52	0.72
122	3	0.3	1										1.963	0.588	1.27	0.72
123	3	0.3	1										1.594	0.588	0.85	0.72

Run	Lw	hd	hw	y1 high	y1 low	y1 ref	y2 high	y2 low	y2 ref	y3 high	y3 low	y3 ref	H1	H1 ref	H2	H2 ref
124	3	0.3	1										1.727	0.588	1	0.72
125	5	0.7	1										1.549	0.588	0.82	0.72
126	5	0.7	1										1.734	0.588	1	0.72
127	5	0.7	1										1.939	0.588	1.25	0.72
128	5	0.7	1										2.131	0.588	1.46	0.72
129	5	0.7	1										2.244	0.588	1.58	0.72
130	5	0.7	0.5										2.243	0.588	1.6	0.72
131	5	0.7	0.5										2.176	0.588	1.52	0.72
132	5	0.7	0.5										1.927	0.588	1.22	0.72
133	5	0.7	0.5										1.716	0.588	0.98	0.72
134	5	0.7	0.5										1.543	0.588	0.82	0.72
135	5	0.7	0.5										1.544	0.588	0.82	0.72
136	5	0.7	0.5										1.484	0.588	0.76	0.72
137	5	0.7	0.5										1.912	0.588	1.22	0.72
138	5	0.7	0.5										2.114	0.588	1.45	0.72
139	5	0.7	0.5										2.211	0.588	1.61	0.72
140	3	0.7	0.5										2.208	0.576	1.56	0.73
141	3	0.7	0.5										2.104	0.576	1.47	0.73
142	3	0.7	0.5										1.911	0.576	1.23	0.73
143	3	0.7	0.5										1.529	0.576	0.81	0.73
144	5	0.7	0.4										1.534	0.576	0.82	0.73
145	5	0.7	0.4										1.926	0.576	1.25	0.73
146	5	0.7	0.4										2.15	0.576	1.52	0.73
147	5	0.7	0.4										2.215	0.576	1.61	0.73
148	5	0.7	0.8										1.434	0.576	0.73	0.73
149	5	0.7	0.8										1.877	0.576	1.17	0.73
150	5	0.7	0.8										2.077	0.576	1.44	0.73
151	5	0.7	0.8										2.206	0.576	1.55	0.73
152	5	0.7	0.8										2.2	0.576	1.58	0.73
153	5	0.7	0.8										2.127	0.576	1.49	0.73
154	5	0.7	0.8										1.814	0.576	1.11	0.73
155	5	0.7	0.8										1.404	0.576	0.68	0.73
156	5	1	0.8										2.094	0.576	1.45	0.73
157	5	1	0.8										1.851	0.576	1.14	0.73
158	5	1	0.8										1.422	0.576	0.73	0.73
159	5	1	0.8										2.189	0.576	1.55	0.73
160	5	1	0.8										2.185	0.576	1.55	0.73
161	5	1	0.8										2.106	0.576	1.45	0.73
162	5	1	0.8										1.854	0.576	1.15	0.73
163	5	1	0.8										1.447	0.576	0.73	0.73

Jump Type	Run	Lw	hd	hw	Q	Current Meter V3
A Jump	79	5	0.319	0.5	2.21	7.39
B-Jump	79	5	0.319	0.5	2.21	7.39
B-Min	36	7	0.71	0.5	2.06	7.52
B-Min	48	5	0.71	0.5	2.20	6.54
B-Min	60	3	0.71	0.5	2.18	7.85
A Jump	41	7	0.71	1	2.11	7.11
A Jump	55	5	0.71	1	2.33	8.89
A-Sloped Jump	85	5	0.319	1	2.22	9.17
A-Sloped Jump	78	3	0.319	1	2.23	8.83
A-Sloped Jump	47	7	0.71	1.5	2.18	8.09
A-Sloped Jump	70	3	0.71	1.5	2.25	9.78

Jump Type	Run	Lw	hd	hw	Q	Current Meter V3
A Jump	72	3	0.319	0.5	5.10	8.23
B-Jumps	80	5	0.319	0.5	4.97	7.58
B-Min	37	7	0.71	0.5	4.92	6.54
B-Min	49	5	0.71	0.5	4.98	8.29
Wave Jump	42	7	0.71	1	4.89	8.17
Wave Jump	54	5	0.71	1	5.12	8.22
A-Sloped Jump	84	5	0.319	1	4.98	10.49
A-Sloped Jump	77	3	0.319	1	4.93	10.49
A-Sloped Jump	46	7	0.71	1.5	4.90	8.87
A-Sloped Jump	57	5	0.71	1.5	5.25	12.09
A-Sloped Jump	69	3	0.71	1.5	5.09	10.88

Jump Type	Run	Lw	hd	hw	Q	Current Meter V3
A Jump	73	3	0.319	0.5	6.63	7.26
B-Jumps	81	5	0.319	0.5	7.17	7.09
B-Min	38	7	0.71	0.5	7.30	3.84
B-Min	50	5	0.71	0.5	6.70	6.48
Wave Jump	43	7	0.71	1	6.68	5.05
Wave Jump	53	5	0.71	1	6.90	9.78
A-Sloped Jump	86	5	0.319	1	7.18	10.62
A-Sloped Jump	76	3	0.319	1	6.86	9.34
A-Sloped Jump	45	7	0.71	1.5	7.01	9.09
A-Sloped Jump	56	5	0.71	1.5	6.96	12.33
A-Sloped Jump	68	3	0.71	1.5	7.24	10.21

Jump Type	Run	Lw	hd	hw	Q	Current Meter V3
A Jump	74	3	0.319	0.5	7.88	7.65
B-Jumps	82	5	0.319	0.5	8.25	7.33
B-Min	33	5	1	0.5	7.97	7.35
B-Min	39	7	0.71	0.5	8.32	3.65
B-Min	51	5	0.71	0.5	8.15	7.26
Wave Jump	40	7	0.71	1	8.08	5.04
Wave Jump	52	5	0.71	1	8.08	10.01
A-Sloped Jump	83	5	0.319	1	8.07	7.71
A-Sloped Jump	75	3	0.319	1	7.93	9.07
A-Sloped Jump	58	5	0.71	1.5	8.27	12.88
A-Sloped Jump	67	3	0.71	1.5	8.30	10.24
A-Sloped Jump	44	7	0.71	1.5	8.05	5.76

Run = The run number

x = The transverse distance across the channel

Q = The discharge (cfs)

ref = The point gage channel bed measurement

low = The point gage reading for the loweste water surface in ununiform flow.

high = The point gage reading for the highest water surface in ununiform flow.

y = The flow depth

V = The velocity

Froude = The Froude Number

sloped = Measurements taken in the sloped section

drop= Measurements taken at the drop.

Run	x	Q	ref	low	high	y	V	Fr		
86		7.2	0.940	1.279	1.346	0.373	9.6	2.8	0.37	
86		7.2	0.936	1.248	1.401	0.389	9.2	2.6	9.63	
86		7.2	0.937	1.266	1.324	0.358	10.0	3.0	2.78	sloped
85		2.2	0.937	1.040	1.058	0.112	9.9	5.2	0.12	
85		2.2	0.938	1.054	1.060	0.119	9.3	4.8	9.49	
85		2.2	0.940	1.054	1.065	0.120	9.3	4.7	4.90	sloped
87		7.2	0.937	1.276	1.324	0.363	9.9	2.9	0.37	
87		7.2	0.938	1.278	1.347	0.375	9.6	2.8	9.60	
87		7.2	0.937	1.250	1.397	0.387	9.3	2.6	2.77	sloped
87		7.2	0.176	0.417	0.451	0.258	13.9	4.8	0.31	
87		7.2	0.651	1.039	0.963	0.350	10.3	3.1	11.68	
87		7.2	0.634	0.949	0.983	0.332	10.8	3.3	3.74	drop
88	1.43	5.1	0.648	0.870	0.906	0.240	10.6	3.8	0.21	
88	0.94	5.1	0.648	0.811	0.835	0.175	14.6	6.1	12.21	
88	0.41	5.1	0.651	0.856	0.892	0.223	11.4	4.3	4.74	drop
88	1.47	5.1	0.938	1.179	1.242	0.273	9.4	3.2	0.27	
88	0.97	5.1	0.937	1.163	1.263	0.276	9.2	3.1	9.52	
88	0.97	5.1	0.937	1.173	1.213	0.256	10.0	3.5	3.24	sloped
89	0.81	2.3	0.641	0.736	0.762	0.108	10.4	5.6	0.10	
89	0.39	2.3	0.652	0.747	0.763	0.103	10.9	6.0	10.94	
89	1.35	2.3	0.624	0.720	0.751	0.098	11.5	6.5	6.02	drop
89	0.47	2.3	0.938	1.053	1.069	0.123	9.1	4.6	0.12	
89	0.97	2.3	0.939	1.046	1.072	0.120	9.4	4.8	9.21	
89	1.47	2.3	0.940	1.055	1.072	0.124	9.1	4.6	4.64	sloped
64		5.1	0.21	0.406		0.196	13.1	5.2		
64		5.1	0.21	0.44		0.230	11.2	4.1		
64		5.1	0.21	0.386		0.176	14.6	6.1	0.21	
64		5.1	0.179	0.402		0.223	11.5	4.3	12.20	
64		5.1	0.164	0.407		0.243	10.6	3.8	4.71	drop
90	0.9167	8.0	0.139	0.415		0.276	14.4	4.8	0.33	
90	0.3438	8.0	0.137	0.498	0.546	0.385	10.3	2.9	12.13	
90	1.5	8.0	0.141	0.503	0.464	0.343	11.6	3.5	3.76	drop
90	0.47	8.0	0.939	1.3	1.378	0.400	10.0	2.8	0.41	
90	0.97	8.0	0.937	1.279	1.452	0.429	9.3	2.5	9.71	
90	1.47	8.0	0.937	1.315	1.363	0.402	9.9	2.8	2.67	sloped
91	1.47	7.9	0.937	1.352	1.352	0.415	9.5	2.6	0.41	
91	0.97	7.9	0.937	1.355	1.355	0.418	9.5	2.6	9.66	
91	0.47	7.9	0.937	1.333	1.333	0.396	10.0	2.8	2.66	sloped
93	0.47	4.9	0.937	1.194	1.219	0.270	9.1	3.1	0.26	
93	0.97	4.9	0.937	1.219	1.192	0.269	9.1	3.1	9.42	
93	1.47	4.9	0.938	1.193	1.171	0.244	10.0	3.6	3.26	sloped
94	0.47	6.6	0.937	1.257	1.287	0.335	9.9	3.0	0.34	
94	0.97	6.6	0.937	1.278	1.243	0.324	10.3	3.2	9.80	
94	1.47	6.6	0.938	1.307	1.289	0.360	9.2	2.7	2.97	sloped
95	1.47	2.3	0.938	1.05	1.061	0.118	9.6	4.9	0.11	
95	0.97	2.3	0.937	1.057	1.044	0.114	10.0	5.2	9.84	
95	0.47	2.3	0.937	1.044	1.057	0.114	10.0	5.2	5.12	sloped
96	0.47	2.3	0.938	1.061	1.049	0.117	9.7	5.0	0.12	
96	0.97	2.3	0.938	1.073	1.052	0.125	9.1	4.5	9.46	
96	1.47	2.3	0.939	1.049	1.063	0.117	9.7	5.0	4.83	sloped
97	1.47	5.0	0.939	1.205	1.217	0.272	9.2	3.1	0.27	

Run	x	Q	ref	low	high	y	V	Fr			
97	0.97	5.0	0.938	1.259	1.179	0.281	8.9	3.0	9.37		
97	0.47	5.0	0.938	1.181	1.203	0.254	9.8	3.4	3.20	sloped	
98	0.47	6.7	0.938	1.257	1.309	0.345	9.7	2.9	0.35		
98	0.97	6.7	0.938	1.346	1.234	0.352	9.5	2.8	9.58		
98	1.47	6.7	0.939	1.3	1.274	0.348	9.6	2.9	2.86	sloped	
98	1.33	6.7	0.695	0.958	0.995	0.282	11.9	3.9			
98	0.58	6.7	0.696	0.973	0.95	0.266	12.6	4.3		drop	
99	1.47	7.9	0.939	1.356	1.278	0.378	10.4	3.0	0.39		
99	0.97	7.9	0.938	1.403	1.283	0.405	9.7	2.7	10.12		
99	0.47	7.9	0.938	1.291	1.349	0.382	10.3	2.9	2.86	sloped	
99	1.33	7.9	0.695	0.977	1.029	0.308	12.7	4.0			
99	0.6	7.9	0.696	0.982	1.032	0.311	12.6	4.0		drop	
100	0.47	7.7	0.938	1.356	1.279	0.380	10.2	2.9	0.41		
100	0.97	7.7	0.938	1.279	1.425	0.414	9.3	2.6	9.56		
100	1.47	7.7	0.939	1.361	1.361	0.422	9.2	2.5	2.65	sloped	
100	0.92	7.7	0.696	1.082	1.144	0.417	9.3	2.5	0.38		
100	0.54	7.7	0.696	1.038	1.091	0.369	10.5	3.0	10.15		
100	1.345	7.7	0.696	1.03	1.085	0.3615	10.7	3.1	2.90	drop	
101	1.47	6.9	0.939	1.275	1.339	0.368	9.3	2.7	0.36		
101	0.97	6.9	0.938	1.379	1.239	0.371	9.2	2.7	9.53		
101	0.47	6.9	0.938	1.26	1.3	0.342	10.0	3.0	2.80	sloped	
101	0.96	6.9	0.694	0.999	1.053	0.332	10.3	3.2	0.33		
101	1.34	6.9	0.694	1.047	0.976	0.318	10.8	3.4	10.34		
101	0.56	6.9	0.694	1.008	1.0736	0.347	9.9	3.0	3.17	drop	
102	0.47	5.0	0.938	1.173	1.206	0.252	10.0	3.5	0.27		
102	0.97	5.0	0.938	1.155	1.277	0.278	9.0	3.0	9.40		
102	1.47	5.0	0.939	1.191	1.236	0.2745	9.2	3.1	3.21	sloped	
102	0.96	5.0	0.696	0.94	0.978	0.263	9.6	3.3	0.26		
102	0.57	5.0	0.695	0.988	0.942	0.270	9.3	3.2	9.63		
102	1.34	5.0	0.694	0.921	0.969	0.251	10.0	3.5	3.32	drop	
103	1.47	2.3	0.939	1.06	1.053	0.118	9.6	4.9	0.12		
103	0.97	2.3	0.938	1.042	1.064	0.115	9.8	5.1	9.69		
103	0.47	2.3	0.938	1.059	1.049	0.116	9.7	5.0	5.01	sloped	
103	0.85	2.3	0.689	0.789	0.809	0.110	10.2	5.4	0.12		
103	0.575	2.3	0.690	0.8	0.814	0.117	9.6	5.0	9.70		
103	1.34	2.3	0.695	0.809	0.824	0.1215	9.3	4.7	5.03	drop	
104	0.47	2.3	0.938	1.061	1.049	0.117	9.7	5.0	0.12		
104	0.97	2.3	0.938	1.069	1.048	0.1205	9.4	4.8	9.43		
104	1.47	2.3	0.939	1.052	1.07	0.122	9.3	4.7	4.80	sloped	
104	1.375	2.3	0.692	0.816	0.826	0.129	8.8	4.3			
104	1.105	2.3	0.695	0.799	0.826	0.1175	9.6	4.9	0.12		
104	0.835	2.3	0.698	0.828	0.798	0.115	9.8	5.1	9.55		
104	0.515	2.3	0.702	0.822	0.808	0.113	10.0	5.2	4.90		1
104	0.53	2.3	0.705	0.824	0.813	0.1135	10.0	5.2	0.12		
104	0.99	2.3	0.704	0.806	0.824	0.111	10.2	5.4	9.77		
104	1.4	2.3	0.703	0.835	0.817	0.123	9.2	4.6	5.07		2
104	0.93	2.3	0.702	0.833	0.817	0.123	9.2	4.6	0.14		
104	0.6	2.3	0.705	0.832	0.851	0.1365	8.3	3.9	8.40		
104	1.395	2.3	0.696	0.855	0.829	0.146	7.7	3.6	4.04		3
104	0.94	2.3	0.697	0.823	0.849	0.139	8.1	3.8	0.13		
104	1.31	2.3	0.694	0.812	0.825	0.1245	9.1	4.5	8.49		

Run	x	Q	ref	low	high	y	V	Fr			
104	0.56	2.3	0.703	0.848	0.831	0.1365	8.3	3.9	3.95	Outlet	
105	1.47	5.2	0.940	1.237	1.203	0.28	9.2	3.1	0.27		
105	0.97	5.2	0.939	1.265	1.17	0.2785	9.3	3.1	9.55		
105	0.47	5.2	0.939	1.177	1.211	0.255	10.1	3.5	3.24	sloped	
105	0.54	5.2	0.696	0.909	0.959	0.238	10.9	3.9	0.24		
105	1.02	5.2	0.690	0.943	0.904	0.2335	11.1	4.0	10.75		
105	1.36	5.2	0.685	0.949	0.922	0.2505	10.3	3.6	3.86		1
105	1.33	5.2	0.703	0.893	0.93	0.2085	12.4	4.8	0.21		
105	1.01	5.2	0.705	0.888	0.913	0.1955	13.2	5.3	12.38		
105	0.56	5.2	0.707	0.95	0.913	0.2245	11.5	4.3	4.78		2
105	0.61	5.2	0.704	0.987	0.949	0.264	9.8	3.4	0.28		
105	1	5.2	0.690	1.006	1.054	0.34	7.6	2.3	9.31		
105	1.4	5.2	0.696	0.965	0.918	0.2455	10.5	3.7	3.13		3
105	0.58	5.2	0.702	0.984	0.959	0.2695	9.6	3.3	0.27		
105	1.045	5.2	0.697	0.948	0.988	0.271	9.5	3.2	9.63		
105	1.425	5.2	0.691	0.938	0.973	0.2645	9.8	3.3	3.28	Outlet	
106	0.47	6.8	0.939	1.295	1.254	0.3355	10.1	3.1	0.34		
106	0.97	6.8	0.939	1.232	1.325	0.3395	10.0	3.0	9.82		
106	1.47	6.8	0.940	1.325	1.272	0.3585	9.4	2.8	2.95	sloped	
106	1.38	6.8	0.688	0.986	1.017	0.3135	10.8	3.4	0.30		
106	0.93	6.8	0.694	0.957	0.988	0.2785	12.1	4.1	11.39		
106	0.55	6.8	0.699	1.021	0.977	0.3	11.3	3.6	3.69		1
106	0.55	6.8	0.706	0.996	1.033	0.3085	11.0	3.5	0.29		
106	1	6.8	0.703	0.996	0.967	0.2785	12.1	4.1	11.66		
106	1.37	6.8	0.701	0.996	0.974	0.284	11.9	3.9	3.82		2
106	1.3	6.8	0.687	1.058	1.014	0.349	9.7	2.9	0.34		
106	0.92	6.8	0.691	1.007	1.048	0.3365	10.0	3.1	10.04		
106	0.61	6.8	0.696	1.002	1.04	0.325	10.4	3.2	3.05		3
106	0.62	6.8	0.699	1.065	1.022	0.3445	9.8	2.9	0.34		
106	0.99	6.8	0.696	1.064	1.019	0.3455	9.8	2.9	9.83		
106	1.38	6.8	0.690	1.06	1.004	0.342	9.9	3.0	2.95	Outlet	
107	1.470	8.0	0.940	1.317	1.388	0.4125	9.7	2.7	0.42		
107	0.97	8.0	0.939	1.296	1.462	0.44	9.1	2.4	9.70		
107	0.47	8.0	0.939	1.366	1.298	0.393	10.2	2.9	2.66	sloped	
107	1.33	8.0	0.688	1.067	1.013	0.352	11.4	3.4	0.34		
107	0.89	8.0	0.694	0.996	1.036	0.322	12.5	3.9	11.70		
107	0.50	8.0	0.702	1.082	1.04	0.359	11.2	3.3	3.52		1
107	1.36	8.0	0.701	1.005	1.054	0.3285	12.2	3.8	0.33		
107	0.94	8.0	0.701	1.026	0.984	0.304	13.2	4.2	12.23		
107	0.53	8.0	0.706	1.027	1.101	0.358	11.2	3.3	3.77		2
107	1.38	8.0	0.687	1.053	1.102	0.3905	10.3	2.9	0.38		
107	1.00	8.0	0.690	1.04	1.094	0.377	10.7	3.1	10.53		
107	0.59	8.0	0.696	1.04	1.109	0.3785	10.6	3.0	3.00		3
107	1.33	8.0	0.693	1.117	1.06	0.3955	10.2	2.8	0.40		
107	0.97	8.0	0.696	1.136	1.092	0.418	9.6	2.6	10.02		
107	0.57	8.0	0.701	1.116	1.069	0.3915	10.3	2.9	2.79	Outlet	
112	1.47	8.0	0.939	1.388	1.322	0.416	9.6	2.6	0.41		
112	0.97	8.0	0.936	1.45	1.26	0.4205	9.5	2.6	9.74		
112	0.47	8.0	0.936	1.38	1.29	0.3975	10.1	2.8	2.68	sloped	
112	0.55	8.0	0.702	1.10	1.05	0.3735	10.7	3.1	0.41		
112	1.05	8.0	0.698	1.18	1.14	0.462	8.7	2.2	9.97		

Run	x	Q	ref	low	high	y	V	Fr		
112	1.45	8.0	0.699	1.05	1.11	0.3805	10.5	3.0	3.01	toe
112	0.55	8.0	0.694	1.74	2.04	1.196	3.3	0.5	1.20	
112	1.00	8.0	0.689	1.71	2.08	1.2075	3.3	0.5	3.34	
112	1.52	8.0	0.685	1.70	2.06	1.1925	3.4	0.5	0.54	Y2
112	0.55	8.0	0.697	1.46	1.17	0.6215	6.4	1.4	0.62	
112	1.02	8.0	0.687	1.50	1.17	0.6485	6.2	1.4	6.50	
112	1.47	8.0	0.687	1.39	1.15	0.5825	6.9	1.6	1.46	Outlet
113	0.47	6.8	0.936	1.34	1.24	0.355	9.6	2.8	0.36	
113	0.97	6.8	0.936	1.24	1.35	0.3565	9.6	2.8	9.46	
113	1.47	6.8	0.939	1.34	1.28	0.37	9.2	2.7	2.78	sloped
113	0.68	6.8	0.702	1.03	1.08	0.349	9.8	2.9	0.35	
113	0.97	6.8	0.699	1.06	1.10	0.3765	9.1	2.6	9.89	
113	1.45	6.8	0.699	0.99	1.04	0.3145	10.8	3.4	2.97	toe
113	1.45	6.8	0.690	1.65	1.99	1.1265	3.0	0.5	1.16	
113	1.03	6.8	0.692	2.11	1.68	1.2055	2.8	0.5	2.93	
113	0.64	6.8	0.697	1.99	1.73	1.162	2.9	0.5	0.48	Y2
113	0.66	6.8	0.700	1.09	1.35	0.5205	6.6	1.6	0.53	
113	0.96	6.8	0.698	1.12	1.35	0.5395	6.3	1.5	6.49	
113	1.44	6.8	0.692	1.07	1.35	0.5165	6.6	1.6	1.58	Outlet
114	0.47	5.2	0.936	1.18	1.22	0.2645	9.9	3.4	0.29	
114	0.97	5.2	0.936	1.17	1.29	0.291	9.0	2.9	9.06	
114	1.47	5.2	0.938	1.32	1.18	0.3125	8.4	2.6	2.98	sloped
114	1.46	5.2	0.687	1.24	1.06	0.4625	5.6	1.5	0.46	
114	0.97	5.2	0.698	1.25	1.10	0.475	5.5	1.4	5.65	
114	0.58	5.2	0.704	1.21	1.09	0.4485	5.8	1.5	1.47	Outlet
114	0.59	5.2	0.696	1.86	1.66	1.062	2.5	0.4	1.07	
114	1.00	5.2	0.685	1.89	1.64	1.079	2.4	0.4	2.44	
114	1.51	5.2	0.686	1.91	1.60	1.0685	2.4	0.4	0.42	Y2
114	1.50	5.2	0.706	1.01	0.94	0.265	9.8	3.4	0.30	
114	0.96	5.2	0.698	1.00	0.96	0.2825	9.2	3.1	8.88	
114	0.56	5.2	0.702	1.11	0.98	0.345	7.6	2.3	2.90	toe
115	0.47	2.4	0.936	1.06	1.07	0.126	9.5	4.7	0.12	
115	0.97	2.4	0.936	1.07	1.05	0.1205	9.9	5.0	9.67	
115	1.47	2.4	0.939	1.06	1.07	0.1245	9.6	4.8	4.85	sloped
115	0.54	2.4	0.701	0.86	0.82	0.14	8.5	4.0	0.14	
115	0.97	2.4	0.694	0.83	0.84	0.1405	8.5	4.0	8.49	
115	1.49	2.4	0.686	0.82	0.84	0.142	8.4	3.9	3.98	toe
115	1.45	2.4	0.687	1.44	1.54	0.803	1.5	0.3	0.80	
115	1.09	2.4	0.689	1.43	1.52	0.788	1.5	0.3	1.50	
115	0.55	2.4	0.697	1.55	1.44	0.7955	1.5	0.3	0.30	Y2
115	0.55	2.4	0.701	0.95	0.88	0.213	5.6	2.1	0.22	
115	1.03	2.4	0.695	0.88	0.96	0.2255	5.3	2.0	5.46	
115	1.44	2.4	0.689	0.88	0.93	0.2185	5.5	2.1	2.06	Outlet
116	1.47	2.2	0.939	1.053	1.066	0.1205	9.1	4.6	0.12	
116	0.97	2.2	0.936	1.04	1.06	0.1155	9.5	4.9	9.32	
116	0.47	2.2	0.937	1.048	1.063	0.1185	9.3	4.8	4.78	sloped
116	1.37	2.2	0.698	0.815	0.831	0.125	8.8	4.4	0.11	
116	1.03	2.2	0.698	0.794	0.807	0.1025	10.7	5.9	9.98	
116	0.56	2.2	0.703	0.803	0.815	0.106	10.4	5.6	5.31	toe
116	0.55	2.2	0.379	1.303	1.223	0.884	1.2	0.2	0.89	
116	0.97	2.2	0.374	1.307	1.24	0.8995	1.2	0.2	1.23	

Run	x	Q	ref	low	high	y	V	Fr		
116	1.43	2.2	0.372	1.321	1.221	0.899	1.2	0.2	0.23	Y2
116	1.44	2.2	0.37	0.521	0.607	0.194	5.7	2.3	0.21	
116	1.05	2.2	0.37	0.561	0.637	0.229	4.8	1.8	5.23	
116	0.56	2.2	0.381	0.563	0.622	0.2115	5.2	2.0	2.01	Outlet
117	0.47	5.1	0.936	1.175	1.204	0.2535	10.1	3.5	0.27	
117	0.97	5.1	0.937	1.181	1.236	0.2715	9.4	3.2	9.57	
117	1.47	5.1	0.938	1.202	1.23	0.278	9.2	3.1	3.26	sloped
117	0.56	5.1	0.703	0.908	0.92	0.211	12.1	4.7	0.20	
117	0.98	5.1	0.698	0.894	0.879	0.1885	13.6	5.5	12.56	
117	1.43	5.1	0.695	0.897	0.92	0.2135	12.0	4.6	4.91	toe
117	1.41	5.1	0.37	1.706	1.534	1.25	2.0	0.3	1.28	
117	1	5.1	0.371	1.594	1.734	1.293	2.0	0.3	2.00	
117	0.57	5.1	0.376	1.595	1.747	1.295	2.0	0.3	0.31	Y2
117	0.6	5.1	0.38	0.709	0.842	0.3955	6.5	1.8	0.40	
117	0.92	5.1	0.374	0.705	0.85	0.4035	6.3	1.8	6.46	
117	1.46	5.1	0.368	0.687	0.826	0.3885	6.6	1.9	1.81	Outlet
118	0.47	6.7	0.937	1.284	1.253	0.3315	10.1	3.1	0.35	
118	0.97	6.7	0.936	1.253	1.313	0.347	9.6	2.9	9.66	
118	1.47	6.7	0.937	1.315	1.28	0.3605	9.3	2.7	2.90	sloped
118	1.47	6.7	0.691	0.961	0.996	0.2875	11.6	3.8	0.29	
118	0.96	6.7	0.696	0.934	0.986	0.264	12.7	4.3	11.59	
118	0.48	6.7	0.705	1.004	1.043	0.3185	10.5	3.3	3.81	toe
118	0.53	6.7	0.372	1.907	1.728	1.4455	2.3	0.3	1.43	
118	1.02	6.7	0.368	1.895	1.677	1.418	2.4	0.3	2.35	
118	1.46	6.7	0.368	1.874	1.685	1.4115	2.4	0.4	0.35	Y2
118	0.58	6.7	0.38	0.717	0.961	0.459	7.3	1.9	0.46	
118	1.11	6.7	0.369	0.763	0.919	0.472	7.1	1.8	7.26	
118	1.47	6.7	0.369	0.691	0.949	0.451	7.4	1.9	1.88	Outlet
119	1.47	7.9	0.94	1.301	1.377	0.402	9.8	2.7	1.89	sloped
119	0.49	7.9	0.705	1.042	1.1107	0.3714	10.6	3.1	0.33	
119	0.93	7.9	0.696	0.969	1.016	0.2965	13.3	4.3	12.02	
119	1.36	7.9	0.694	0.983	1.05	0.3225	12.2	3.8	3.71	toe
119	1.4	7.9	0.37	1.937	1.752	1.4745	2.7	0.4	1.51	
119	0.95	7.9	0.371	1.983	1.773	1.507	2.6	0.4	2.61	
119	0.58	7.9	0.375	2.042	1.802	1.547	2.5	0.4	0.37	Y2
119	0.59	7.9	0.379	0.802	1.026	0.535	7.4	1.8	0.52	
119	1	7.9	0.373	0.797	0.984	0.5175	7.6	1.9	7.51	
119	1.39	7.9	0.369	0.745	1.032	0.5195	7.6	1.9	1.83	Outlet
120	1.47	8.0	0.938	1.297	1.395	0.408	9.7	2.7	0.41	
120	0.97	8.0	0.937	1.435	1.272	0.4165	9.5	2.6	9.68	
120	0.47	8.0	0.938	1.371	1.32	0.4075	9.8	2.7	2.66	sloped
120	0.45	8.0	0.378	2.321	2.34	1.9525	2.0	0.3	1.95	
120	1	8.0	0.377	2.325	2.318	1.9445	2.0	0.3	2.04	
120	1.45	8.0	0.38	2.33	2.31	1.94	2.0	0.3	0.26	Y2
120	0.59	8.0	0.378	0.77	1.018	0.516	7.7	1.9	0.52	
120	0.95	8.0	0.374	1.045	0.778	0.5375	7.4	1.8	7.70	
120	1.46	8.0	0.371	1.004	0.733	0.4975	8.0	2.0	1.89	Outlet
121	0.47	7.4	0.938	1.276	1.34	0.37	10.0	2.9	0.39	
121	0.97	7.4	0.937	1.248	1.428	0.401	9.2	2.6	9.57	
121	1.47	7.4	0.938	1.283	1.367	0.387	9.5	2.7	2.72	sloped
121	0.82	7.4	0.132	1.904	2.109	1.8745	2.0	0.3	1.88	

Run	x	Q	ref	low	high	y	V	Fr		
121	1.39	7.4	0.129	1.905	2.114	1.8805	2.0	0.3	1.96	
121	0.57	7.4	0.136	1.923	2.12	1.8855	2.0	0.3	0.25	Y2
121	0.54	7.4	0.134	0.703	0.5	0.4675	7.9	2.0	0.48	
121	0.95	7.4	0.138	0.479	0.767	0.485	7.6	1.9	7.68	
121	1.44	7.4	0.125	0.733	0.496	0.4895	7.5	1.9	1.95	Outlet
122	1.47	5.3	0.939	1.191	1.252	0.2825	9.4	3.1	0.27	
122	0.97	5.3	0.937	1.165	1.255	0.273	9.7	3.3	9.71	
122	0.47	5.3	0.938	1.181	1.22	0.2625	10.1	3.5	3.28	sloped
122	1.41	5.3	0.126	1.746	1.913	1.7035	1.6	0.2	1.69	
122	0.94	5.3	0.128	1.742	1.896	1.691	1.6	0.2	1.56	
122	0.51	5.3	0.136	1.758	1.888	1.687	1.6	0.2	0.21	Y2
122	0.63	5.3	0.183	0.421	0.569	0.312	8.5	2.7	0.35	
122	1	5.3	0.126	0.552	0.417	0.3585	7.4	2.2	7.66	
122	1.44	5.3	0.124	0.587	0.403	0.371	7.1	2.1	2.30	Outlet
123	0.47	2.5	0.939	1.074	1.061	0.1285	9.8	4.8	0.13	
123	0.97	2.5	0.937	1.052	1.078	0.128	9.8	4.8	9.58	
123	1.47	2.5	0.939	1.07	1.082	0.137	9.2	4.4	4.66	sloped
123	0.51	2.5	0.132	1.502	1.573	1.4055	0.9	0.1	1.41	
123	0.94	2.5	0.124	1.5	1.578	1.415	0.9	0.1	0.89	
123	1.46	2.5	0.118	1.559	1.488	1.4055	0.9	0.1	0.13	Y2
123	1.41	2.5	0.106	0.262	0.354	0.202	6.2	2.4	0.20	
123	0.97	2.5	0.107	0.256	0.34	0.191	6.6	2.6	6.15	
123	0.51	2.5	0.119	0.304	0.377	0.2215	5.7	2.1	2.40	Outlet
124	1.47	3.4	0.939	1.105	1.136	0.1815	9.5	3.9	0.18	
124	0.97	3.4	0.938	1.164	1.095	0.1915	9.0	3.6	9.56	
124	0.47	3.4	0.938	1.096	1.117	0.1685	10.2	4.4	3.97	sloped
124	1.43	3.4	0.113	1.665	1.559	1.499	1.1	0.2	1.51	
124	0.99	3.4	0.114	1.573	1.687	1.516	1.1	0.2	1.14	
124	0.56	3.4	0.118	1.696	1.573	1.5165	1.1	0.2	0.16	Y2
124	0.51	3.4	0.12	0.329	0.435	0.262	6.6	2.3	0.27	
124	0.98	3.4	0.112	0.435	0.33	0.2705	6.4	2.2	6.46	
124	1.43	3.4	0.11	0.452	0.301	0.2665	6.5	2.2	2.21	Outlet
125	0.47	2.2	0.939	1.05	1.06	0.116	9.7	5.0	0.12	
125	0.97	2.2	0.939	1.049	1.068	0.1195	9.4	4.8	9.35	
125	1.47	2.2	0.941	1.058	1.072	0.124	9.0	4.5	4.76	sloped
125	0.56	2.2	0.734	0.835	0.849	0.108	10.4	5.6	0.11	
125	1	2.2	0.738	0.837	0.854	0.1075	10.4	5.6	10.15	
125	1.45	2.2	0.729	0.838	0.852	0.116	9.7	5.0	5.39	toe
125	0.59	2.2	0.023	1.374	1.513	1.4205	0.8	0.1	1.41	
125	0.98	2.2	0.017	1.335	1.519	1.41	0.8	0.1	0.80	
125	1.45	2.2	0.015	1.495	1.31	1.3875	0.8	0.1	0.12	Y2
125	1.43	2.2	0.022	0.156	0.322	0.217	5.2	2.0	0.20	
125	0.97	2.2	0.022	0.179	0.264	0.1995	5.6	2.2	5.48	
125	0.59	2.2	0.028	0.178	0.274	0.198	5.7	2.2	2.14	Outlet
126	1.47	3.5	0.94	1.109	1.141	0.185	9.3	3.8	0.18	
126	0.97	3.5	0.938	1.137	1.111	0.186	9.3	3.8	9.49	
126	0.47	3.5	0.937	1.103	1.12	0.1745	9.9	4.2	3.93	sloped
126	1.46	3.5	0.728	0.867	0.89	0.1505	11.5	5.2	0.15	
126	1	3.5	0.729	0.873	0.888	0.1515	11.4	5.2	11.55	
126	0.58	3.5	0.734	0.869	0.891	0.146	11.8	5.4	5.27	toe
126	0.58	3.5	0.023	1.677	1.527	1.579	1.1	0.2	1.58	

Run	x	Q	ref	low	high	y	V	Fr		
126	1.03	3.5	0.018	1.53	1.683	1.5885	1.1	0.2	1.10	
126	1.45	3.5	0.014	1.519	1.632	1.5615	1.1	0.2	0.15	Y2
126	1.43	3.5	0.018	0.196	0.339	0.2495	6.9	2.4	0.28	
126	0.98	3.5	0.019	0.378	0.234	0.287	6.0	2.0	6.26	
126	0.55	3.5	0.027	0.239	0.405	0.295	5.8	1.9	2.10	Outlet
127	0.47	5.1	0.938	1.209	1.173	0.253	10.0	3.5	0.27	
127	0.97	5.1	0.937	1.252	1.159	0.2685	9.4	3.2	9.45	
127	1.47	5.1	0.939	1.239	1.21	0.2855	8.9	2.9	3.22	sloped
127	0.59	5.1	0.973	1.169	1.186	0.2045	12.4	4.8	0.20	
127	1	5.1	0.968	1.15	1.169	0.1915	13.2	5.3	12.41	
127	1.42	5.1	0.966	1.176	1.193	0.2185	11.6	4.4	4.85	toe
127	1.43	5.1	0.254	2.132	1.714	1.669	1.5	0.2	1.65	
127	0.98	5.1	0.257	1.656	2.079	1.6105	1.6	0.2	1.54	
127	0.58	5.1	0.262	2.1	1.759	1.6675	1.5	0.2	0.21	Y2
127	0.55	5.1	0.026	0.586	0.312	0.423	6.0	1.6	0.45	
127	0.97	5.1	0.019	0.683	0.325	0.485	5.2	1.3	5.63	
127	1.43	5.1	0.014	0.619	0.304	0.4475	5.7	1.5	1.48	Outlet
128	1.47	6.9	0.939	1.324	1.267	0.3565	9.6	2.8	0.35	
128	0.97	6.9	0.938	1.342	1.246	0.356	9.6	2.8	9.83	
128	0.47	6.9	0.938	1.306	1.243	0.3365	10.2	3.1	2.93	sloped
128	0.6	6.9	0.971	1.249	1.224	0.2655	12.9	4.4	0.26	
128	0.98	6.9	0.97	1.22	1.203	0.2415	14.2	5.1	13.05	
128	1.43	6.9	0.968	1.244	1.265	0.2865	12.0	3.9	4.49	toe
128	0.6	6.9	0.261	1.749	2.02	1.6235	2.1	0.3	1.61	
128	1.02	6.9	0.253	1.736	2.006	1.618	2.1	0.3	2.13	
128	1.44	6.9	0.254	1.687	1.997	1.588	2.2	0.3	0.30	Y2
128	0.56	6.9	0.26	0.535	0.926	0.4705	7.3	1.9	0.47	
128	0.97	6.9	0.255	0.9	0.514	0.452	7.6	2.0	7.27	
128	1.45	6.9	0.255	0.985	0.519	0.497	6.9	1.7	1.87	Outlet
129	0.47	8.1	0.938	1.307	1.374	0.4025	10.0	2.8	0.41	
129	0.97	8.1	0.938	1.274	1.405	0.4015	10.0	2.8	9.95	
129	1.47	8.1	0.939	1.326	1.377	0.4125	9.8	2.7	2.75	sloped
129	0.62	8.1	0.968	1.292	1.286	0.321	12.6	3.9	0.32	
129	1	8.1	0.964	1.25	1.267	0.2945	13.7	4.4	12.79	
129	1.4	8.1	0.964	1.272	1.323	0.3335	12.1	3.7	4.02	toe
129	0.61	8.1	0.261	2.035	1.758	1.6355	2.5	0.3	1.63	
129	0.97	8.1	0.253	1.714	2.03	1.619	2.5	0.3	2.48	
129	1.45	8.1	0.254	1.708	2.05	1.625	2.5	0.3	0.34	Y2
129	0.6	8.1	0.26	0.572	0.949	0.5005	8.1	2.0	0.53	
129	1.01	8.1	0.255	1.01	0.646	0.573	7.0	1.6	7.68	
129	1.42	8.1	0.255	0.54	0.985	0.5075	8.0	2.0	1.87	Outlet
130	0.47	8.0	0.937	1.314	1.398	0.419	9.6	2.6	0.43	
130	0.97	8.0	0.937	1.498	1.294	0.459	8.7	2.3	9.38	
130	1.47	8.0	0.94	1.3	1.393	0.4065	9.9	2.7	2.53	sloped
130	0.56	8.0	0.974	1.375	1.309	0.368	10.9	3.2	0.33	
130	1.01	8.0	0.97	1.287	1.256	0.3015	13.3	4.3	12.14	
130	1.43	8.0	0.968	1.32	1.27	0.327	12.2	3.8	3.73	toe
130	0.6	8.0	0.259	1.71	2.072	1.632	2.5	0.3	1.60	
130	0.97	8.0	0.253	1.656	1.948	1.549	2.6	0.4	2.50	
130	1.42	8.0	0.248	1.67	2.075	1.6245	2.5	0.3	0.35	Y2
130	0.59	8.0	0.259	0.759	0.093	0.167	24.0	10.3	0.46	

Run	x	Q	ref	low	high	y	V	Fr		
130	0.99	8.0	0.252	0.787	1.041	0.662	6.0	1.3	6.61	
130	1.42	8.0	0.251	0.659	0.959	0.558	7.2	1.7	1.50	Outlet
131	0.47	7.3	0.937	1.287	1.344	0.3785	9.6	2.8	0.38	
131	0.97	7.3	0.937	1.363	1.261	0.375	9.7	2.8	9.60	
131	1.47	7.3	0.94	1.297	1.358	0.3875	9.4	2.7	2.74	sloped
131	0.6	7.3	0.972	1.262	1.314	0.316	11.6	3.6	0.30	
131	0.98	7.3	0.969	1.228	1.269	0.2795	13.1	4.4	12.03	
131	1.43	7.3	0.965	1.26	1.306	0.318	11.5	3.6	3.85	toe
131	0.58	7.3	0.258	1.889	1.684	1.5285	2.4	0.3	1.50	
131	1.02	7.3	0.252	1.597	1.874	1.4835	2.5	0.4	2.43	
131	1.45	7.3	0.245	1.564	1.902	1.488	2.5	0.4	0.35	Y2
131	0.6	7.3	0.262	0.659	0.924	0.5295	6.9	1.7	0.54	
131	0.97	7.3	0.254	0.696	0.95	0.569	6.4	1.5	6.78	
131	1.42	7.3	0.252	0.63	0.914	0.52	7.0	1.7	1.63	Outlet
132	0.47	5.0	0.938	1.172	1.207	0.2515	9.9	3.5	0.26	
132	0.97	5.0	0.939	1.228	1.158	0.254	9.8	3.4	9.56	
132	1.47	5.0	0.941	1.238	1.199	0.2775	9.0	3.0	3.30	sloped
132	0.58	5.0	0.976	1.215	1.182	0.2225	11.2	4.2	0.21	
132	1.02	5.0	0.971	1.175	1.142	0.1875	13.3	5.4	11.96	
132	1.43	5.0	0.969	1.201	1.173	0.218	11.4	4.3	4.63	toe
132	0.6	5.0	0.26	1.465	1.673	1.309	1.9	0.3	1.31	
132	1	5.0	0.255	1.649	1.469	1.304	1.9	0.3	1.91	
132	1.42	5.0	0.251	1.64	1.471	1.3045	1.9	0.3	0.29	Y2
132	0.58	5.0	0.265	0.772	0.558	0.4	6.2	1.7	0.41	
132	0.97	5.0	0.255	0.566	0.758	0.407	6.1	1.7	6.09	
132	1.45	5.0	0.253	0.584	0.764	0.421	5.9	1.6	1.68	Outlet
133	0.47	3.3	0.938	1.103	1.114	0.1705	9.7	4.2	0.18	
133	0.97	3.3	0.938	1.103	1.144	0.1855	8.9	3.7	9.40	
133	1.47	3.3	0.941	1.108	1.123	0.1745	9.5	4.0	3.94	sloped
133	0.6	3.3	0.975	1.114	1.132	0.148	11.2	5.1	0.17	
133	0.99	3.3	0.972	1.198	1.118	0.186	8.9	3.6	10.12	
133	1.42	3.3	0.969	1.149	1.114	0.1625	10.2	4.5	4.42	toe
133	0.58	3.3	0.26	1.318	1.438	1.118	1.5	0.2	1.11	
133	0.98	3.3	0.258	1.291	1.433	1.104	1.5	0.3	1.49	
133	1.42	3.3	0.254	1.314	1.425	1.1155	1.5	0.2	0.25	Y2
133	0.6	3.3	0.265	0.475	0.599	0.272	6.1	2.1	0.30	
133	1.02	3.3	0.256	0.488	0.671	0.3235	5.1	1.6	5.57	
133	1.43	3.3	0.256	0.488	0.629	0.3025	5.5	1.8	1.80	Outlet
134	0.47	2.2	0.938	1.053	1.063	0.12	9.2	4.7	0.12	
134	0.97	2.2	0.938	1.045	1.055	0.112	9.9	5.2	9.36	
134	1.47	2.2	0.941	1.058	1.069	0.1225	9.0	4.5	4.81	sloped
134	0.59	2.2	0.972	1.089	1.097	0.121	9.1	4.6	0.12	
134	1	2.2	0.972	1.076	1.093	0.1125	9.8	5.2	9.39	
134	1.42	2.2	0.969	1.079	1.099	0.12	9.2	4.7	4.82	toe
134	0.58	2.2	0.26	1.146	1.256	0.941	1.2	0.2	0.94	
134	1.02	2.2	0.255	1.167	1.255	0.956	1.2	0.2	1.18	
134	1.45	2.2	0.251	1.138	1.213	0.9245	1.2	0.2	0.21	Y2
134	0.55	2.2	0.266	0.437	0.549	0.227	4.9	1.8	0.24	
134	1.02	2.2	0.258	0.457	0.563	0.252	4.4	1.5	4.68	
134	1.43	2.2	0.249	0.437	0.522	0.2305	4.8	1.8	1.70	Outlet
135	0.47	2.2	0.937	1.051	1.058	0.1175	9.4	4.9	0.12	

Run	x	Q	ref	low	high	y	V	Fr		
135	0.97	2.2	0.938	1.057	1.049	0.115	9.7	5.0	9.53	
135	1.47	2.2	0.941	1.065	1.053	0.118	9.4	4.8	4.92	sloped
135	0.55	2.2	0.973	1.081	1.093	0.114	9.7	5.1	0.11	
135	1.02	2.2	0.969	1.075	1.085	0.111	10.0	5.3	9.75	
135	1.4	2.2	0.968	1.09	1.079	0.1165	9.5	4.9	5.10	toe
135	0.6	2.2	0.259	1.148	1.249	0.9395	1.2	0.2	0.94	
135	1	2.2	0.256	1.154	1.248	0.945	1.2	0.2	1.19	
135	1.43	2.2	0.253	1.132	1.216	0.921	1.2	0.2	0.22	Y2
135	0.57	2.2	0.267	0.434	0.539	0.2195	5.1	1.9	0.23	
135	1.02	2.2	0.258	0.438	0.554	0.238	4.7	1.7	4.74	
135	1.45	2.2	0.253	0.442	0.557	0.2465	4.5	1.6	1.73	Outlet
136	0.47	1.9	0.937	1.05	1.038	0.107	8.8	4.8	0.11	
136	0.97	1.9	0.938	1.031	1.055	0.105	9.0	4.9	8.93	
136	1.47	1.9	0.941	1.04	1.053	0.1055	9.0	4.9	4.84	sloped
136	0.6	1.9	0.975	1.073	1.092	0.1075	8.8	4.7	0.11	
136	1	1.9	0.971	1.073	1.085	0.108	8.8	4.7	8.61	
136	1.43	1.9	0.973	1.095	1.079	0.114	8.3	4.3	4.58	drop
136	0.58	1.9	0.259	1.194	1.124	0.9	1.1	0.2	0.90	
136	0.98	1.9	0.253	1.122	1.206	0.911	1.0	0.2	1.05	
136	1.45	1.9	0.254	1.115	1.191	0.899	1.1	0.2	0.19	Y2
136	0.55	1.9	0.265	0.449	0.516	0.2175	4.3	1.6	0.23	
136	1	1.9	0.257	0.458	0.547	0.2455	3.8	1.4	4.15	
136	1.43	1.9	0.256	0.431	0.526	0.2225	4.2	1.6	1.53	Outlet
137	0.47	4.8	0.938	1.158	1.197	0.2395	10.1	3.6	0.26	
137	0.97	4.8	0.937	1.151	1.249	0.263	9.2	3.2	9.46	
137	1.47	4.8	0.939	1.181	1.227	0.265	9.1	3.1	3.30	sloped
137	0.58	4.8	0.972	1.17	1.199	0.2125	11.4	4.3	0.21	
137	1	4.8	0.968	1.162	1.144	0.185	13.1	5.3	11.65	
137	1.43	4.8	0.963	1.172	1.213	0.2295	10.5	3.9	4.52	drop
137	0.59	4.8	0.257	1.53	1.745	1.3805	1.7	0.3	1.37	
137	0.98	4.8	0.256	1.532	1.687	1.3535	1.8	0.3	1.77	
137	1.45	4.8	0.25	1.524	1.709	1.3665	1.8	0.3	0.27	Y2
137	0.6	4.8	0.26	0.564	0.742	0.393	6.1	1.7	0.43	
137	1	4.8	0.255	0.594	0.831	0.4575	5.3	1.4	5.67	
137	1.43	4.8	0.256	0.609	0.767	0.432	5.6	1.5	1.53	Outlet
138	0.47	6.7	0.937	1.247	1.303	0.338	9.9	3.0	0.35	
138	0.97	6.7	0.937	1.224	1.337	0.3435	9.7	2.9	9.59	
138	1.47	6.7	0.939	1.266	1.341	0.3645	9.2	2.7	2.86	sloped
138	0.6	6.7	0.978	1.233	1.276	0.2765	12.1	4.0	0.27	
138	1	6.7	0.967	1.198	1.227	0.2455	13.6	4.8	12.59	
138	1.43	6.7	0.966	1.218	1.267	0.2765	12.1	4.0	4.31	drop
138	0.58	6.7	0.253	1.659	1.976	1.5645	2.1	0.3	1.53	
138	0.98	6.7	0.246	1.609	1.869	1.493	2.2	0.3	2.18	
138	1.42	6.7	0.244	1.673	1.886	1.5355	2.2	0.3	0.31	Y2
138	0.59	6.7	0.253	0.632	0.876	0.501	6.7	1.7	0.51	
138	1.02	6.7	0.248	0.715	0.877	0.548	6.1	1.5	6.58	
138	1.45	6.7	0.247	0.613	0.838	0.4785	7.0	1.8	1.63	Outlet
139	0.47	7.6	0.938	1.385	1.301	0.405	9.3	2.6	0.40	
139	0.97	7.6	0.937	1.279	1.397	0.401	9.4	2.6	9.38	
139	1.47	7.6	0.937	1.298	1.384	0.404	9.4	2.6	2.60	sloped
139	0.58	7.6	0.966	1.352	1.288	0.354	10.7	3.2	0.32	

Run	x	Q	ref	low	high	y	V	Fr		
139	0.99	7.6	0.963	1.275	1.243	0.296	12.8	4.1	12.35	
139	1.45	7.6	0.965	1.259	1.306	0.3175	11.9	3.7	3.94	drop
139	0.55	7.6	0.246	1.709	2.071	1.644	2.3	0.3	1.62	
139	0.98	7.6	0.245	1.693	2.015	1.609	2.4	0.3	2.34	
139	1.45	7.6	0.248	1.706	1.993	1.6015	2.4	0.3	0.32	Y2
139	0.6	7.6	0.254	0.972	0.657	0.5605	6.8	1.6	0.61	
139	1	7.6	0.246	0.959	0.703	0.585	6.5	1.5	6.23	
139	1.43	7.6	0.246	0.963	0.915	0.693	5.5	1.2	1.41	Outlet
140	0.47	7.8	0.937	1.304	1.366	0.398	9.8	2.7	0.41	
140	0.97	7.8	0.936	1.292	1.443	0.4315	9.0	2.4	9.52	
140	1.47	7.8	0.936	1.301	1.377	0.403	9.7	2.7	2.62	sloped
140	0.6	7.8	0.967	1.294	1.362	0.361	10.8	3.2	0.33	
140	1	7.8	0.965	1.286	1.249	0.3025	12.9	4.1	11.90	
140	1.43	7.8	0.966	1.276	1.309	0.3265	12.0	3.7	3.67	drop
140	0.58	7.8	0.256	1.209	1.136	0.9165	4.3	0.8	0.95	
140	0.98	7.8	0.254	1.22	1.314	1.013	3.9	0.7	4.11	
140	1.45	7.8	0.25	1.102	1.251	0.9265	4.2	0.8	0.74	Y2
140	0.55	7.8	0.252	0.684	0.858	0.519	7.5	1.8	0.50	
140	0.97	7.8	0.244	0.613	0.854	0.4895	8.0	2.0	7.86	
140	1.42	7.8	0.245	0.618	0.838	0.483	8.1	2.1	1.97	Outlet
141	0.47	6.7	0.937	1.323	1.259	0.354	9.4	2.8	0.36	
141	0.97	6.7	0.936	1.209	1.38	0.3585	9.3	2.7	9.32	
141	1.47	6.7	0.936	1.268	1.333	0.3645	9.2	2.7	2.74	sloped
141	0.55	6.7	0.966	1.303	1.257	0.314	10.7	3.4	0.29	
141	1.02	6.7	0.973	1.201	1.244	0.2495	13.4	4.7	11.82	
141	1.42	6.7	0.961	1.239	1.27	0.2935	11.4	3.7	3.93	drop
141	0.55	6.7	0.258	1.097	1.21	0.8955	3.7	0.7	0.91	
141	0.97	6.7	0.256	1.166	1.263	0.9585	3.5	0.6	3.66	
141	1.45	6.7	0.253	1.209	1.073	0.888	3.8	0.7	0.68	Y2
141	0.6	6.7	0.25	0.588	0.85	0.469	7.1	1.8	0.48	
141	0.98	6.7	0.244	0.882	0.593	0.4935	6.8	1.7	6.93	
141	1.42	6.7	0.244	0.839	0.623	0.487	6.9	1.7	1.76	Outlet
142	0.47	4.9	0.937	1.179	1.208	0.2565	9.6	3.4	0.26	
142	0.97	4.9	0.937	1.165	1.234	0.2625	9.4	3.2	9.42	
142	1.47	4.9	0.94	1.179	1.236	0.2675	9.2	3.1	3.24	sloped
142	0.55	4.9	0.966	1.207	1.193	0.234	10.6	3.8	0.22	
142	0.98	4.9	0.964	1.148	1.177	0.1985	12.4	4.9	11.22	
142	1.42	4.9	0.96	1.172	1.212	0.232	10.6	3.9	4.22	drop
142	0.57	4.9	0.26	1.009	1.176	0.8325	3.0	0.6	0.83	
142	0.97	4.9	0.255	1.186	1.053	0.8645	2.9	0.5	2.96	
142	1.45	4.9	0.252	1.01	1.106	0.806	3.1	0.6	0.57	Y2
142	0.6	4.9	0.256	0.57	0.73	0.394	6.3	1.8	0.42	
142	1	4.9	0.249	0.558	0.854	0.457	5.4	1.4	5.85	
142	1.43	4.9	0.249	0.589	0.749	0.42	5.9	1.6	1.59	Outlet
143	0.47	2.2	0.937	1.056	1.065	0.1235	8.9	4.5	0.12	
143	0.97	2.2	0.937	1.049	1.052	0.1135	9.7	5.1	9.42	
143	1.47	2.2	0.939	1.047	1.059	0.114	9.6	5.0	4.86	sloped
143	0.55	2.2	0.968	1.079	1.089	0.116	9.5	4.9	0.12	
143	0.98	2.2	0.965	1.066	1.085	0.1105	10.0	5.3	9.35	
143	1.42	2.2	0.963	1.098	1.083	0.1275	8.6	4.3	4.81	drop
143	0.57	2.2	0.258	1.394	1.251	1.0645	1.0	0.2	1.08	

Run	x	Q	ref	low	high	y	V	Fr		
143	0.97	2.2	0.256	1.412	1.279	1.0895	1.0	0.2	1.02	
143	1.45	2.2	0.252	1.257	1.394	1.0735	1.0	0.2	0.17	Y2
143	0.6	2.2	0.257	0.514	0.448	0.224	4.9	1.8	0.23	
143	1	2.2	0.25	0.538	0.446	0.242	4.5	1.6	4.73	
143	1.43	2.2	0.25	0.519	0.446	0.2325	4.7	1.7	1.73	Outlet
144	0.47	2.2	0.938	1.056	1.065	0.1225	9.1	4.6	0.12	
144	0.97	2.2	0.939	1.046	1.077	0.1225	9.1	4.6	8.94	
144	1.47	2.2	0.94	1.076	1.063	0.1295	8.6	4.2	4.46	sloped
144	0.58	2.2	0.966	1.079	1.092	0.1195	9.3	4.8	0.12	
144	1	2.2	0.965	1.067	1.086	0.1115	10.0	5.3	9.34	
144	1.43	2.2	0.964	1.08	1.105	0.1285	8.7	4.3	4.77	drop
144	0.6	2.2	0.251	1.148	1.039	0.8425	1.3	0.3	0.85	
144	0.97	2.2	0.246	1.029	1.17	0.8535	1.3	0.2	1.31	
144	1.44	2.2	0.238	1.03	1.15	0.852	1.3	0.2	0.25	Y2
144	0.57	2.2	0.258	0.486	0.562	0.266	4.2	1.4	0.27	
144	0.98	2.2	0.25	0.482	0.557	0.2695	4.1	1.4	4.18	
144	1.44	2.2	0.246	0.474	0.549	0.2655	4.2	1.4	1.42	Outlet
145	0.47	5.1	0.937	1.209	1.179	0.257	9.8	3.4	0.27	
145	0.97	5.1	0.937	1.169	1.254	0.2745	9.2	3.1	9.38	
145	1.47	5.1	0.94	1.24	1.198	0.279	9.1	3.0	3.18	sloped
145	0.58	5.1	0.967	1.179	1.226	0.2355	10.7	3.9	0.22	
145	1	5.1	0.962	1.144	1.171	0.1955	12.9	5.2	11.84	
145	1.45	5.1	0.971	1.2	1.17	0.214	11.8	4.5	4.52	drop
145	0.6	5.1	0.252	1.37	1.568	1.217	2.1	0.3	1.19	
145	0.97	5.1	0.247	1.286	1.553	1.1725	2.2	0.4	2.13	
145	1.43	5.1	0.243	1.282	1.54	1.168	2.2	0.4	0.35	Y2
145	0.5	5.1	0.256	0.785	0.643	0.458	5.5	1.4	0.47	
145	1	5.1	0.247	0.799	0.634	0.4695	5.4	1.4	5.39	
145	1.43	5.1	0.243	0.798	0.65	0.481	5.3	1.3	1.39	Outlet
146	0.47	7.2	0.937	1.274	1.348	0.374	9.6	2.8	0.37	
146	0.97	7.2	0.937	1.234	1.349	0.3545	10.1	3.0	9.70	
146	1.47	7.2	0.939	1.284	1.354	0.38	9.4	2.7	2.81	sloped
146	0.58	7.2	0.965	1.254	1.303	0.3135	11.4	3.6	0.30	
146	1.02	7.2	0.962	1.212	1.249	0.2685	13.3	4.5	12.08	
146	1.45	7.2	0.962	1.254	1.294	0.312	11.5	3.6	3.92	drop
146	0.59	7.2	0.248	1.776	1.47	1.375	2.6	0.4	1.34	
146	0.97	7.2	0.24	1.384	1.716	1.31	2.7	0.4	2.66	
146	1.43	7.2	0.238	1.732	1.442	1.349	2.7	0.4	0.40	Y2
146	0.58	7.2	0.258	0.729	0.926	0.5695	6.3	1.5	0.58	
146	0.98	7.2	0.248	0.742	0.916	0.581	6.2	1.4	6.19	
146	1.4	7.2	0.245	0.937	0.723	0.585	6.1	1.4	1.43	Outlet
147	0.47	7.8	0.937	1.307	1.381	0.407	9.6	2.6	0.41	
147	0.97	7.8	0.936	1.43	1.278	0.418	9.3	2.5	9.46	
147	1.47	7.8	0.938	1.385	1.316	0.4125	9.5	2.6	2.59	sloped
147	0.6	7.8	0.962	1.275	1.359	0.355	11.0	3.2	0.33	
147	1	7.8	0.964	1.239	1.286	0.2985	13.1	4.2	11.85	
147	1.43	7.8	0.962	1.317	1.286	0.3395	11.5	3.5	3.65	drop
147	0.58	7.8	0.251	1.866	1.564	1.464	2.7	0.4	1.45	
147	0.97	7.8	0.243	1.536	1.845	1.4475	2.7	0.4	2.69	
147	1.45	7.8	0.242	1.826	1.547	1.4445	2.7	0.4	0.39	Y2
147	0.59	7.8	0.255	0.804	1.065	0.6795	5.7	1.2	0.67	

Run	x	Q	ref	low	high	y	V	Fr		
147	0.98	7.8	0.247	1.042	0.809	0.6785	5.7	1.2	5.84	
147	1.43	7.8	0.247	0.999	0.808	0.6565	5.9	1.3	1.26	Outlet
148	0.47	1.7	0.94	1.028	1.023	0.0855	9.9	6.0	0.09	
148	0.97	1.7	0.942	1.028	1.018	0.081	10.4	6.5	9.74	
148	1.47	1.7	0.937	1.026	1.039	0.0955	8.9	5.1	5.83	sloped
148	0.59	1.7	0.967	1.064	1.059	0.0945	9.0	5.1	0.10	
148	1.02	1.7	0.963	1.074	1.065	0.1065	7.9	4.3	8.23	
148	1.44	1.7	0.963	1.074	1.069	0.1085	7.8	4.2	4.53	drop
148	0.6	1.7	0.251	1.365	1.173	1.018	0.8	0.1	1.04	
148	0.97	1.7	0.247	1.385	1.212	1.0515	0.8	0.1	0.81	
148	1.45	1.7	0.24	1.371	1.22	1.0555	0.8	0.1	0.14	Y2
148	0.58	1.7	0.258	0.535	0.416	0.2175	3.9	1.5	0.20	
148	1	1.7	0.25	0.536	0.398	0.217	3.9	1.5	4.23	
148	1.43	1.7	0.249	0.362	0.481	0.1725	4.9	2.1	1.68	Outlet
149	0.47	4.7	0.937	1.159	1.149	0.217	10.7	4.1	0.24	
149	0.97	4.7	0.937	1.207	1.15	0.2415	9.6	3.5	9.93	
149	1.47	4.7	0.939	1.168	1.205	0.2475	9.4	3.3	3.62	sloped
149	0.59	4.7	0.965	1.18	1.153	0.2015	11.6	4.5	0.20	
149	1.02	4.7	0.962	1.15	1.124	0.175	13.3	5.6	11.96	
149	1.44	4.7	0.961	1.159	1.186	0.2115	11.0	4.2	4.79	drop
149	0.6	4.7	0.253	1.886	1.456	1.418	1.6	0.2	1.37	
149	0.97	4.7	0.249	1.828	1.324	1.327	1.8	0.3	1.70	
149	1.45	4.7	0.246	1.903	1.316	1.3635	1.7	0.3	0.26	Y2
149	0.58	4.7	0.252	0.798	0.539	0.4165	5.6	1.5	0.44	
149	1	4.7	0.244	0.887	0.517	0.458	5.1	1.3	5.25	
149	1.43	4.7	0.246	0.557	0.852	0.4585	5.1	1.3	1.39	Outlet
150	0.47	6.4	0.936	1.218	1.298	0.322	10.0	3.1	0.34	
150	0.97	6.4	0.937	1.233	1.345	0.352	9.1	2.7	9.48	
150	1.47	6.4	0.939	1.31	1.257	0.3445	9.3	2.8	2.87	sloped
150	0.6	6.4	0.965	1.24	1.274	0.292	11.0	3.6	0.29	
150	1	6.4	0.962	1.184	1.238	0.249	12.9	4.6	11.32	
150	1.43	6.4	0.96	1.264	1.296	0.32	10.0	3.1	3.76	drop
150	0.58	6.4	0.252	1.375	1.9	1.3855	2.3	0.3	1.32	
150	1.02	6.4	0.248	1.336	1.61	1.225	2.6	0.4	2.44	
150	1.45	6.4	0.239	1.382	1.79	1.347	2.4	0.4	0.38	Y2
150	0.55	6.4	0.252	0.904	0.543	0.4715	6.8	1.7	0.48	
150	0.97	6.4	0.246	0.879	0.539	0.463	6.9	1.8	6.74	
150	1.43	6.4	0.247	0.869	0.619	0.497	6.5	1.6	1.72	Outlet
151	0.47	7.8	0.936	1.37	1.291	0.3945	9.9	2.8	0.42	
151	0.97	7.8	0.937	1.423	1.37	0.4595	8.5	2.2	9.42	
151	1.47	7.8	0.939	1.36	1.306	0.394	9.9	2.8	2.59	sloped
151	0.58	7.8	0.964	1.323	1.289	0.342	11.4	3.4	0.33	
151	1	7.8	0.962	1.267	1.262	0.3025	12.9	4.1	11.85	
151	1.45	7.8	0.96	1.317	1.296	0.3465	11.3	3.4	3.65	drop
151	0.56	7.8	0.252	2.213	1.693	1.701	2.3	0.3	1.44	
151	0.98	7.8	0.248	2.163	1.498	1.5825	2.5	0.3	2.85	
151	1.42	7.8	0.239	1.074	1.457	1.0265	3.8	0.7	0.44	Y2
151	0.57	7.8	0.252	0.59	0.978	0.532	7.3	1.8	0.55	
151	1	7.8	0.247	0.618	0.962	0.543	7.2	1.7	7.11	
151	1.42	7.8	0.247	0.678	0.961	0.5725	6.8	1.6	1.69	Outlet
152	0.47	7.7	0.937	1.269	1.354	0.3745	10.2	2.9	0.39	

Run	x	Q	ref	low	high	y	V	Fr		
152	0.97	7.7	0.937	1.285	1.409	0.41	9.4	2.6	9.54	
152	1.47	7.7	0.938	1.305	1.36	0.3945	9.7	2.7	2.65	sloped
152	0.57	7.7	0.966	1.324	1.285	0.3385	11.3	3.4	0.32	
152	1	7.7	0.962	1.266	1.23	0.286	13.4	4.4	11.93	
152	1.45	7.7	0.958	1.285	1.325	0.347	11.1	3.3	3.72	drop
152	0.6	7.7	0.256	1.848	2.097	1.7165	2.2	0.3	1.70	
152	1.01	7.7	0.25	2.128	1.818	1.723	2.2	0.3	2.25	
152	1.4	7.7	0.242	1.773	2.048	1.6685	2.3	0.3	0.30	Y2
152	0.58	7.7	0.249	0.695	0.977	0.587	6.5	1.5	0.59	
152	1.01	7.7	0.244	0.781	0.923	0.608	6.3	1.4	6.46	
152	1.43	7.7	0.243	0.714	0.944	0.586	6.5	1.5	1.48	Outlet
153	0.47	6.9	0.937	1.268	1.302	0.348	10.0	3.0	0.36	
153	0.97	6.9	0.937	1.265	1.355	0.373	9.3	2.7	9.60	
153	1.47	6.9	0.939	1.284	1.319	0.3625	9.6	2.8	2.82	sloped
153	0.58	6.9	0.965	1.234	1.291	0.2975	11.6	3.8	0.30	
153	1	6.9	0.963	1.216	1.253	0.2715	12.8	4.3	11.76	
153	1.4	6.9	0.96	1.255	1.302	0.3185	10.9	3.4	3.83	drop
153	0.6	6.9	0.25	1.828	2.032	1.68	2.1	0.3	4.73	
153	0.97	6.9	0.247	1.78	20.37	10.828	0.3	0.0	1.48	
153	1.45	6.9	0.241	2.034	1.833	1.6925	2.0	0.3	0.19	Y2
153	0.55	6.9	0.253	0.908	0.7	0.551	6.3	1.5	0.57	
153	1.02	6.9	0.246	0.954	0.748	0.605	5.7	1.3	6.07	
153	1.43	6.9	0.246	0.722	0.891	0.5605	6.2	1.5	1.42	Outlet
154	0.47	4.2	0.937	1.13	1.158	0.207	10.0	3.9	0.22	
154	0.97	4.2	0.937	1.145	1.194	0.2325	8.9	3.3	9.45	
154	1.47	4.2	0.939	1.146	1.173	0.2205	9.4	3.5	3.56	sloped
154	0.58	4.2	0.967	1.149	1.174	0.1945	10.7	4.3	0.19	
154	1	4.2	0.962	1.122	1.143	0.1705	12.2	5.2	11.19	
154	1.42	4.2	0.959	1.145	1.16	0.1935	10.7	4.3	4.58	drop
154	0.6	4.2	0.254	1.608	1.698	1.399	1.5	0.2	1.37	
154	1.02	4.2	0.246	1.548	1.708	1.382	1.5	0.2	1.51	
154	1.45	4.2	0.244	1.506	1.651	1.3345	1.6	0.2	0.23	Y2
154	0.61	4.2	0.255	0.698	0.578	0.383	5.4	1.5	0.39	
154	0.97	4.2	0.246	0.556	0.705	0.3845	5.4	1.5	5.38	
154	1.45	4.2	0.244	0.673	0.593	0.389	5.3	1.5	1.53	Outlet
155	0.47	1.7	0.937	1.021	1.031	0.089	9.5	5.6	0.09	
155	0.97	1.7	0.937	1.009	1.022	0.0785	10.8	6.8	9.94	
155	1.47	1.7	0.939	1.021	1.034	0.0885	9.5	5.7	6.01	sloped
155	0.58	1.7	0.966	1.043	1.058	0.0845	10.0	6.1	0.09	
155	1.02	1.7	0.962	1.055	1.066	0.0985	8.6	4.8	9.05	
155	1.45	1.7	0.96	1.05	1.067	0.0985	8.6	4.8	5.23	drop
155	0.6	1.7	0.254	1.223	1.183	0.949	0.9	0.2	0.96	
155	0.98	1.7	0.249	1.183	1.236	0.9605	0.9	0.2	0.88	
155	1.43	1.7	0.243	1.253	1.186	0.9765	0.9	0.2	0.16	Y2
155	0.55	1.7	0.258	0.432	0.394	0.155	5.5	2.4	0.16	
155	1	1.7	0.25	0.408	0.492	0.2	4.2	1.7	5.26	
155	1.45	1.7	0.247	0.402	0.369	0.1385	6.1	2.9	2.33	Outlet
156	0.47	6.6	0.937	1.28	1.241	0.3235	10.2	3.2	0.34	
156	0.97	6.6	0.937	1.24	1.314	0.34	9.7	2.9	9.73	
156	1.47	6.6	0.938	1.31	1.277	0.3555	9.3	2.7	2.95	sloped
156	0.58	6.6	1.044	1.349	1.314	0.2875	11.5	3.8	0.28	

Run	x	Q	ref	low	high	y	V	Fr		
156	0.98	6.6	1.04	1.279	1.3	0.2495	13.2	4.7	12.23	
156	1.43	6.6	1.038	1.349	1.315	0.294	11.2	3.6	4.16	drop
156	0.6	6.6	0.029	1.68	1.904	1.763	1.9	0.2	1.74	
156	1	6.6	0.019	1.638	1.852	1.726	1.9	0.3	1.90	
156	1.45	6.6	0.017	1.629	1.874	1.7345	1.9	0.3	0.25	Y2
156	0.55	6.6	0.031	0.494	0.65	0.541	6.1	1.5	0.53	
156	0.97	6.6	0.026	0.459	0.656	0.5315	6.2	1.5	6.23	
156	1.44	6.6	0.022	0.419	0.66	0.5175	6.4	1.6	1.51	Outlet
157	0.47	4.5	0.937	1.142	1.175	0.2215	10.0	3.8	0.24	
157	0.97	4.5	0.937	1.156	1.218	0.25	8.9	3.1	9.41	
157	1.47	4.5	0.938	1.163	1.193	0.24	9.3	3.3	3.41	sloped
157	0.58	4.5	1.042	1.223	1.243	0.191	11.6	4.7	0.19	
157	1.02	4.5	1.04	1.205	1.23	0.1775	12.5	5.2	11.83	
157	1.45	4.5	1.038	1.22	1.25	0.197	11.3	4.5	4.81	drop
157	0.6	4.5	0.019	1.64	1.47	1.536	1.4	0.2	1.51	
157	1	4.5	0.018	1.456	1.562	1.491	1.5	0.2	1.47	
157	1.42	4.5	0.017	1.594	1.442	1.501	1.5	0.2	0.21	Y2
157	0.55	4.5	0.036	0.263	0.425	0.308	7.2	2.3	0.34	
157	0.98	4.5	0.028	0.316	0.441	0.3505	6.3	1.9	6.55	
157	1.45	4.5	0.023	0.472	0.306	0.366	6.1	1.8	1.98	Outlet
158	0.47	1.6	0.937	1.026	1.032	0.092	8.9	5.1	0.09	
158	0.97	1.6	0.937	1.015	1.025	0.083	9.8	6.0	9.33	
158	1.47	1.6	0.939	1.023	1.03	0.0875	9.3	5.5	5.57	sloped
158	0.6	1.6	1.042	1.128	1.126	0.085	9.6	5.8	0.09	
158	1.02	1.6	1.04	1.128	1.136	0.092	8.9	5.1	8.79	
158	1.45	1.6	1.038	1.139	1.143	0.103	7.9	4.3	5.10	drop
158	0.55	1.6	0.023	1.076	1.116	1.073	0.8	0.1	1.07	
158	0.97	1.6	0.023	1.073	1.104	1.0655	0.8	0.1	0.76	
158	1.43	1.6	0.023	1.076	1.118	1.074	0.8	0.1	0.13	Y2
158	0.56	1.6	0.037	0.166	0.249	0.1705	4.8	2.0	0.16	
158	0.99	1.6	0.029	0.159	0.226	0.1635	5.0	2.2	5.22	
158	1.44	1.6	0.025	0.123	0.204	0.1385	5.9	2.8	2.33	Outlet
159	0.47	7.6	0.937	1.292	1.353	0.3855	9.8	2.8	0.39	
159	0.97	7.6	0.937	1.269	1.394	0.3945	9.6	2.7	9.73	
159	1.47	7.6	0.938	1.299	1.355	0.389	9.7	2.8	2.75	sloped
159	0.6	7.6	1.044	1.366	1.404	0.341	11.1	3.4	0.32	
159	1	7.6	1.04	1.316	1.348	0.292	13.0	4.2	12.05	
159	1.43	7.6	1.039	1.336	1.37	0.314	12.1	3.8	3.79	drop
159	0.56	7.6	0.028	1.748	2.117	1.9045	2.0	0.3	1.85	
159	0.98	7.6	0.025	1.687	1.975	1.806	2.1	0.3	2.05	
159	1.42	7.6	0.022	1.669	2.027	1.826	2.1	0.3	0.27	Y2
159	0.56	7.6	0.034	0.52	0.768	0.61	6.2	1.4	0.61	
159	0.99	7.6	0.027	0.519	0.784	0.6245	6.1	1.4	6.17	
159	1.44	7.6	0.024	0.5	0.768	0.61	6.2	1.4	1.39	Outlet
160	0.47	7.5	0.937	1.285	1.333	0.372	10.1	2.9	0.38	
160	0.97	7.5	0.937	1.268	1.377	0.3855	9.8	2.8	9.79	
160	1.47	7.5	0.939	1.306	1.366	0.397	9.5	2.7	2.78	sloped
160	0.6	7.5	1.043	1.36	1.416	0.345	10.9	3.3	0.31	
160	1	7.5	1.039	1.297	1.337	0.278	13.5	4.5	12.08	
160	1.43	7.5	1.037	1.334	1.379	0.3195	11.8	3.7	3.82	drop
160	0.55	7.5	0.028	1.695	1.988	1.8135	2.1	0.3	1.79	

Run	x	Q	ref	low	high	y	V	Fr		
160	0.97	7.5	0.018	1.649	1.928	1.7705	2.1	0.3	2.11	
160	1.45	7.5	0.015	1.695	1.928	1.7965	2.1	0.3	0.28	Y2
160	0.58	7.5	0.027	0.557	0.804	0.6535	5.8	1.3	0.63	
160	1.02	7.5	0.028	0.556	0.729	0.6145	6.1	1.4	6.03	
160	1.44	7.5	0.025	0.488	0.778	0.608	6.2	1.4	1.34	Outlet
161	0.47	6.8	0.937	1.234	1.296	0.328	10.3	3.2	0.34	
161	0.97	6.8	0.937	1.244	1.323	0.3465	9.7	2.9	9.83	
161	1.47	6.8	0.938	1.273	1.316	0.3565	9.5	2.8	2.96	sloped
161	0.58	6.8	1.041	1.306	1.348	0.286	11.8	3.9	0.27	
161	1.02	6.8	1.039	1.268	1.303	0.2465	13.7	4.9	12.44	
161	1.43	6.8	1.039	1.312	1.336	0.285	11.8	3.9	4.22	drop
161	0.56	6.8	0.026	1.626	1.916	1.745	1.9	0.3	1.70	
161	1.01	6.8	0.02	1.608	1.786	1.677	2.0	0.3	1.98	
161	1.42	6.8	0.018	1.586	1.819	1.6845	2.0	0.3	0.27	Y2
161	0.6	6.8	0.032	0.458	0.676	0.535	6.3	1.5	0.53	
161	0.98	6.8	0.026	0.456	0.668	0.536	6.3	1.5	6.31	
161	1.45	6.8	0.024	0.425	0.688	0.5325	6.3	1.5	1.52	Outlet
162	0.47	4.5	0.937	1.148	1.169	0.2215	10.1	3.8	0.24	
162	0.97	4.5	0.937	1.16	1.21	0.248	9.0	3.2	9.38	
162	1.47	4.5	0.938	1.176	1.194	0.247	9.0	3.2	3.39	sloped
162	0.58	4.5	1.045	1.243	1.278	0.2155	10.4	3.9	0.20	
162	1.02	4.5	1.039	1.198	1.224	0.172	13.0	5.5	11.53	
162	1.43	4.5	1.038	1.219	1.255	0.199	11.2	4.4	4.63	drop
162	0.56	4.5	0.026	1.425	1.598	1.4855	1.5	0.2	1.46	
162	1.02	4.5	0.019	1.39	1.546	1.449	1.5	0.2	1.53	
162	1.42	4.5	0.017	1.354	1.557	1.4385	1.6	0.2	0.22	Y2
162	0.6	4.5	0.035	0.344	0.493	0.3835	5.8	1.7	0.40	
162	0.98	4.5	0.025	0.313	0.549	0.406	5.5	1.5	5.62	
162	1.45	4.5	0.025	0.342	0.515	0.4035	5.5	1.5	1.57	Outlet
163	0.47	1.8	0.937	1.028	1.038	0.096	9.2	5.2	0.09	
163	0.97	1.8	0.937	1.018	1.025	0.0845	10.4	6.3	9.63	
163	1.47	1.8	0.939	1.029	1.038	0.0945	9.3	5.3	5.62	sloped
163	0.56	1.8	1.045	1.129	1.135	0.087	10.1	6.0	0.10	
163	0.97	1.8	1.039	1.136	1.142	0.1	8.8	4.9	8.98	
163	1.43	1.8	1.039	1.142	1.155	0.1095	8.0	4.3	5.08	drop
163	0.58	1.8	0.032	0.989	1.052	0.9885	0.9	0.2	1.01	
163	1.02	1.8	0.023	1.01	1.071	1.0175	0.9	0.2	0.87	
163	1.44	1.8	0.025	1	1.077	1.0135	0.9	0.2	0.15	Y2
163	0.6	1.8	0.037	0.18	0.23	0.168	5.2	2.3	0.19	
163	1	1.8	0.027	0.208	0.279	0.2165	4.1	1.5	4.64	
163	1.45	1.8	0.028	0.188	0.25	0.191	4.6	1.9	1.88	Outlet
164	close	2.2	0.038	0.16	0.331	0.2075	5.2	2.0	0.22	
164	mid	2.2	0.03	0.174	0.358	0.236	4.6	1.7	4.92	
164	far	2.2	0.02	0.157	0.319	0.218	5.0	1.9	1.85	Outlet
164	close	2.2	0.025	1.139	1.237	1.163	0.9	0.2	1.17	
164	mid	2.2	0.017	1.137	1.248	1.1755	0.9	0.1	0.92	
164	far	2.2	0.014	1.121	1.263	1.178	0.9	0.1	0.15	Y2
164	close	2.2	1.032	1.139	1.139	0.107	10.1	5.5	0.11	
164	mid	2.2	1.033	1.137	1.137	0.104	10.4	5.7	9.95	
164	far	2.2	1.029	1.145	1.145	0.116	9.3	4.8	5.32	drop
165	far	5.2	1.023	1.224	1.224	0.201	12.8	5.0	0.19	

Run	x	Q	ref	low	high	y	V	Fr		
165	mid	5.2	1.034	1.21	1.21	0.176	14.7	6.2	13.68	
165	close	5.2	1.032	1.235	1.235	0.203	12.7	5.0	5.56	drop
165	close	5.2	0.02	1.51	1.75	1.61	1.6	0.2	1.59	
165	mid	5.2	0.023	1.516	1.705	1.5875	1.6	0.2	1.62	
165	far	5.2	0.017	1.478	1.704	1.574	1.6	0.2	0.23	Y2
165	close	5.2	0.026	0.338	0.527	0.4065	6.3	1.8	0.41	
165	mid	5.2	0.023	0.339	0.522	0.4075	6.3	1.7	6.25	
165	far	5.2	0.022	0.324	0.568	0.424	6.1	1.6	1.72	Outlet

APPENDIX D

DATA ANALYSIS

Length of Hydraulic Jumps

The location of the weir is an important design parameter. If the weir is located too close to the drop a jump may not fully develop and energy loss is incomplete. If the weir is located too far downstream, a complete jump forms and there is tranquil water upstream of the weir. Minimal energy dissipation occurs when the flow is tranquil, but the added length costs money. Designing the location of the weir is a balance between insuring a jump occurs and cost.

The variation in jump type observed with location of weir is provided in Table 3. The effect of the weir location depends on the type of jump.

For a Sloped-A-jump there is no change in the location of the toe or the type of jump that occurs with the change in weir location. For example, pictures of three weir locations with a weir height of 1.5 ft, a drop height of 0.71 ft, and a discharge ~5.0 cfs are shown in Figure D1. For each weir location the turbulent part of the jump (the part that dissipates energy) ends around the drop. The additional space between the end of the turbulence and the weir is just calm flow, which dissipates little energy. The extra length costs money to build, with little energy dissipation added.

For wave jumps, A-jumps, B-jumps, and Min-B-Jumps the primary effect of the weir's location is development of the jump. For example, pictures of three weir locations with a weir height of 1.5 ft, a 1.0 ft drop height of, and a discharge ~8.0 cfs are shown in

Figure D2. As the weir is moved from 3 ft downstream of the drop to 7 ft the jump goes from incomplete to developed. The type of jump that forms is somewhere between an A-jump and a Wave Jump and not ideal for design, but the sequence demonstrates that the type of jump is not changing only the level of its development.

In a few cases it appears that the type of jump does change with sill location. For example, pictures of three weir locations with a weir height of 0.5 ft, a drop height of 0.32 ft, and a discharge ~7.0 cfs are shown in Figure D3. It appears that the toe of the jump is moving downstream as the weir location is moved downstream. One explanation for this is that the discharge is also increasing slightly as the weir location is moved. This small increase in discharge could be enough to move the toe of the jump downstream. Also, the toe location is fairly unsteady, so the pictures may be showing an extreme position. The other explanation is that the jump toe location is dependent on the weir location.

Analyzing all of the data it can be concluded that the weir location has little effect on the type of jump that occurs. The principle effect of weir location is jump development. At a weir located 3 ft downstream of the drop, 43.8% of the flows were either skimming flows or undeveloped jumps. The percentages drop to 12.5% for a weir 5 ft downstream of the drop, and 3.1% for a weir 7 ft downstream of the drop.

To design a weir location the literature suggests using the equation $Lj = 2\ y2$, for $4<Fr<12$. Comparing this equation with collected data is provided in Table D1.

Table D1. Comparison of Measured and Predicted Length.

Run	Distance Between Drop and Weir	Predicted Length of Jump Using Peterka	Observation of Jump
80	5	6.4	Turbulence is seen all the way to weir. Surface is level as it approaches the weir.
81	5	7.1	Turbulence is seen all the way to weir. Surface is still rising as it approaches the weir.
82	5	7.4	Turbulence is seen all the way to weir. Surface is still rising as it approaches the weir.
87	7	7	Turbulence is seen all the way to sill. Surface level peaks upstream of weir and falls as it approaches the weir.
88	7	6.5	Turbulence is seen all the way to weir. Surface is level as it approaches the weir.
89	7	5.2	Turbulence ends 5 feet downstream of the weir. Surface is level as it approaches the weir.
90	7	7.3	Turbulence is seen all the way to weir. Surface is level as it approaches the weir.

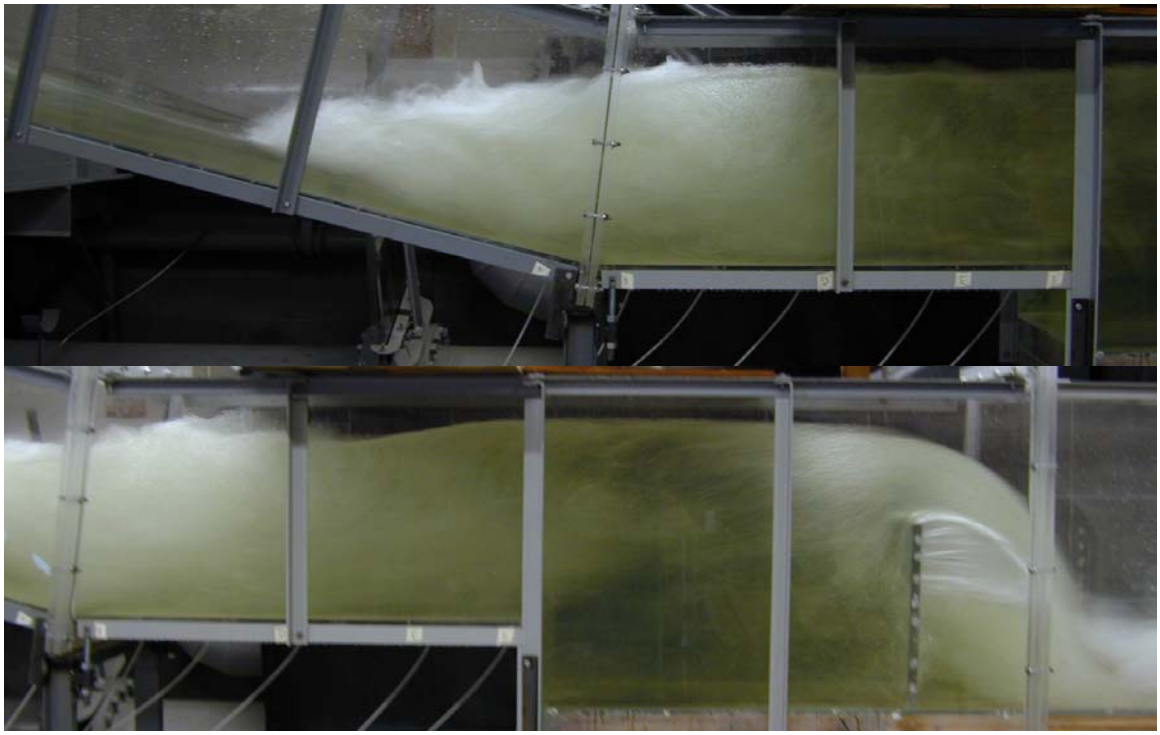

Weir Located 3 ft downstream from drop. Run # 69 Q = 5.1 cfs

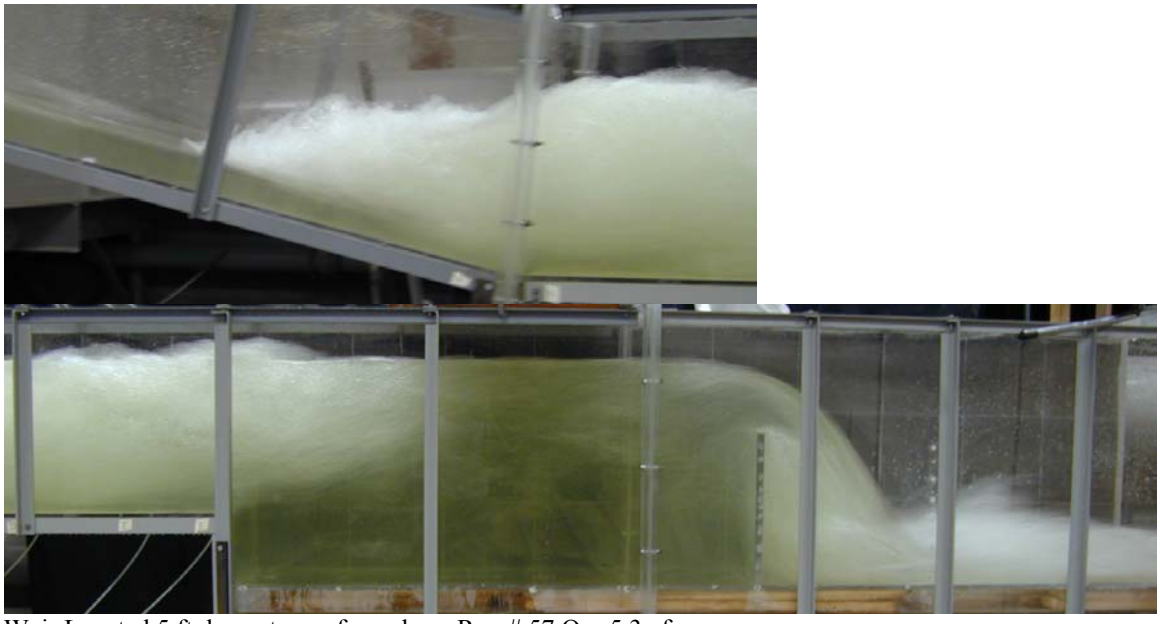

Weir Located 5 ft downstream from drop. Run # 57 Q = 5.3 cfs

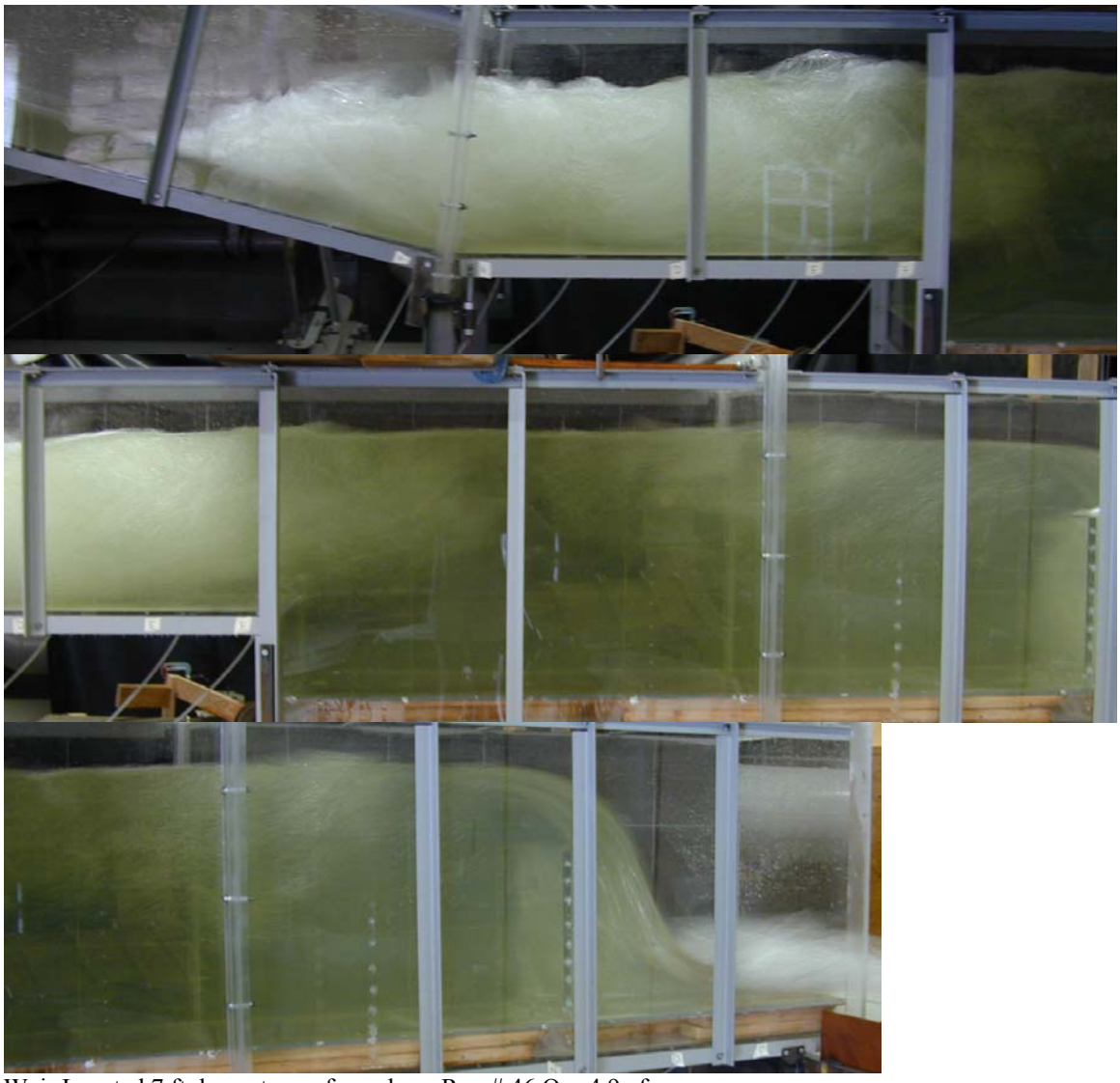

Weir Located 7 ft downstream from drop. Run # 46 Q = 4.9 cfs

Figure D1. Sloped-A-Jump Weir Location Series

Weir Located 3 ft downstream from drop. Run # 9 Q = 8.2 cfs

Weir Located 5 ft downstream from drop. Run # 25 Q = 8.1 cfs

Weir Located 7 ft downstream from drop. Run # 16 Q = 8.3 cfs

Figure D2. A/Wave-Jump Weir Location Series.

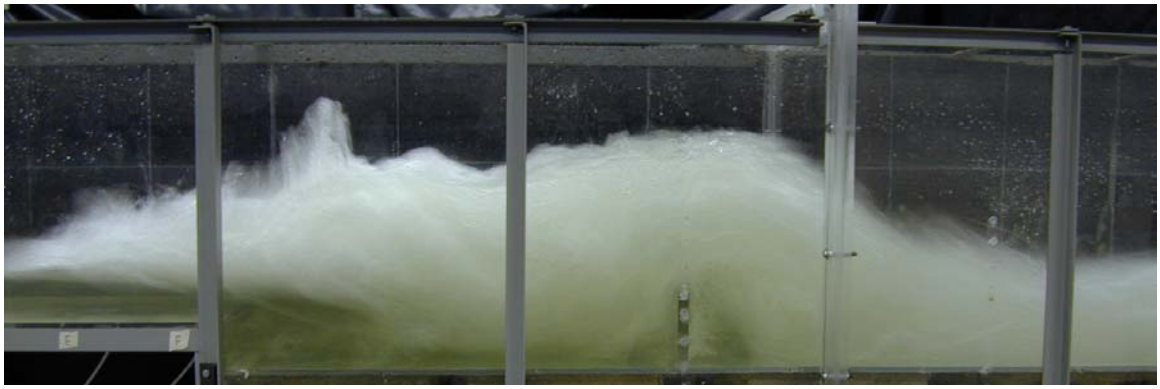

Weir Located 3 ft downstream from drop. Run # 73 Q = 6.6 cfs

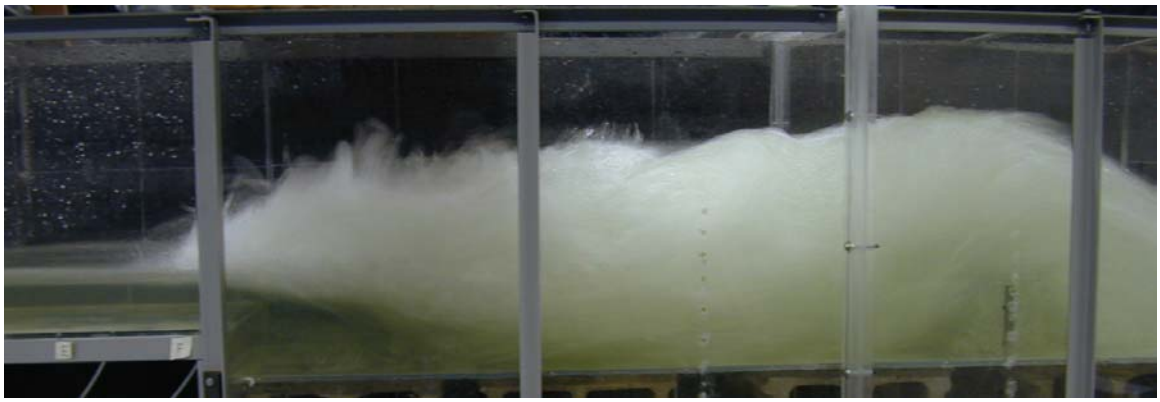

Weir Located 5 ft downstream from drop. Run # 81 Q = 7.2 cfs

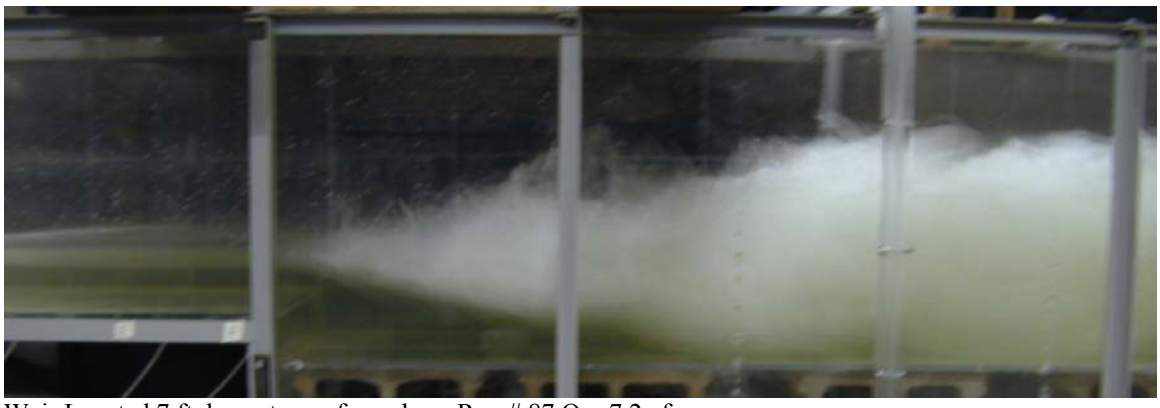

Weir Located 7 ft downstream from drop. Run # 87 Q = 7.2 cfs

Figure D3. A/B-Jump Weir Location Series

Comparison to Literature

Drag Force on Weir

When the tailwater depth is not known the momentum equation can be used to predict downstream flow characteristics. The momentum equation can be solved for tailwater depth if the drag coefficient is known. The literature discusses three methods to find the drag coefficient. The drag on the weir can be determined indirectly by measuring the depth of flow upstream and downstream from the weir and solving the momentum equation for drag. For a weir with no tailwater, the drag coefficient found using the indirect method ranged from 0.46 to 0.62 (*9*). The drag on the weir can also be calculated by installing manometer taps along both sides of the weir. Integrating these point measurements determines the drag over the entire weir (*10,11*). For a weir without tailwater, the drag coefficient found using manometer taps ranged from 0.4 to 0.65. A transducer can also be used to measure the drag force on the entire weir (*12,13*). The drag coefficient values found using a transducer were 0 to 0.5. In each method, the value of the drag coefficient is dependent on the distance from the jump toe to the weir.

The drag coefficient was found using the indirect method discussed above. The drag coefficient was found to range from 0.2-1.1. The drag coefficient is found to vary with approach depth, weir height, and jump length (Figure D4).

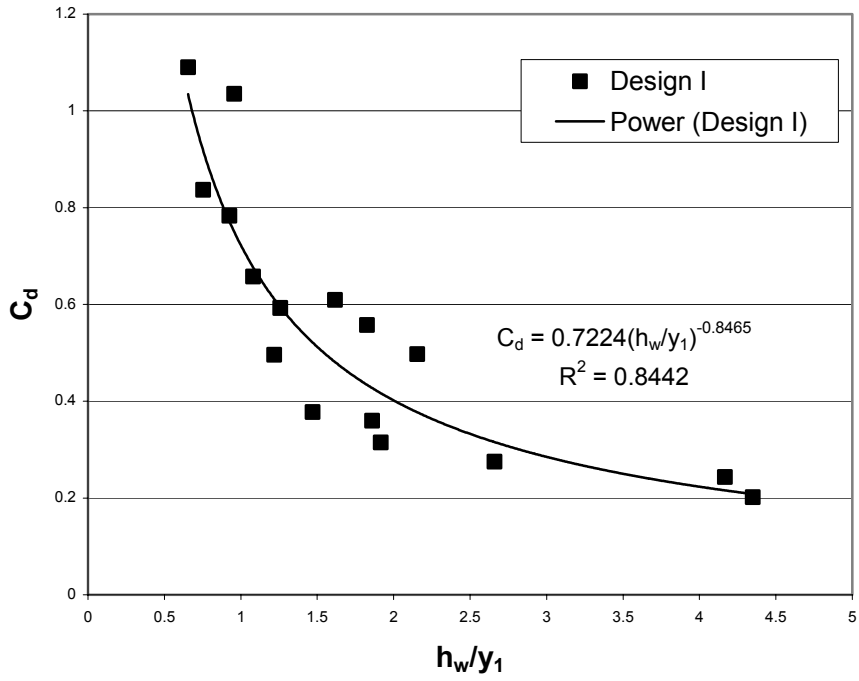

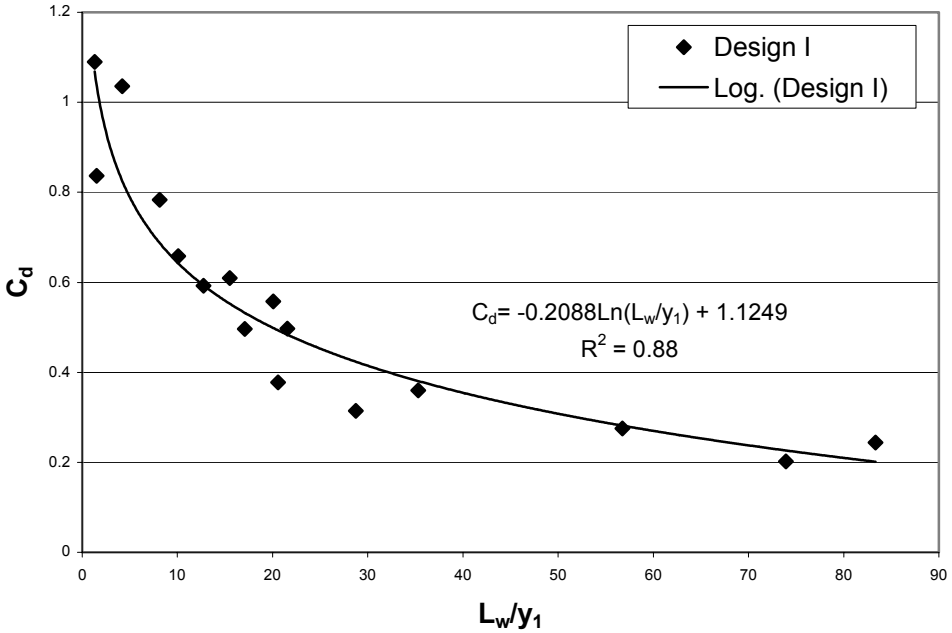

Figure D4: Variation of Drag Coefficient with approach depth, weir height, and jump length.

Jump Geometry

The theoretical equations derived for A- and B-jumps over drops relate the following dimensionless parameters (*7*).

$$Fr_1^2 = \frac{\left(\frac{y_2}{y_1} - \frac{h_d}{y_1}\right)^2 - 1}{2\left(1 - \frac{y_1}{y_2}\right)} \quad \text{(D1)}$$

$$Fr_1^2 = \frac{\left(\frac{y_2}{y_1}\right)^2 - \left(1 + \frac{h_d}{y_1}\right)^2}{2\left(1 - \frac{y_1}{y_2}\right)} \quad \text{(D2)}$$

The results of solving the equations with measured values of y_2, h_d, and y_1 are represented in Figure D5. The results of calculating Fr_1 by estimating y_2 with $y_c + h_w$ is also plotted.

Moore and Morgan (1957) provided a series of plots for their experimental data. The plots with y_2/y_1 on the abscissa and Fr_1 on the ordinate showed the region that each jump type was observed. A different plot was provided for each value. Plots of $(y_c + h_w)/ y_1$ are shown with the Moore Morgan data in Figure D6. The measured y_2/y_1 is also plotted with this data. The range of h_d/y_1 tested in the current study extended below

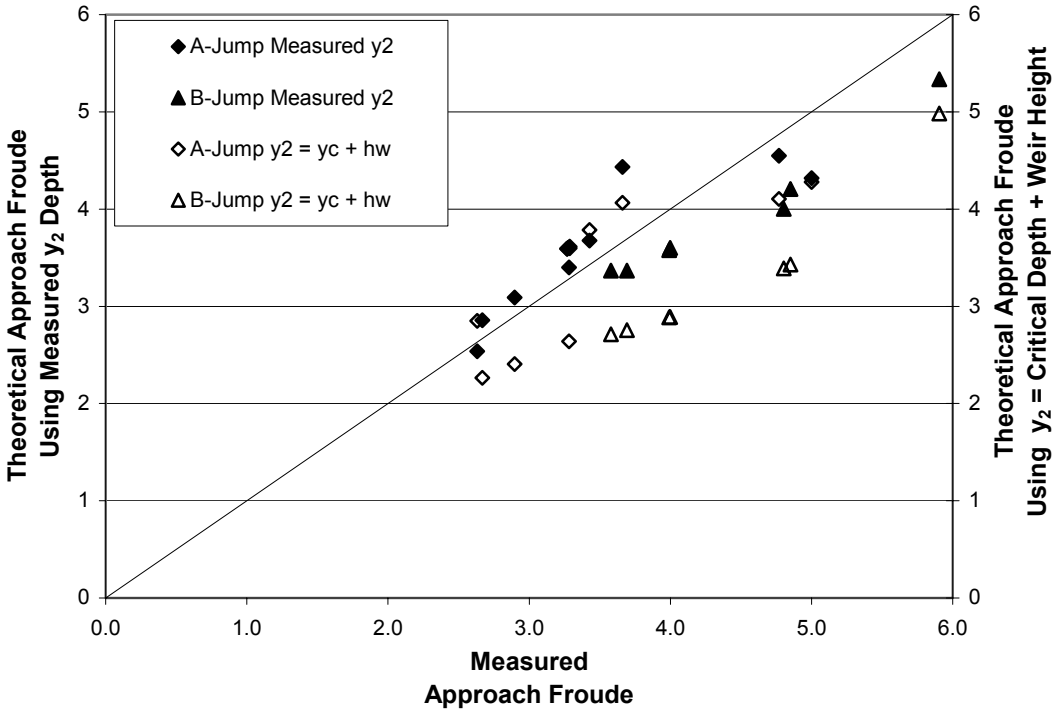

Figure D5. Theoretical vs. Measured Froude Over Drops.

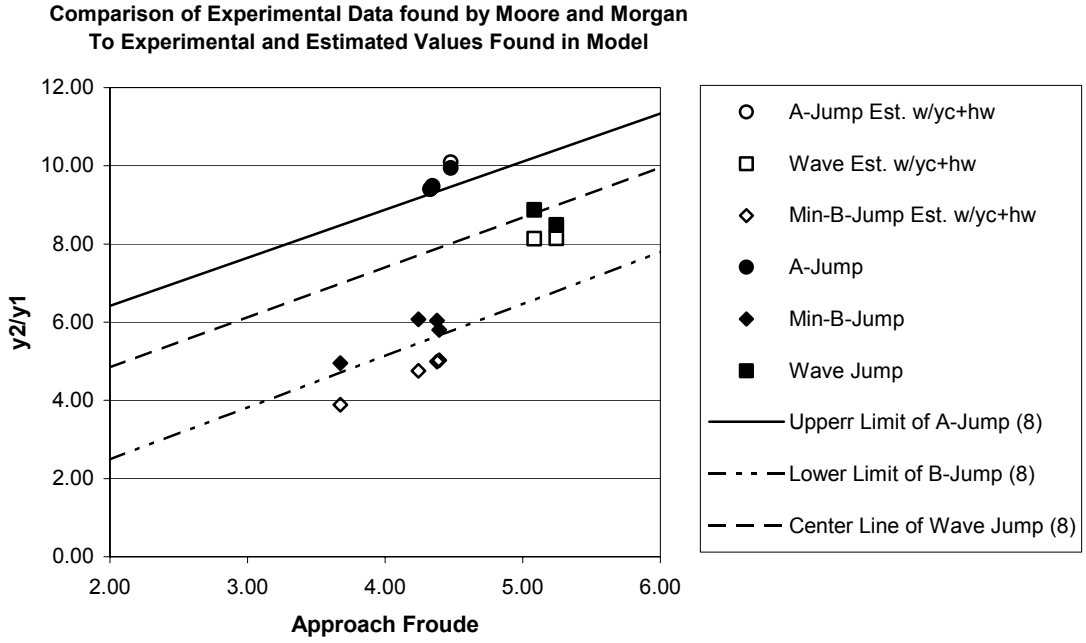

a)

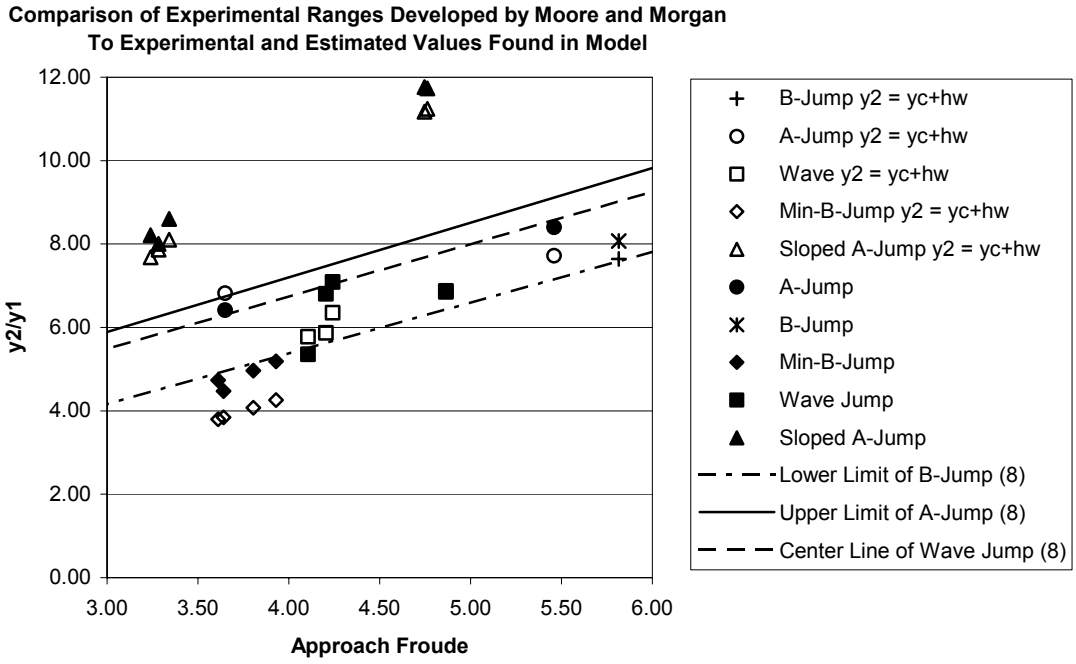

b)

Figure D6. Moore and Morgan a) 3<hd/y1<5 b) 2<hd/y1<3.

and above that provided by Moore and Morgan. This data followed the same trends as the plotted data.

The jump types observed during the testing match those created with tailwater described in the literature (7, 8, 9). The geometric characteristics of these jumps also match the theoretical data derived by Hsu and the experimental data presented by Moore and Morgan. The approximation of $y_2 = y_c + h_w$ allows the design engineer to predict if a jump will be triggered, however due to the sensitivity of jump type to small variation in y_2, the approximation will not be useful in predicting jump type.

Discharge Measurements

Depth measurements were taken with point gages, in the headtank, upstream and downstream of the weir. Villemonte's (1947) equations for a submerged V-notch weir were used to find discharge.

$$Q_1 = 0.58 \cdot \frac{8}{15} \cdot \sqrt{2g} \cdot H_1^{5/2} \tag{D3}$$

$$\frac{Q}{Q_1} = \left[1 - \left(\frac{H_2}{H_1} \right)^{5/2} \right]^{0.385} \tag{D4}$$

Where Q = [cfs], H = [ft],g = [ft/s^2].

APPENDIX E

ALTERNATIVE DESIGNS

Incomplete Hydraulic Jumps

Introduction

If a hydraulic jump occurs inside a culvert, the sequent depth may be greater then the height of the culvert. In this situation, the jump is incomplete and flow is pressurized downstream of the jump. Depending on the height of the channel and the sequent depth, the pressure inside the culvert may be different than that predicted with the Belanger equation.

Literature Review

There has been research completed on incomplete hydraulic jumps in closed conduits. Incomplete jumps have been studied in sloping and horizontal circular (1,2,3), exponential (2), and rectangular culverts (4,5,6).

Haindl (4) used the momentum equation to derive the pressure head above the ceiling of the conduit (Equation E1).

$$H = \frac{1}{D}\left[\frac{\alpha_1 q^2}{g y_1} - \frac{\alpha_2 q^2}{g y_2} + \frac{y_1^2}{2} - \frac{D^2}{2}\right] \quad \text{(E1)}$$

Where:

H = pressure head above ceiling of the conduit

D = height of the conduit cross section

He assumed hydrostatic pressure upstream and downstream of the jump (Figure E1). His results showed that this derivation over predicted the measure pressure head on the ceiling. The difference between measured and derived results is attributed to the assumptions of negligible friction forces and velocity coefficients equal to one. Haindl concluded that the downstream velocity coefficient varies and can be much larger than one. He also concluded that incomplete jumps dissipate less energy than complete jumps with the same approach Froude number.

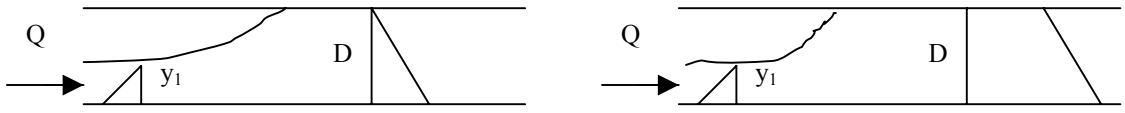

a) b)

Figure E1. a) Hydrostatic pressure at downstream cross-section is taken as a function of D. b) Hydrostatic pressure at downstream cross-section is taken as a function of y_2.

Smith and Chen (5) expanded on the work of Haindl. They derived the equation for an incomplete hydraulic jump using the momentum equation and added friction and weight (for sloped conduits) forces into the equation. They also changed the downstream hydrostatic pressure force so that it was a function of y_2 not just D (Figure E1b). This derivation had too many unknowns to solve, but if simplified for the case of a horizontal rectangular channel with negligible friction forces:

$$\frac{H}{D} = Fr_1^2\left(\frac{y_1}{D}\right)^2\left(1-\frac{y_1}{D}\right)+\frac{1}{2}\left[\left(\frac{y_1}{D}\right)^2+1\right] \qquad \text{(E2)}$$

Smith and Chen ran several experiments and found that the prediction over predicts the measured pressure head on the ceiling of the conduit. They developed a set of empirical equations to fit the measured data.

Ezzeldin, et. al. (6) studied the relationship between approach depth, conduit height, tailwater depth, and conduit slope. They reasoned that H is a function of tailwater depth and developed a set of empirical equations predicting the ratio of tailwater depth over conduit height to approach Froude number.

Experimental Setup and Procedure

Experiments were conducted in a horizontal rectangular flume measuring 0.5 ft (0.153 m) wide and 6 ft (1.83 m) long. 20 peizometers taps were spaced along the channel bed centerline. An adjustable 5 ft (1.524 m) long acrylic roof was fabricated, and runs were conducted at roof heights of 0.2, 0.25, and 0.3 ft (0.061, 0.076, and 0.91 m). The inflow was controlled using the pump inlet valve. The flow rate was held steady at 0.2 cfs (0.0056cms) for every run. The sluice gate was adjusted to create the desired Froude number (from 2 to 7) at a point 0.48ft downstream of the sluice gate, and the tailgate was raised or lowered to keep the toe of each jump approximately 1.5ft (0.457m) from the sluice gate.

Results and Discussion

Data collected from 15 experimental runs is presented in Table E1. The resulting pressures measured were compared to those predicted using the Belanger equation. The data is plotted in Figure E2. On average, the Belanger equation over predicts the pressure by 15.5% and the proposed derivation over predicts the pressure by 18.5%. In both

equations the over prediction comes primarily from the assumption that there are no friction losses in channel.

The measured data was compared to theoretical and measured data presented by Smith and Chen. The current data follows a similar trend of that seen in the literature. The literature over predicts the results found in the current study.

Table E1. Incomplete Hydraulic Jump Data.

Run #	Approach Froude Number	Sluice Gate Heights (ft)	Roof Heights (ft)	Max Pressure Observed (ft)
1A	2	0.108	0.2	0.20
2A	3	0.082	0.2	0.28
3A	4	0.068	0.2	0.30
4A	5	0.058	0.2	0.34
5A	6	0.052	0.2	0.38
6A	7	0.047	0.2	0.42
7A	7	0.047	0.3	0.39
8A	6	0.052	0.3	0.37
9A	5	0.058	0.3	0.34
10A	4	0.068	0.3	0.30
11A	3	0.082	0.25	0.25
12A	4	0.068	0.25	0.29
13A	5	0.058	0.25	0.33
14A	6	0.052	0.25	0.36
15A	7	0.047	0.25	0.39

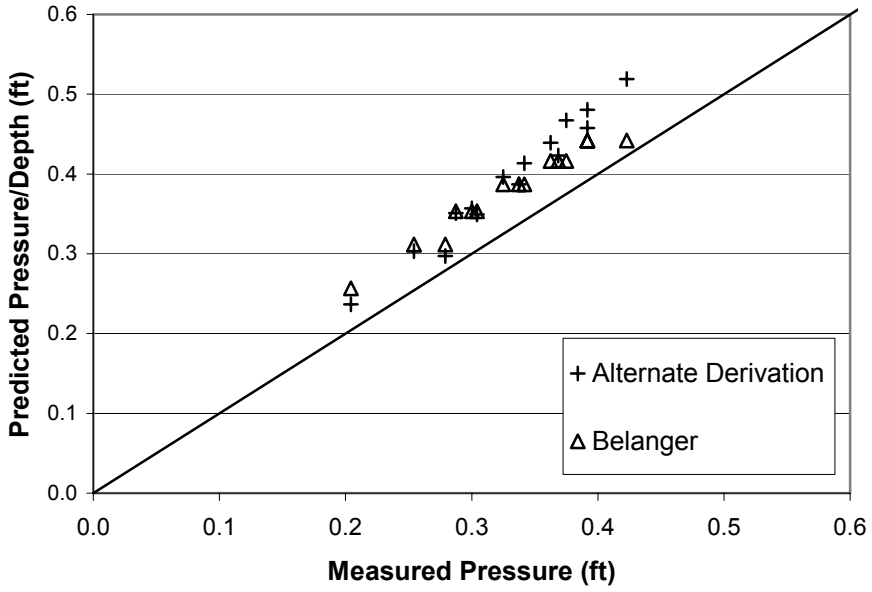

Figure E2: Comparison of Predictive Equations to Measured Data for Incomplete Jumps.

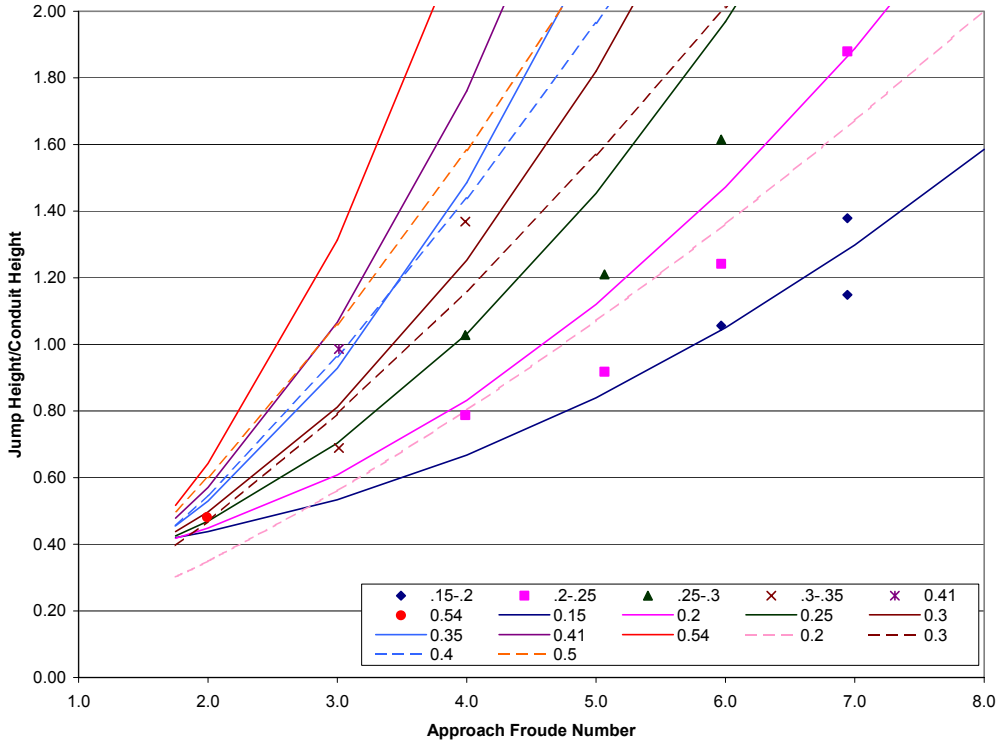

Figure E3. Comparison of measured data (points) to derived data by Smith and Chen (solid lines) and empirical equations by Smith and Chen (dashed lines).

References

1. Kalinske, A.A. and J.M. Robertson. Closed Conduit Flow. *Trans. Of the ASCE* Vol. 108 (1943) pg. 1435.

2. Rajaratnam, N. Hydraulic Jumps, Advances in Hydroscience, V.T. Chow, ed. Vol. 4, Academic Press, New York (1967).

3. Lane, E.W. and C.E. Kindsvater. Hydraulic Jump in Enclosed Conduit. *Eng. News Record*, 106 Dec 29, 1938. P. 815.

4. Haindl, K. Hydraulic Jump in Closed Conduit. Proc., International Association of Hydraulic Research. Lisbon, Vol. 2 (1957).

5. Smith, C.D. and Wentao Chen. The hydraulic jump in a steeply sloping square conduit. Journal of Hydraulic Research. 27(3), 1989.

6. Ezzeldin, M.M., A.M. Negm, and M.I. Attia. Experimental investigation on the hydraulic jump in sloping rectangular closed conduits.

Drop With Two Weirs

Introduction

Watching flow patterns during experimentation led us to consider other design options. There was not enough time or funds to fully explore these other options, but several were tested to give an idea if they show promise for future research or not. The two weir design was inspired by the Contra Costa stilling basin which has two rows of baffles and an end sill.

Design Setup

For runs 136-139 the two weir results were compared to the one weir results. The second weir was half as tall as the first and located 2 ft downstream. For runs 140-143 the second weir was 0.375 ft, the first weir was 0.5 ft, and they were 2 ft apart.

Results

The change in y_3 is less then $\pm$10% in all cases, except at a minimum flow rate. In this case the tailwater depth increased by 23%. These values are still within the range of measurement error.

Table E2. Comparison of One and Two Weir Configurations

Run	Ls	hd	hw		y1	y2	y3	Q	V1	V2	V3
48	5	0.71	0.5		0.097	0.892	0.242	2.20	11.34	1.23	4.56
136	5	0.71	0.5		0.11	0.903	0.229	1.89	8.59	1.05	4.13
	7		0.25	% Δ	-13.40	-1.29	5.18	14.11	24.26	15.21	9.42
49	5	0.71	0.5		0.196	1.303	0.397	4.98	12.70	1.91	6.27
137	5	0.71	0.5		0.209	1.367	0.428	4.83	7.92	1.77	5.64
	7		0.25	% Δ	-6.63	-4.91	-7.81	2.99	37.66	7.53	10.01
50	5	0.71	0.5		0.255	1.465	0.485	6.70	13.14	2.29	6.91
138	5	0.71	0.5		0.266	1.531	0.509	6.68	12.56	2.18	6.56
	7		0.25	% Δ	-4.31	-4.51	-4.95	0.33	4.45	4.63	5.03
51	5	0.71	0.5		0.311	1.516	0.600	8.15	13.11	2.69	6.80
139	5	0.71	0.5		0.323	1.618	0.557	7.57	11.72	2.34	6.80
	7		0.25	% Δ	-3.86	-6.73	7.09	7.17	10.62	13.02	0.09
59	3	0.71	0.5		0.3	0.974	0.552	8.21	13.68	4.22	7.43
140	3	0.71	0.5		0.33	0.952	0.497	7.81	11.83	4.10	7.86
	7		0.375	% Δ	-10.00	2.21	9.96	4.85	13.50	2.70	-5.68
60	3	0.71	0.5		0.113	1.034	0.189	2.18	9.63	1.05	5.76
143	3	0.71	0.5		0.118	1.076	0.233	2.20	9.32	1.02	4.72
	7		0.375	% Δ	-4.42	-4.11	-23.28	-1.06	3.22	2.93	18.03
61	3	0.71	0.5		0.193	0.816	0.426	5.01	12.99	3.07	5.89
142	3	0.71	0.5		0.222	0.834	0.424	4.94	11.13	2.96	5.83
	7		0.375	% Δ	-15.03	-2.21	0.35	1.46	14.33	3.59	1.11
62	3	0.71	0.5		0.253	0.896	0.511	6.74	13.32	3.76	6.60
141	3	0.71	0.5		0.286	0.914	0.483	6.69	11.70	3.66	6.93
	7		0.375	% Δ	-13.04	-2.07	5.39	0.76	12.21	2.77	-4.89

Drop With a Raised Weir

Introduction

Another design idea was to look at weirs that are raised slightly off the culvert floor, so that the water can flow both over and under the weir. This is based loosely on the USBR VII. This is a basin that allows low flows pass through, so sediment will not build up.

Design Setup

For runs 144-147 the results of a weir raised 0.125 ft off the floor were compared to the results of a weir of comparable height.

Results

The change in y_3 is less than $\pm$20% in all cases, except at a maximum flow rate. In this case the tailwater depth increased by 45.5%. In all cases the y_3 depth was deeper with a raised weir.

Table E3. Comparison of One and Raised Weir Configurations

Run	144 (raised sill)	134		145 (raised sill)	132		146 (raised sill)	131		147 (raised sill)	130	
Ls	5	5		5	5		5	5		5	5	
hd	0.71	0.71		0.71	0.71		0.71	0.71		0.71	0.71	
hw	0.375	0.5		0.375	0.5		0.375	0.5		0.375	0.5	
			%Δ			%Δ			%Δ			%Δ
Sloped	0.125	0.118	-5.93	0.27	0.261	-3.45	0.37	0.38	2.63	0.413	0.428	3.50
d1	0.12	0.118	-1.69	0.215	0.209	-2.87	0.298	0.305	2.30	0.331	0.332	0.30
d2	0.849	0.941	9.78	1.186	1.306	9.19	1.345	1.5	10.33	1.452	1.602	9.36
d3	0.267	0.237	-12.66	0.47	0.409	-14.91	0.579	0.54	-7.22	0.672	0.462	-45.45
Q	2.23	2.21	-0.80	5.06	4.98	-1.66	7.16	7.30	1.88	7.80	8.01	2.64

Weir with Drain Holes

Introduction

All experimental runs for Design I and II were performed with a solid rectangular weir. If this weir were used on the prototype the area upstream of the weir would fill with sediment and reduce the design effectiveness. Eight runs were performed with a weir with drain holes to determine its effect on outlet conditions and jump type.

Results

The effectiveness of the jump was found to be comparable to a weir without drain holes (Table E4). The jets coming through the slots were observed to break up at the nappe base. Jump type did not change.

Table E4. Weir with drain holes.

Run	Ld	hd	hw	y1	y2	y3	Q
148 (test)	5	0.71	0.75	0.103	1.042	0.202	1.69
155 (cut)	5	0.71	0.75	0.094	0.962	0.165	1.55
				8.74	7.68	18.32	8.51
149 (test)	5	0.71	0.75	0.196	1.37	0.444	4.66
154 (cut)	5	0.71	0.75	0.186	1.372	0.386	4.15
				5.10	-0.15	13.06	11.13
150 (test)	5	0.71	0.75	0.287	1.319	0.477	6.43
153 (cut)	5	0.71	0.75	0.296	1.678	0.572	6.93
				-3.14	-27.22	-19.92	-7.78
151 (test)	5	0.71	0.75	0.33	1.437	0.549	7.80
152 (cut)	5	0.71	0.75	0.324	1.703	0.594	7.67
				1.82	-18.51	-8.20	1.71
156	5	1	0.75	0.277	1.741	0.53	6.60
161 (cut)	5	1	0.75	0.273	1.702	0.535	6.75
				1.44	2.24	-0.94	-2.28
157	5	1	0.75	0.189	1.509	0.342	4.45
162 (cut)	5	1	0.75	0.196	1.458	0.398	4.47
				-3.70	3.38	-16.37	-0.39
158	5	1	0.75	0.093	1.071	0.158	1.63
163 (cut)	5	1	0.75	0.099	1.007	0.192	1.76
				-6.45	5.98	-21.52	-7.55
159	5	1	0.75	0.316	1.846	0.615	7.58
160 (cut)	5	1	0.75	0.314	1.794	0.625	7.53
				0.63	2.82	-1.63	0.73